

Copyright
by
Walter Orlando Tangarife García
2014

The Dissertation Committee for Walter Orlando Tangarife García
certifies that this is the approved version of the following dissertation:

**Holographic studies of thermalization and dissipation in
strongly coupled theories**

Committee:

Willy Fischler, Supervisor

Jacques Distler

Vadim Kaplunovsky

Eiichiro Komatsu

Sonia Pabán

**Holographic studies of thermalization and dissipation in
strongly coupled theories**

by

Walter Orlando Tangarife García, B.S.

DISSERTATION

Presented to the Faculty of the Graduate School of

The University of Texas at Austin

in Partial Fulfillment

of the Requirements

for the Degree of

DOCTOR OF PHILOSOPHY

THE UNIVERSITY OF TEXAS AT AUSTIN

August 2014

Dedicated to my family:

Edilma, Duván, Jeimy, Milena, Simón, Juan, Carlos Alberto, Henry, Andrés
and René.

Acknowledgments

Many people contributed in many ways to the research presented in this thesis.

I want to start by thanking my supervisor, Willy Fischler, for the superb guidance that he has offered during these years. Not only his great intuition and profound understanding of fundamental physics have provided me with a very significant learning experience, but also his sense of practicality and affable nature have been integral parts of his role as adviser and collaborator.

I am very grateful to the faculty members of the theory group. Particularly, I really enjoyed Vadim Kaplunovsky's courses on QFT and SUSY. I also thank him for sharing his vast knowledge in individual discussions and during brown bag meetings. Likewise, I thank Jacques Distler for his courses on string theory and for his willingness to discuss any question I had. I'm also grateful to Sonia Pabán, for individual physics discussions and her constant advice on practical matters. I thank Eiichiro Komatsu for conversations and support when he was at the TCC. And I thank Can Kilic for many discussions about phenomenology and bearing my many naïve questions.

My collaborators have been essential in this process. I want to thank specially Juan F. Pedraza, who has been not only an excellent research co-author but also a very good friend, I know he has a great academic career

in front of him. I thank Elena Cáceres for invaluable contributions to my research, for her advice and her friendship. I also wish to thank Arnab Kundu and Mohammad Edalati for the productive collaboration we have had. Many thanks to Alejandro de la Puente who has constantly motivated me to get more involved in phenomenology projects. I am thankful to Dustin Lorshbough and Phuc Nguyen for the recent fruitful collaboration that has been established with each of them recently.

I am also thankful to my fellow students and postdocs in the group with whom I spent lots of time discussing physics and non-physics related topics. I am in big debt with my friends in Austin, for many coffee conversations and for their valuable support.

Special thanks to Jan Duffy for her incredible job and patience while keeping the group running. Every interaction with her made the day much better.

And, finally, I would like to thank my family in Colombia for everything they have done for me.

This material is based upon work partially supported by the National Science Foundation under Grant Numbers PHY-1316033 and PHY-0969020 and by the Texas Cosmology Center.

Holographic studies of thermalization and dissipation in strongly coupled theories

Walter Orlando Tangarife García, Ph.D.
The University of Texas at Austin, 2014

Supervisor: Willy Fischler

This thesis presents a series of studies of thermalization and dissipation in a variety of strongly coupled systems. The main tool for these investigations is the *Gauge/Gravity duality*, which establishes a correspondence between a $d + 1$ -dimensional quantum theory of gravity and a d -dimensional quantum field theory.

We study the decay rates of fluctuations around the thermal equilibrium in theories in non-commutative geometry. Rapid thermalization of such fluctuations is found and motivates the conjecture that the phenomena at the black hole horizon is described by non-local physics. In the same type of environment, we analyze the Langevin dynamics of a heavy quark, which undergoes Brownian motion. We find that the late-time behavior of the displacement squared is unaffected by the non-commutativity of the geometry.

In a different scenario, we study the correlation functions in theories with quantum critical points. We compute the response of these quantum crit-

ical points to a disturbance caused by a massive charged particle and analyze its late time behavior.

Finally, we analyze systems far-from-equilibrium as they evolve towards a thermal state. We characterize this evolution for systems with chemical potential by focusing on the “strong subadditivity” property of their entanglement entropy. This is achieved on the gravity side by using time dependent functions for mass and charge in an AdS-Vaydia metric.

Table of Contents

Acknowledgments	v
Abstract	vii
List of Tables	xii
List of Figures	xiii
Chapter 1. Introduction	1
1.1 The Gauge/Gravity correspondence	2
1.2 Outline	6
Chapter 2. Fast thermalization in Non-Commutative Super Yang Mills Theories	9
2.1 Preliminaries	9
2.2 Holographic description of non-commutative theories	13
2.2.1 A Gravity Dual For Non-commutative SYM	17
2.3 Approach to Thermalization	19
2.3.1 Minimally-Coupled Scalar	21
2.3.2 Dilaton and Axion Fluctuations	31
2.4 Discussion	36
Chapter 3. Holographic Brownian Motion in Magnetic Environments	39
3.1 Preliminaries	39
3.2 Heavy quarks in a magnetic environment and holographic Brownian motion	42
3.3 Brownian Motion in SYM with a Magnetic Field	50
3.3.1 Langevin dynamics in the presence of a magnetic field .	50
3.3.2 Bulk dynamics and the drag coefficient	57

3.3.3	Diffusion and the fluctuation-dissipation theorem	61
3.4	Brownian Motion in NCSYM	64
3.4.1	Langevin dynamics in the non-commutative plasma . . .	64
3.4.2	Bulk dynamics and the drag coefficient	67
3.4.3	Diffusion and the fluctuation-dissipation theorem	71
3.5	Discussion	73
Chapter 4.	Quantum Fluctuations in Holographic Theories with Hyperscaling Violation	76
4.1	Preliminaries	76
4.2	Bulk metric	79
4.3	Quantum fluctuations and the two-point function	82
4.4	Response function and the fluctuation-dissipation theorem . .	88
4.5	Quantum Fluctuations in Holographic QCPs with $z = \infty$. . .	91
4.6	Final remarks	97
Chapter 5.	Strong Subadditivity, Null Energy Condition and Charged Black Holes	99
5.1	Introduction	99
5.2	A brief review of known results	104
5.2.1	Strong subadditivity, concavity and monotone-increasing	104
5.2.1.1	AdS-Vaidya background and entanglement entropy	105
5.2.1.2	Strong subadditivity and the null energy condition	107
5.3	The AdS-RN-Vaidya background	109
5.3.1	The bulk action and the backgrounds	110
5.3.2	Tests of strong subadditivity	116
5.3.3	Thin shells and junction conditions	119
5.3.4	Examples in $d = 3$	123
5.3.4.1	Backgrounds that respect SSA	124
5.3.4.2	Backgrounds that violate SSA	128
5.3.5	Examples in $d = 4$	131
5.3.5.1	Backgrounds that respect SSA	132
5.3.5.2	Backgrounds that violate SSA	133
5.4	Discussion and conclusions	134

Chapter 6. Conclusions	138
Appendices	140
Appendix A. Appendix to Fast Scrambling in NCSYM	141
Appendix B. Appendix to Brownian motion in NCSYM	144
B.1 Solutions for the string embedding	144
B.1.1 Solution for the AdS-Schwarzschild black hole	144
B.1.2 Solution for the Maldacena-Russo background	147
Appendix C. Appendix to Quantum Fluctuations in Theories with Hyperscaling Violation	151
C.0.3 Solution for $d = 2$	153
C.0.4 Solution for $d = 3$	154
Bibliography	156
Vita	178

List of Tables

2.1	Fits of the form $\text{Im } \omega = -\alpha T^\gamma$ for the curves shown in Figure 2.3 in the regime of $T\sqrt{\theta} \gg 1$	30
2.2	Fits of the form $\text{Im } \omega = -\alpha T^\gamma$ for the blue and purple curves shown in Figure 2.4 in the regime of $T \gg \theta^{-1/2}$	36

List of Figures

2.1	Quasi-normal modes of a minimally-coupled massless scalar. . .	29
2.2	Imaginary part of ω/T as a function of k/T	30
2.3	Imaginary part of the dominant quasi-normal frequency as a function of T	31
2.4	Imaginary part of the dominant quasi-normal frequency as a function of T for dilaton and axion.	35
2.5	Comparison of the thermalization rates for the commutative (black) and noncommutative (red) cases at weak coupling. . .	37
4.1	Schematic picture of the fluctuating string dual to a charged heavy particle coupled to a quantum critical point. The string stretches in the bulk between a D-brane at $r = r_b$ and the IR region of the geometry at $r = r_\epsilon$	82
5.1	Examples of two functions $m(v)$ where (a) NEC is obeyed, and (b) NEC is violated.	108
5.2	Entropy function for the cases where (a) NEC is obeyed, and (b) NEC is violated.	109
5.3	$m(v)$, $q(v)$ and $S(\ell)$ functions.	124
5.4	Profiles of a family of geodesics when SSA is obeyed.	125
5.5	$m(v)$, $q(v)$ given in (5.68) and $S(\ell)$	127
5.6	$m(v)$, $q(v)$ given in (5.69) and $S(\ell)$	128
5.7	$m(v)$, $q(v)$ given in (5.70) and $S(\ell)$	129
5.8	Profile of geodesic when SSA is violated corresponding to the choice (5.70).	130
5.9	$m(v)$, $q(v)$ given in (5.71) and $S(\ell)$	131
5.10	Example 1 of $m(v)$, $q(v)$ and $S(\ell)$ in $d = 4$	132
5.11	Example 2 of $m(v)$, $q(v)$ and $S(\ell)$ in $d = 4$	133
5.12	Example 3 of $m(v)$, $q(v)$ and $S(\ell)$ in $d = 4$	134
5.13	Example 1 of violation of SSA in $d = 4$	135
5.14	Example 2 of violation of SSA in $d = 4$	136

Chapter 1

Introduction

At the end of last century, the holographic principle was introduced in theoretical physics [165, 158]. This states that the description of a volume of space can be encoded on the boundary to the region. A remarkable development in this direction was the AdS/CFT correspondence proposal [121], more generally known as *Gauge/Gravity duality* [121, 79, 169]. This idea establishes the equivalence between two theories: a $d + 1$ -dimensional quantum theory of gravity and a d -dimensional quantum field theory.

Over the years, the study of thermal properties in quantum field theories has been of great interest. The gauge/gravity correspondence has provided tools for the study of a large class of strongly-coupled non-abelian gauge theories. Aside from pure theoretical motivation, one the the main reasons for pursuing such studies is the possible connection with the phenomenology of ultra-relativistic heavy ion collisions and/or strongly correlated condensed matter systems. An account of these efforts can be found in the reviews [78, 38, 83, 126] and the references therein. The prescription to compute correlation functions using the gauge/gravity duality was developed in [79, 169] and was subsequently generalized to the real-time finite-temperature formal-

ism in [155, 91]. This thesis explores applications of this correspondence to the study of thermalization, quantum fluctuation and dissipation processes in various strongly coupled theories. The dynamics in these theories is probed by using several techniques such as the computation of quasi-normal frequencies of bulk perturbations, calculation of entanglement entropy, introducing a heavy quark and studying its Langevin dynamics and the calculation of two-point functions. In the following paragraphs, we present an overview of the gauge/gravity correspondence.

1.1 The Gauge/Gravity correspondence

The simplest and best-understood example of the gauge/gravity duality relates four-dimensional $\mathcal{N} = 4$ Super-Yang-Mills (SYM) to type-IIB string theory (or supergravity) in asymptotically $\text{AdS}_5 \times S^5$, hence the name *AdS/CFT*. AdS_{d+1} spacetime is a solution to Einstein equations with negative cosmological constant and can be seen as a 5-dimensional hyperboloid embedded in a 6-dimensional spacetime $R^{2,d}$ [2],

$$-X_{-1} - X_0 + X_1 + \cdots + X_d = -R^2, \quad (1.1)$$

which has isometry $SO(d, 2)$. There is useful parametrization of this hyperboloid called the *Poincaré coordinates* $(u, t, x_{i=1, \dots, d-1})$,

$$\begin{aligned} X_0 &= \frac{1}{2u} (1 + u^2(R^2 + \vec{x}^2 - t^2)), \\ X^i &= R u x^i, \quad X_{-1} = R u t \\ X^d &= \frac{1}{2u} (1 - u^2(R^2 - \vec{x}^2 + t^2)), \end{aligned} \quad (1.2)$$

which provides for AdS_{d+1} the metric

$$ds^2 = R^2 \left(\frac{du^2}{u^2} + u^2(-dt^2 + d\vec{x}^2) \right). \quad (1.3)$$

In fact, most of the backgrounds studied in this thesis will resemble this parametrization of AdS .

The AdS/CFT conjecture postulates that the physics of the AdS space-time (gravity side) bulk can be described by a quantum field theory that lives on the boundary of this spacetime. The isometry group of AdS, acting on the boundary, turns out to be the conformal group $SO(2, d)$.

The theory on the boundary, in the simplest example, is $\mathcal{N} = 4$ $SU(N)$ Super Yang-Mills (SYM) with an $\mathcal{N} = 4$ vector supermultiplet living in d dimensions. Considering the specific case of $d = 3 + 1$, this theory arises from having a large stack of N $D3$ -branes along a $3 + 1$ dimensional hyperplane in the 10-dimensional spacetime. The action that describes the open string excitations contains the action for this theory plus higher derivative terms. Additionally, there is an action that corresponds to the massless closed string excitations and there is an action that mixes the two types of strings. In the low energy limit, these two sectors are completely decoupled by taking $\alpha' \rightarrow 0$, *i.e.* $l_s \rightarrow 0$, while keeping N and the string coupling g_s constant. Thus, the open string action describes the physics of $\mathcal{N} = 4$ $SU(N)$ SYM on the 4-dimensional boundary.

On the other hand, this system can be seen from the supergravity point of view. The $D3$ -branes act as sources for type IIB supergravity fields. In the

limit where N is very large, the geometry that is a solution to the equations of motion is called a black 3-brane and has a horizon and a singularity. When these two coincide, it is called an extremal black 3-brane and its mass is given by

$$M = \frac{N}{(2\pi)^3 g_s l_s^4}.$$

In the low energy limit, there are two kinds of excitations; one is composed by free supergravity fields and the other corresponds to the excitations living near the horizon of the *black* 3-branes. This “near-horizon” geometry is precisely $AdS_5 \times S^5$

$$ds^2 = \frac{r^2}{R^2}(-dt^2 + d\vec{x}^2) + \frac{R^2}{r^2} + R^2 d\Omega_5^2, \quad R^4 \equiv 4\pi g_s \alpha'^2 N, \quad (1.4)$$

where r is related to u in 1.3 by $r = R^2 u$.

Thus, we have two theories that are the same, $\mathcal{N} = 4$ $SU(N)$ SYM in $d = 3 + 1$ spacetime and type IIB supergravity on $AdS_5 \times S^5$. The validity of one or the other descriptions depends on the value of the so-called 't Hooft coupling,

$$\lambda \equiv g_{YM}^2 N = 4\pi g_s N. \quad (1.5)$$

When $\lambda \gg 1$, the boundary theory is strongly coupled and perturbation theory cannot be used while the gravitational description can be trusted. Conversely, when $\lambda \ll 1$, the gauge theory is weakly coupled but the gravity side cannot be trusted anymore.

The “dictionary” that AdS/CFT prescribes works in the following way. Let us take an excitation in the bulk $\phi(r, t, \vec{x})$ which at the boundary ($r \rightarrow 0$)

takes the value $\phi_0(t, \vec{x})$. This field couples like a source to a boundary gauge invariant operator $\mathcal{O}(t, \vec{x})$ through the term $\int d^4x \phi_0(x) \mathcal{O}(x)$ in the boundary Lagrangian. Thus, the correspondence relates the generating function of correlation functions of the field theory with the minimized supergravity action in the bulk [79, 169]:

$$\langle e^{\int d^4x \phi_0(x) \mathcal{O}(x)} \rangle \equiv \mathcal{Z}_{\text{CFT}}[\phi_0(x)] \iff e^{-S_{\text{bulk}}[\phi(r, x)]|_{r=0}} \equiv \mathcal{Z}_{\text{Bulk}}[\phi_0(x)]. \quad (1.6)$$

Then, a straightforward formula gives the n -point correlation function for \mathcal{O} ,

$$\langle \mathcal{O}(x_1) \cdots \mathcal{O}(x_n) \rangle = \frac{\delta}{\delta \phi_0(x_1)} \cdots \frac{\delta}{\delta \phi_0(x_n)} \mathcal{Z}_{\text{Bulk}}[\phi_0(x)]. \quad (1.7)$$

The mass m of the bulk field ϕ and the conformal dimension Δ of the operator \mathcal{O} are related by the expression

$$\Delta = \frac{d}{2} + \sqrt{\frac{d^2}{4} + R^2 m^2}. \quad (1.8)$$

This correspondence has been generalized to more generic gravitational backgrounds. In particular, the inclusion of a black hole in the *AdS* bulk is known to be dual to a strongly-coupled gauge theory at finite temperature [170]. Furthermore, the gravitational background dual to a theory with finite chemical potential is described by an AdS geometry with an electrically charged black hole, this is known as AdS-Reissner-Nordström background.

This opened the possibility of computing a large variety of observables in thermal field theories with string coupling. Some examples are given by the decay rates and time scales for the approach to thermal equilibrium of

certain disturbances [93, 24, 108], which in the gravity side are mapped to the computation of quasinormal frequencies. One interesting result in this front has been the well-known result of $1/4\pi$ for the shear viscosity to entropy density ratio at strong coupling [139, 109] which in turn led to the holographic calculation of many other transport coefficients [156, 140]. More recently, it has been possible to gain further insight in the previously uncharted out-of-equilibrium regime by considering geometries that evolve in time [94, 14, 15, 31]. In these latter studies, the thermalization process is analyzed by following the formation of a black hole in the bulk. This dynamics is probed by computing non-local observables such as Wilson loops and entanglement entropy.

1.2 Outline

This thesis contains a collection of studies of processes in strongly coupled systems. Such studies are motivated by phenomena that have been observed in condensed matter systems, quark-gluon plasma or environments resembling non-local properties, such as the horizon of black holes. The main tool for the analysis is the correspondence presented above. In Chapter 2, we study rapid thermalization in thermal theories in non-commutative geometry. Specifically, the decay rates of fluctuations around the thermal equilibrium are calculated by considering the imaginary parts of the frequencies of quasinormal modes of fields in the gravitational background. Such analysis is motivated by the fast thermalization features exhibited black hole horizons. The

main result is that, in fact, strongly coupled plasmas in these non-commutative geometries show fast “scrambling” of perturbations, which supports the idea that the physics at the black hole horizon is described by non-local physics. The contents of this work were published in [62].

Following the motivation from Chapter 2, in Chapter 3 the same geometry is considered and a study of Brownian motion of a heavy particle is studied. The holographic realization of Langevin dynamics of this particle, undergoing random motion in a non-commutative strongly couple plasma, provides a description of the diffusion processes within the plasma. It is found, however, that although the non-commutative plasma is less viscous, the late-time behavior of the displacement squared is unaffected by the non-commutativity of the geometry. These results were published in [68].

In Chapter 4, the methods of AdS/CFT are used to explore a different system. We study the correlation functions in theories with a class of quantum critical points. We compute the response of these quantum critical points to a disturbance caused by a massive charged particle. Our results show that, in these theories, the two-point functions become independent of the mass of the probe at late times. Such work has been published in [63].

Finally, in Chapter 5, entanglement entropy is used to analyze systems far-from-equilibrium as they evolve towards a thermal state. We characterize this evolution especially for systems with chemical potential by focusing on the “strong subadditivity” property of their entanglement entropy. On the gravity side, time dependent functions for mass and charge are chosen, in an AdS-

Vaidya metric, in order to resemble the desired dual QFT. Our investigations find that the dual field theory disallows specific choices of the mass and charge functions for which it is possible to penetrate some critical surface that is formed in the bulk. This research has been published in [32].

Chapter 2

Fast thermalization in Non-Commutative Super Yang Mills Theories

2.1 Preliminaries

It has been known since the days of the “membrane paradigm” [166] that the event horizon of black holes, or more precisely the stretched horizon, is endowed with physical properties from the vantage point of some fiducial observers. This is in contrast with the freely falling observers which do not experience the horizon. In particular, from the viewpoint of these fiducial observers, a charge falling into the horizon is seen as having its charge smeared over the horizon in a time that grows logarithmically with the Schwarzschild radius of the black hole.

In a remarkable paper, Preskill and Hayden [86] posed a critical challenge to the resolution of the information paradox. In a nutshell, their observation lead to the conclusion that the time scale involved in possibly sharing information between two observers, one hovering outside the black hole horizon and the other falling through the horizon while carrying information, is dramatically shorter than what was believed possible until then. The fascinating answer to this challenge, the so-called “fast scrambling” property of the

horizon, was conjectured by Sekino and Susskind in [149]. This property is tantamount to the extremely rapid spreading of the charge as we alluded to earlier. The time scale involved in scrambling grows only logarithmically with the entropy. This is a much shorter time scale as a function of the entropy than the time that a particle subject to Brownian motion would take to travel through a distance commensurate with the “size” of the system [149]. The time scale in the latter case grows with a positive power of the entropy. Additional conjectures related to the fate of information on the horizon of a black hole have appeared in the last few years. The most relevant one has been described as the *firewall conjecture* [7], which states that black hole complementarity, [160], is not enough to assure the compatibility of quantum mechanics and the equivalence principle for observers that are falling into a black hole. Instead, the existence of a “firewall” behind the black hole horizon is proposed in order to keep a freely falling observer from falling without noticing any drama at the horizon.

It was argued in [149] that non-locality has to be one of the ingredients that generate fast scrambling. Local interactions, on the other hand, would lead to slow diffusion as in Brownian motion. Another possibly necessary ingredient to generate the fast scrambling property of the stretched horizon is the presence of strong coupling interactions among the horizon’s degrees of freedom.

In this chapter, we present the results published in [62], in which we emulate non-locality and strong coupling by considering a strongly-coupled

non-commutative gauge theory at high temperature: four-dimensional non-commutative (supersymmetric) Yang-Mills theory, to be precise. As the non-commutative system under consideration is strongly coupled, we use the gauge/gravity correspondence, described in the introduction to this thesis, as a toolbox for analyzing various thermal aspects of the system. We show that the rate of decay of a disturbance propagating in this thermal medium is parametrically much larger than in the local setting of conventional field theories. This inevitably leads to rapid thermalization¹. It is noteworthy that computations at weak coupling do not exhibit an enhancement of the thermalization rate. This could then imply that fast thermalization in non-commutative field theories is a consequence of having both strong coupling and non-commutativity. See [159, 11, 18, 113] for other works in analyzing the fast scrambling conjecture.

The existence of a connection between the ultraviolet and the infrared in the non-commutative setting has been well studied over the years [23]. One of its manifestations is the large transverse size of any degree of freedom moving with a large momentum k , where transversality here is with respect to the direction of k . The transverse size grows with k when the momentum in the non-commutative direction is larger than $\theta^{-1/2}$ where θ is the Moyal area. Indeed, the transverse size scales like θk . This property is at the heart of the rapid decay of high momenta modes into excitations of the heat bath.

¹It should be noted that the rapid thermalization that we observe here is for the boundary non-commutative thermal bath and does not seem to be directly connected to the properties of the stretched horizon of the dual black brane background as observed by a fiducial observer hovering outside the horizon.

The chapter is organized as follows: in the next section we briefly review the gravity dual of a strongly coupled large- N non-commutative gauge theory at finite temperature and then set-up the study of the approach to thermalization in this context. In section three, we exhibit the computation of the decay rates in the non-commutative heat bath and compare it to the results for the local case of strongly-coupled commutative gauge theories. More specifically, we compute the decay rates in three cases: once when the non-commutative thermal bath is perturbed by an operator dual to a minimally-coupled massless scalar field in the bulk, then with the operator dual to the dilaton fluctuation of the bulk, and finally with the operator dual to the bulk axion fluctuation. Furthermore, we compute the decay rates in the regime of parameters where the temperature of the bath is taken to be larger than $\theta^{-1/2}$ along with the momentum of the modes in the non-commutative plane being greater than the temperature (which necessarily implies that the momentum is also greater than $\theta^{-1/2}$). This is the regime where one expects the deviations from the results of the commutative setting to be more pronounced².

²This is due to the fact that at temperatures larger than $\theta^{-1/2}$, the typical momenta in the heat bath is of the order of temperature and hence the transverse size of the modes of the heat bath is large and gets larger as the temperature increases. One therefore expects the non-local effects to be important at those high temperatures.

2.2 Holographic description of non-commutative theories

In order to motivate the physics of theories in non-commutative geometries, let us consider a classical pair of particles with opposite electric charge in the presence of a strong magnetic field B and with an additional harmonic potential. In the regime where the Coulomb potential can be neglected, the effective Lagrangian can be written as [23]

$$\mathcal{L} = \frac{B}{2}\epsilon_{ij}(\dot{x}_1^i x_1^j - \dot{x}_2^i x_2^j) - \frac{K}{2}(\vec{x}_1 - \vec{x}_2)^2, \quad (2.1)$$

where $\epsilon_{ij} = -\epsilon_{ji}$.

This can be rewritten in terms of center of mass and the relative coordinates,

$$X^i \equiv \frac{1}{2}(x_1^i + x_2^i), \quad \Delta \equiv \frac{1}{2}(x_1^i - x_2^i),$$

as

$$\mathcal{L} = 2B\epsilon_{ij}\dot{X}^i\Delta^j - 2K\Delta^2. \quad (2.2)$$

Notice that the center of mass momentum, conjugate to X^i , is

$$P_i = 2B\epsilon_{ij}\Delta^j, \quad (2.3)$$

and the Hamiltonian is

$$\mathcal{H} = \frac{K}{2B^2}P^2. \quad (2.4)$$

Thus, what we have here is a system that behaves as a free particle of mass B^2/K but whose “size” depends on its momentum. That means that the

system “grows” as the momentum increases. This resembles the UV/IR connection, mentioned in the previous paragraphs, that characterizes the theories in non-commutative geometries; the physics at low energies (large distances) are directly connected to the phenomena at high energies (large momentum).

Non-commutative geometries are defined by the commutator between two coordinates

$$[x^\mu, x^\nu] = i\theta^{\mu\nu}, \quad (2.5)$$

where θ is a rank-2 antisymmetric tensor. The algebra of functions in this non-commutative spacetime is defined using the *Moyal product*,

$$(\phi_1 \star \phi_2)(x) \equiv e^{i\theta^{\mu\nu} \partial_\mu^y \partial_\nu^z} \phi_1(y) \phi_2(z) \Big|_{z=y=x}. \quad (2.6)$$

A quantum field theory in this type of geometry is, then, defined by the functional action $S = \int d^4x \mathcal{L}[\phi]$, with the property that the multiplication of fields in \mathcal{L} is performed using the Moyal product [127, 60]. Specifically, in perturbative field theory, the quadratic terms are left unchanged respect to ordinary QFT, but the interaction terms are modified by a phase factor. In momentum space, this is

$$\lambda_n \phi^n \rightarrow \lambda_n \phi_1 \cdots \phi_n e^{-\frac{i}{2} \sum_{i < j} k_i \times k_j}, \quad (2.7)$$

where $k_i \times k_j = k_i^\mu k_j^\nu \theta_{\mu\nu}$.

In string theory, non-commutative theories can be easily realized on the worldvolume of Dp -branes with a constant Neveu-Schwarz $B_{\mu\nu}$ field provided that one takes a special limit to decouple the open and closed string modes [59,

10, 148]. Basically, one scales the string tension to infinity and the closed string metric to zero while keeping the background $B_{\mu\nu}$ field fixed. The worldsheet action for the open strings, with Euclidean signature, is given by

$$\begin{aligned} S &= \frac{1}{4\pi\alpha'} \int_{\Sigma} (g_{ij} \partial_a x^i \partial^a x^j - 2\pi i \alpha' B_{ij} \epsilon^{ab} \partial_a x^i \partial_b x^j) \\ &= \frac{1}{4\pi\alpha'} \int_{\Sigma} g_{ij} \partial_a x^i \partial^a x^j - \frac{i}{2} \int_{\partial\Sigma} B_{ij} x^i \partial_t x^j, \end{aligned} \quad (2.8)$$

where Σ is the string worldsheet and the rank of B is r . The boundary conditions dictated by the equations of motion along the Dp -branes are

$$g_{ij} \partial_n x^j + 2\pi i \alpha' B_{ij} \partial_t x^j \Big|_{\partial\Sigma} = 0, \quad (2.9)$$

with ∂_n normal to $\partial\Sigma$. These can be rewritten for the case where Σ is a disc that is conformally mapped to the upper half complex plane:

$$g_{ij} (\partial - \bar{\partial}) x^j + 2\pi i \alpha' B_{ij} (\partial + \bar{\partial}) x^j \Big|_{z=\bar{z}} = 0. \quad (2.10)$$

Thus, the propagator results in

$$\langle x^i(z) x^j(z') \rangle = -\alpha' [g^{ij} \text{Log}|z - z'| - g^{ij} \text{Log}|z - \bar{z}'|] \quad (2.11)$$

$$+ G^{ij} \text{Log}|z - \bar{z}'|^2 + \frac{1}{2\pi\alpha'} \theta^{ij} \text{Log} \left| \frac{z - \bar{z}'}{z - z'} \right| + \text{const.} \quad (2.12)$$

where

$$G^{ij} = \left(\frac{1}{g + 2\pi\alpha'} g \frac{1}{g - 2\pi\alpha'} \right)^{ij}, \text{ and} \quad (2.13)$$

$$\theta^{ij} = -(2\pi\alpha')^2 \left(\frac{1}{g + 2\pi\alpha'} B \frac{1}{g - 2\pi\alpha'} \right)^{ij}. \quad (2.14)$$

At the boundary, and restricting to real z , this propagator becomes

$$\langle x^i(z)x^j(z') \rangle = \alpha' G^{ij} \text{Log}(z - z')^2 + \frac{i}{2} \theta^{ij} \epsilon(z - z'), \quad (2.15)$$

where $\epsilon(z)$ is 1 or -1 for positive or negative z . In the last expression, G^{ij} has an interpretation as the open string metric. θ^{ij} on the other hand, is interpreted as the Moyal tensor, given that

$$[x^i(\tau), x^j(\tau)] = i\theta^{ij}. \quad (2.16)$$

Here, τ is interpreted as time and the time ordering is taken as the operator order.

Furthermore, the product of two tachyon vertex operators produce

$$e^{ip \cdot x}(z) \cdot e^{iq \cdot x}(z) \approx (z - z')^{2\alpha' G^{ij} p_i q_j} e^{-\frac{i}{2} \theta^{ij} p_i q_j} e^{i(p+q) \cdot x}(z') + \dots. \quad (2.17)$$

Notice that this coincides with the Moyal product in the limit in which $\alpha' \rightarrow 0$. In order to keep G and θ fixed in this limit, a double decoupling limit is taken to realize a theory in non-commutative geometry:

$$\alpha' \sim \sqrt{\epsilon} \rightarrow 0, \quad (2.18)$$

$$g_{ij} \sim \epsilon \rightarrow 0, \quad i, j = 1, \dots, r. \quad (2.19)$$

When background gauge fields are added to the theory, the term

$$-i \int d\tau A_i(x) \partial_\tau x^i \quad (2.20)$$

is added to the action 2.8. This is invariant under the gauge transformation

$$\delta A_i = \partial_i \lambda + i\lambda \star A_i - iA_i \star \lambda. \quad (2.21)$$

2.2.1 A Gravity Dual For Non-commutative SYM

We now present a gravitational dual to the the strong 't Hooft coupling and large N limit of a non-commutative super Yang-Mills theory, in the spirit of the AdS/CFT correspondence [121]. For much of this chapter, we focus on the four-dimensional non-commutative Yang-Mills theory at finite temperature. We also take the non-commutativity parameter to be non-zero only in the (x^2, x^3) -plane, that is $[x^2, x^3] \sim i\theta$.

A proposal for the dual gravity background of such a theory was given in [85, 123] which, in the string frame, reads

$$\begin{aligned} ds^2 &= L^2 \left[-u^2 f(u) dt^2 + u^2 dx_1^2 + u^2 h(u) (dx_2^2 + dx_3^2) + \frac{du^2}{u^2 f(u)} + d\Omega_5^2 \right], \\ B_{23} &= L^2 a^2 u^4 h(u), \quad e^{2\Phi} = \hat{g}^2 h(u), \\ C_{01} &= L^2 a^2 \hat{g}^{-1} u^4, \quad F_{0123u} = 4L^4 \hat{g}^{-1} u^3 h(u), \end{aligned} \tag{2.22}$$

where $L^4 = 4\pi \hat{g} N \alpha'^2$ with \hat{g} being the value of the string coupling in the IR, and

$$h(u) = \frac{1}{1 + a^4 u^4}, \quad f(u) = 1 - \frac{u_h^4}{u^4}, \tag{2.23}$$

where u_h is the horizon radius.

The parameter a which appears in the above expressions is related to the non-commutativity parameter θ of the boundary theory through $a = \lambda^{1/4} \sqrt{\theta}$. Here, $\lambda = L^4/\alpha'^2$ is the 't Hooft coupling of the boundary large- N non-commutative Yang-Mills theory. For $u \ll a^{-1}$, the background (2.22) goes over to the $AdS_5 \times S^5$ solution. As expected, this observation just reflects

the fact that the non-commutative boundary theory goes over to the ordinary commutative Yang-Mills theory at length scales much greater than $\lambda^{1/4}\sqrt{\theta}$. For $u \gg a^{-1}$, on the other hand, the background (2.22) shows significant deviation from the $AdS_5 \times S^5$ geometry. In particular, the bulk spacetime is no longer asymptotically AdS_5 . The boundary theory interpretation of this regime just means that the effect of non-commutativity becomes pronounced for length scales which are at the order of, or smaller than, $\lambda^{1/4}\sqrt{\theta}$ ³. To summarize, the background (2.22) represents a flow in the boundary theory from a UV fixed point which is non-commutative Yang-Mills at large N and large λ to an IR fixed point given by the ordinary commutative Yang-Mills (again, at large N and large λ)⁴.

Also, the Hawking temperature of the above solution, which is interpreted as the temperature of the non-commutative boundary theory, is given by $T = u_h/\pi$. Notice that this temperature is the same as the temperature one obtains for the Schwarzschild AdS_5 solution, which is dual to a thermal state of four-dimensional commutative Yang-Mills theory. Indeed, it is easy to show that all the thermodynamic quantities obtained from (2.22) are the same as the ones obtained from the Schwarzschild AdS_5 solution [123]. In the

³Since the reliability of the solution (2.22) requires $L^4/\alpha'^2 = \lambda$ to be large, the effect of non-commutativity in the boundary theory is visible even at large length scales [123]. This should be compared with the weak-coupling regime of the theory where the threshold length scale (beyond which the theory becomes effectively commutative) is roughly at the order of $\sqrt{\theta}$.

⁴Throughout this work, we use the terms “UV” and “IR” with respect to the boundary energy. Then, in bulk terms, UV means near the boundary whereas IR means near the horizon.

limit of vanishing temperature ($u_h \rightarrow 0$), we are left with a geometry that is dual to the vacuum of the NCSYM.

2.3 Approach to Thermalization

In the context of the AdS/CFT correspondence, turning on the fluctuations of the bulk background translates into deforming the boundary field theory by the operators dual to the bulk fluctuations. In the case where the background is a large black hole, which describes a thermal state in the boundary field theory [170], the bulk fluctuations correspond to the perturbations of the thermal bath in the boundary field theory. Due to the existence of the horizon in the bulk, the fluctuations of the black hole background fall into the horizon. From the perspective of the boundary field theory, the decay of the bulk fluctuations into the horizon translates into the decay of the perturbations of the thermal bath and their eventual thermalization, after some time scale, with the rest of the bath [93]. In other words, the decay of the bulk fluctuations into the horizon holographically describes the approach to thermal equilibrium in the boundary field theory.

In the linear response theory, the time scale required for a perturbation to thermalize with the rest of the bath can be read off from the imaginary part of the poles in the retarded Green's function of the operator by which the thermal bath has been perturbed. Indeed, the late-time decay is dominated by the imaginary part of the lowest of such poles (in the complex frequency plane). While the computation of the thermalization time scales is relatively

easy in the perturbation theory [103, 116], it is a formidable task when the thermal bath is strongly coupled. Fortunately, this is the regime where the AdS/CFT correspondence is most useful. In fact, the poles in the retarded Green's function of the boundary theory operators are mapped, through the correspondence, to the quasi-normal frequencies of the bulk fluctuations which are dual to those operators, a connection which was first proposed in [24] and later sharpened in [155, 108]. See [21] for a relatively recent review on the quasi-normal modes of various backgrounds (with different asymptotics) from the perspectives of both general relativity and the AdS/CFT correspondence.

The quasi-normal modes of a perturbation of a gravitational background are defined as the solutions to the equation of motion of that perturbation which are infalling near the horizon and normalizable at the boundary (when the background is asymptotically AdS). The quasi-normal frequencies are then the set of complex frequencies for which such solutions exist. Thus, for strong-coupling thermal baths, the thermalization time scales can simply be obtained by computing the quasi-normal modes of the dual black hole backgrounds. While there are semi-analytic methods for computing special values of the quasi-normal frequencies, their generic values, however, cannot be computed analytically for most backgrounds. In such cases, one can compute them numerically with high precision using a variety of techniques developed over the years in the literature [21].

Our goal is to study the approach to thermalization in a strongly coupled non-commutative thermal bath, which is dual to the non-extremal back-

ground given in (2.22). In particular, we would like to analyze to what extent the thermalization properties of a non-commutative thermal bath deviate from its commutative counterpart. To do so, we will consider three examples of fluctuations of the dual supergravity background: a minimally-coupled scalar field, fluctuation of the dilaton as well as the fluctuation of the Ramond-Ramond (axion) scalar field.

2.3.1 Minimally-Coupled Scalar

We start by considering perhaps the simplest possibility. That is, we perturb the non-extremal background (2.22) with a minimally-coupled massless scalar φ , which we assume to be dual to some scalar operator \mathcal{O} in the non-commutative boundary theory. Our goal is to calculate the time scale for this perturbation to thermalize with the non-commutative bath. As mentioned above, we need to compute the quasi-normal modes of the minimally-coupled scalar field fluctuations around the background (2.22). The equation of motion for φ (with no dependence on the coordinates of S^5) reads

$$\frac{e^{2\Phi}}{\sqrt{-g}} \partial_\mu (\sqrt{-g} e^{-2\Phi} g^{\mu\nu} \partial_\nu \varphi) = 0, \quad (2.24)$$

which, in the non-extremal background (2.22), takes the form

$$0 = \partial_u [u^5 f(u) \partial_u \varphi] + u \left[-\frac{1}{f(u)} \partial_t^2 + \partial_{x^1}^2 + \frac{1}{h(u)} (\partial_{x^2}^2 + \partial_{x^3}^2) \right] \varphi. \quad (2.25)$$

We emphasize that the minimally-coupled massless scalar that we are studying here is not related to the metric fluctuations of the background (2.22)

such as $\delta g_{x^1}^t$. As shown in [123], the equation of motion for $\delta g_{x^1}^t$ (with no dependence on S^5) satisfies the same equation as in (2.24) provided that $\delta g_{x^1}^t$ depends neither on t nor on x^1 directions. The analysis in this section should be regarded as a warm-up exercise. Nevertheless, we believe that the lesson we learn by analyzing the case of a minimally-coupled massless scalar will prove useful when we consider, in the subsequent section, some genuine fluctuations of the background such as the dilaton and axion fluctuations.

To solve the equation (2.25), we go to momentum space by Fourier transforming $\varphi(u, t, \vec{x})$:

$$\varphi(u, t, \vec{x}) \sim e^{-i\omega t + i\vec{k} \cdot \vec{x}} \varphi(u; \omega, \vec{k}). \quad (2.26)$$

To avoid clutter in the notation, we have denote the Fourier modes of the scalar field also by φ . The distinction should be clear from the arguments of φ , or the context in which it is being used. In order to see any non-trivial effect on the behavior of the modes $\varphi(u; \omega, \vec{k})$ due to the existence of a non-zero Neveu-Schwarz $B_{\mu\nu}$ field in the bulk, especially in the asymptotic $u \rightarrow \infty$ region where the behavior of $\varphi(u \rightarrow \infty; \omega, \vec{k})$ holographically encodes information about the source and the condensate of the dual operator $\mathcal{O}(\omega, \vec{k})$, one should consider the modes with a non-vanishing momentum in the (x^2, x^3) plane. Without loss of generality, we take $k_2 = 0$ and $k_3 \neq 0$ and, for simplicity, we also consider the modes with $k_1 = 0$. The equation of motion (2.25) then becomes

$$\partial_u [u^5 f(u) \partial_u \varphi] + u \left[\frac{\omega^2}{f(u)} - \frac{k^2}{h(u)} \right] \varphi = 0, \quad (2.27)$$

where $k \equiv k_3$.

Some comments on the boundary theory operator dual to $\varphi(u, t, \vec{x})$ are in order here. Normally, in the AdS/CFT correspondence, one associates a gauge invariant operator $\mathcal{O}(t, \vec{x})$ in the boundary theory to the bulk fluctuation $\varphi(u, t, \vec{x})$ in the sense that near the boundary of the spacetime the non-normalizable mode of $\varphi(u \rightarrow \infty, t, \vec{x})$ sources the dual operator $\mathcal{O}(t, \vec{x})$ while its normalizable mode gives the vacuum expectation value of $\mathcal{O}(t, \vec{x})$. The situation is less clear when the boundary gauge theory is non-commutative. This is partly due to the fact that in non-commutative gauge theories, non-commutativity of the space mixes with the gauge transformations and, as such, there are no gauge invariant operators in position space. In momentum space, however, one can construct gauge invariant operators $\mathcal{O}(k^\mu)$ by smearing the gauge covariant operators $\mathcal{O}(x^\mu)$ transforming in the adjoint over an open Wilson line $W(x, C)$ of definite size according to [98, 74, 54]

$$\mathcal{O}(k) = \int d^4x \mathcal{O}(x) \star W(x, C) \star e^{ik \cdot x}, \quad (2.28)$$

where \star denotes the Moyal product. The expression in (2.28) reduces to the corresponding ordinary gauge invariant local operators in the IR. In the UV, on the other hand, this very simple modification, has a drastic consequence for the behavior of the correlation functions of the gauge invariant operators $\mathcal{O}(k)$.

In the following we assume that the bulk fluctuation $\varphi(u; \omega, \vec{k})$ is dual to a gauge invariant operator $\mathcal{O}(\omega, \vec{k})$ of the form (2.28) in the sense that in

the boundary non-commutative gauge theory there exists a coupling of the following form in the momentum space,

$$\int d\omega d^3k \varphi_0(-\omega, -\vec{k}) \mathcal{O}(\omega, \vec{k}), \quad (2.29)$$

where $\varphi_0(\omega, \vec{k})$ is the source term which is determined from the asymptotic non-normalizable behavior of $\varphi(u, \omega, \vec{k})$ given some suitable boundary condition near the horizon.

To obtain the retarded Green's function of the dual operator $\mathcal{O}(\omega, k)$, equation (2.27) should then be solved with infalling boundary condition at the horizon [155]. Close to the horizon, the solution behaves as

$$\varphi(u) \sim f(u)^{\pm i\omega/(4\pi T)}, \quad u \rightarrow u_h, \quad (2.30)$$

where the $+$ and $-$ signs represent outgoing and infalling waves, respectively. So, we discard the solution with the $+$ sign. Near the boundary $u = \Lambda \rightarrow \infty$, the equation (2.27) can be conveniently cast into a Mathieu differential equation. The asymptotic behavior of the solution then takes the form

$$\varphi(u) \sim A(\omega, k) u^{-5/2} e^{ka^2 u} + B(\omega, k) u^{-5/2} e^{-ka^2 u}. \quad (2.31)$$

The first term in the above equation blows up as the cutoff $\Lambda \rightarrow \infty$. So, in the spirit of the AdS/CFT correspondence, the source for the operator dual to φ in the boundary theory should be read off from that term. However, extracting the source of the dual operator from (2.31) is ambiguous. The ambiguity arises because, as seen from (2.31), for any cutoff Λ the relation

between the would-be source $A(\omega, k)$ and the asymptotic behavior of φ involves a function of k , namely $e^{ka^2\Lambda}$. As a result, the normalization of the dual operator, and hence the normalization of the correlation functions, in the boundary theory is not fixed⁵. This feature, which also arises in [2, 128], can ultimately be attributed to the non-local nature of the boundary theory in the UV. As advocated in [123] (see also [53]), a reasonable way forward is to define the source for the dual operator from the asymptotic behavior of the bulk fluctuation in such a way that the correlation functions of the operator reproduce the ordinary commutative results in the IR. Nevertheless, regardless of how the normalization of the boundary theory operator is fixed, the ratios of the correlation functions are unambiguous [123, 74]. Also, note that the overall k -dependent normalization should not affect the poles (in the complex frequency plane) of the retarded Green's function of the dual operator.

In order to find the poles in the retarded Green's function of the dual operator $\mathcal{O}(\omega, k)$, we numerically solve (2.27) with infalling boundary condition near the horizon and normalizable boundary condition near the boundary⁶. In other words, we compute the quasi-normal frequencies of φ in the non-extremal

⁵This is in contrast to the usual examples in the AdS/CFT correspondence where the background is asymptotically AdS and the relation between the asymptotic behavior of a bulk fluctuation and the source of the corresponding dual operator does not depend on k . Indeed, such a relation is fixed by the conformal symmetry of the boundary theory.

⁶The normalizable boundary condition near the boundary seems to be a natural choice given that the potential term in equation (2.27), once written in the form of a Schrödinger equation, blows up near the boundary, see the equation (A.2) in the appendix. This is similar to the case where the background is asymptotically AdS where the potential term in the equation of motion for a minimally-coupled scalar also blows up at the boundary of the spacetime.

background (2.22). To proceed, we find it convenient to define a new radial coordinate $z = u_h/u$. In terms of this new radial coordinate, the horizon is now at $z = 1$ while $z \rightarrow 0$ is the asymptotic boundary of the spacetime. Using the relation $u_h = \pi T$ with T being the Hawking temperature of the background, the equation of motion (2.27), expressed in terms of the new radial coordinate, takes the form

$$0 = f(z)z^2\varphi''(z) + [zf'(z) - 3f(z)]z\varphi'(z) + \frac{z^2}{\pi^2 T^2} \left[\frac{\omega^2}{f(z)} - \frac{k^2}{h(z)} \right] \varphi(z), \quad (2.32)$$

where the primes denote derivatives with respect to z . Equation (2.32) has three (real-valued) regular singular points at $z = -1, 1, \infty$ and one irregular singularity at $z = 0$, thus we must proceed with some care. To numerically compute the quasi-normal frequencies, we employ a method first developed in [115]. That is, we pull out from φ its infalling behavior near the horizon as well as its leading normalizable behavior near the boundary and define a new function $\tilde{\varphi}$ according to

$$\varphi(z; \omega, k) = f(z)^{-i\omega/(4\pi T)} z^{5/2} e^{-\pi k a^2 T/z} \tilde{\varphi}(z; \omega, k). \quad (2.33)$$

The equation for $\tilde{\varphi}$, obtained from (2.32), does not have any singular points in the interval $z \in [1, 0]$. Hence, we can approximate $\tilde{\varphi}$ in that interval by a series expansion, with M terms in it, around a point inside the interval, say $z_0 = 1/2$ (so that the radius of convergence of the series covers the two endpoints of the interval):

$$\tilde{\varphi}(z; \omega, k) = \sum_{m=0}^M a_m(\omega, k) \left(z - \frac{1}{2} \right)^m. \quad (2.34)$$

The equation for $\tilde{\varphi}$ can then be cast in the following form

$$\sum_{m=0}^M A_{mn}(\omega, k) a_n(\omega, k) = 0, \quad (2.35)$$

which is a matrix equation describing $M + 1$ linear equations for $M + 1$ unknowns $a_n(\omega, k)$. For any fixed k , the quasi-normal frequencies, denoted by ω_n , are then obtained by solving the following polynomial equation in ω :

$$\det A_{mn}(\omega, k) = 0. \quad (2.36)$$

As we increase the size of the matrix A defined above, the poles are found to move around in the complex frequency plane slightly. However, depending on the desired precision, they converge for a large but finite value of M . For concreteness, we ran all our computations with $M = 300$, for which we found a confidence level up to fourteen significant digits for the imaginary part of the first mode.

Now, since the boundary field theory under consideration is non-commutative, there is another scale in the problem besides the temperature, namely, the length scale $\sqrt{\theta}$ (or rather $\lambda^{1/4}\sqrt{\theta}$ for our strong coupling setting). As such, the poles in the retarded Green's function of the operator $\mathcal{O}(\omega, k)$, or equivalently, the quasi-normal frequencies of the dual bulk fluctuation, depend on k , T and $1/\sqrt{\theta}$ and can be conveniently parametrized as

$$\omega_n(k, T, \theta) = T f_n\left(\frac{k}{T}, T\sqrt{\theta}\right). \quad (2.37)$$

The index $n \geq 0$ which is sometime referred to as overtone number denotes the number of poles. For instance, $n = 0$ is assigned to the pole with the smallest

magnitude. Aside from special regions in the parameter space of k/T and $T\sqrt{\theta}$, where one can determine the functions f_n semi-analytically, f_n s should, in general, be determined numerically. As we alluded to earlier, one expects the deviations from the commutative results to be more pronounced in the region of parameter space with $T \gg \theta^{-1/2}$ and $k \gg T^{-1}$ which also implies $k \gg \theta^{-1/2}$. As we demonstrate below, this expectation is confirmed in our numerical computations.

The plots (a), (b) and (c) in Figure 2.1 show, respectively, the location of the first few quasi-normal frequencies for $k = \pi T/10$, $k = \pi T$ and $k = 10\pi T$ for a fixed value of $\pi a T = 1$. The red dots show the location of the quasi-normal frequencies of φ on the non-extremal background (2.22) while the black dots represent the quasi-normal frequencies of φ on the AdS_5 Schwarzschild background. Note that even in the presence of a non-zero non-commutativity parameter, the poles are all located in the lower half of the complex frequency plane. Indeed, one can easily show that regardless of the range of parameters no poles will move to the upper half plane, indicating the stability of the system. See the appendix for a proof.

Focusing on the dominant quasi-normal frequency (the one with the largest imaginary part), Figure 2.2 shows the imaginary part of ω/T as a function k/T , with $T\sqrt{\theta}$ held fixed, for that mode for both non-commutative and commutative cases. We have also plotted the behavior of its imaginary part versus temperature for $k = 5/100$, $k = 1$ and $k = 10$ (in units of a^{-1}) where we have fixed $a = \lambda^{1/4}\sqrt{\theta} = 1$. Those results are shown in Figure 2.3.

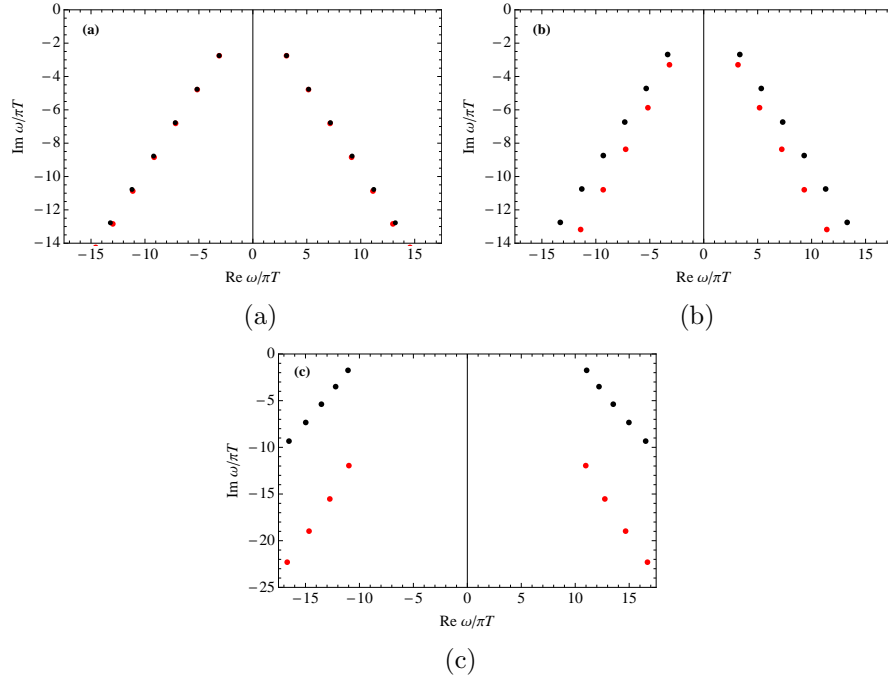


Figure 2.1: Quasi-normal modes of a minimally-coupled massless scalar. The red and black dots show, respectively, the location in the complex frequency plane of the first few quasi-normal frequencies of the scalar on the non-extremal background (2.22) and the AdS_5 Schwarzschild background for (a) $k = \pi T/10$, (b) $k = \pi T$ and (c) $k = 10\pi T$, where we have kept fixed $\pi a T = 1$. The plots have been generated with $M = 300$.

In each plot, the red curve shows the non-commutative result while the black curve shows the commutative result ($\theta = 0$) for the same value of momentum k . Fitting those curves with a simple power law $\text{Im } \omega_0 = -\alpha T^\gamma$ in the regime of $T\sqrt{\theta} \gg 1$, we obtain the results reported in the Table I.

From our numerical results above one can then conclude that in the regime of parameters with both $T\sqrt{\theta} \gg 1$ and $k\sqrt{\theta} \gg 1$, the decay rate of a mode with momentum k into the non-commutative bath is parametrically faster compared to the decay of the same mode into an ordinary commutative

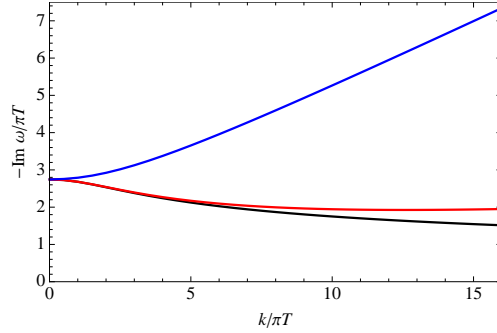


Figure 2.2: Imaginary part of ω/T as a function of k/T . The behavior of the (negative of the) imaginary part of ω/T as a function of k/T for the dominant quasi-normal frequency in the commutative case ($\theta = 0$) shown by the black curve, and in the non-commutative cases with $\pi aT = 1/5$ and $\pi aT = 3/5$ which are shown by the red and blue curves, respectively.

Commutative			Non-commutative	
k	α	γ	α	γ
0.05	5.941	1.318	8.629	1.000
1.00	13.398	1.910	8.623	1.000
10.00	103.64	1.986	8.623	1.000

Table 2.1: Fits of the form $\text{Im } \omega = -\alpha T^\gamma$ for the curves shown in Figure 2.3 in the regime of $T\sqrt{\theta} \gg 1$.

bath. In the regime of high temperatures (as compared to $\theta^{-1/2}$), the non-local effects in non-commutative thermal baths are due to the large transverse size of the typical modes in the bath. These modes provide for a rapid dissipation of the high energy modes injected into the non-commutative bath. In the case of a black hole or deSitter space, the event horizon appears to an observer who is hovering outside the horizon increasingly hotter as the observer gets closer to the horizon. Our analysis does show that at increasingly higher temperatures the rate of dissipation increases parametrically much faster in the non-commutative case. This appears consistent with the fast scrambling

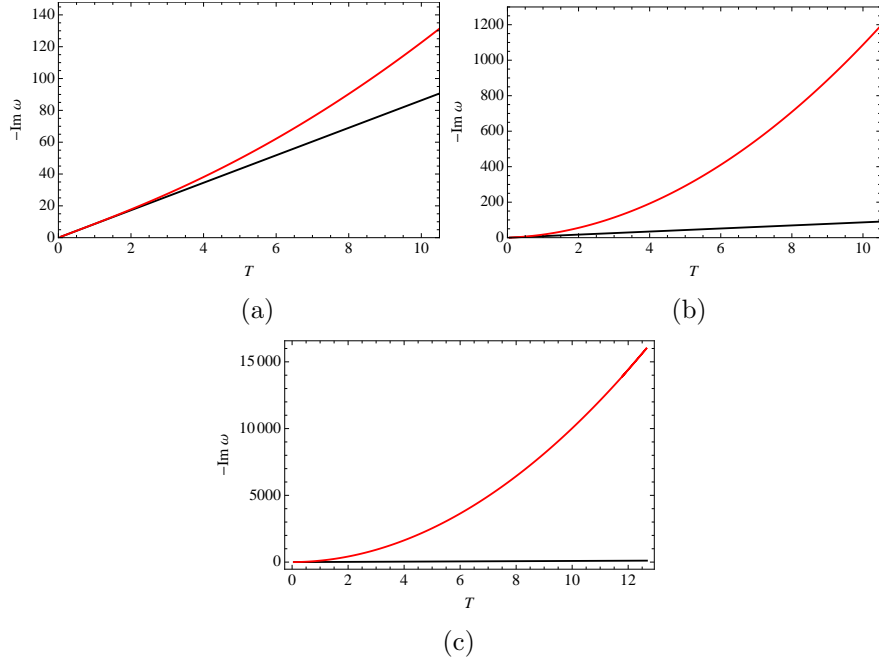


Figure 2.3: Imaginary part of the dominant quasi-normal frequency as a function of T .

The behavior of the (negative of the) imaginary part of the dominant quasi-normal frequency as a function of temperature for $k = 5/100$ (a), $k = 1$ (b) and $k = 10$ (c) in units of $1/\sqrt{\theta}$. The red curves show the behavior for the non-commutative boundary theory while the black curves show the behavior of the same mode in the commutative theory ($\theta = 0$).

property of horizons.

2.3.2 Dilaton and Axion Fluctuations

Similar to our analysis in the previous section, we consider in this section the fluctuations of the dilaton and the axion in the background (2.22) and analyze the approach to thermalization of the boundary non-commutative bath when it gets perturbed by their dual operators.

To start, consider the bosonic part of the action for type IIB super-

gravity. In the Einstein frame, $ds_E^2 = \sqrt{\hat{g}} e^{-\Phi/2} ds_{\text{str}}^2$, we can write it as

$$S = \frac{1}{2\kappa^2} \int d^{10}x \sqrt{-g} \mathcal{R} - \frac{1}{4\kappa^2} \int \left(d\Phi \wedge *d\Phi + e^{2\Phi} dC \wedge *dC \right. \\ \left. + \hat{g} e^{-\Phi} H_3 \wedge *H_3 + \hat{g} e^{\Phi} \tilde{F}_3 \wedge *\tilde{F}_3 + \frac{1}{2} \hat{g}^2 \tilde{F}_5 \wedge *\tilde{F}_5 + \hat{g}^2 C_4 \wedge H_3 \wedge F_3 \right), \quad (2.38)$$

where

$$\begin{aligned} \tilde{F}_3 &= F_3 - C H_3, & F_3 &= dC_2, \\ \tilde{F}_5 &= F_5 - C_2 \wedge H_3, & F_5 &= dC_4. \end{aligned} \quad (2.39)$$

The type IIB equations of motion can be deduced from (2.38), supplemented by the self-duality condition

$$*\tilde{F}_5 = \tilde{F}_5. \quad (2.40)$$

In particular, the background (2.22) is a solution to the equations of motion obtained from the above action.

We now proceed by considering the fluctuations of the dilaton and axion around the background (2.22). As we alluded to earlier, whereas there are no dual gauge invariant local operators in position space, it is possible to write down the linearized coupling of a supergravity field to the noncommutative Yang-Mills modes in momentum space as shown in (2.29), with $\mathcal{O}(k)$ being a gauge invariant operator of the type given in (2.28) (see, for example, [118, 119, 55]). For the dilaton and the axion, we can think of these operators as the non-commutative gauge invariant generalizations of $\text{Tr } F^2$ and $\text{Tr } F\tilde{F}$, respectively.

The equations of motion that result from the above action for the dilaton Φ and the axion C are [147]

$$\begin{aligned}\nabla^2\Phi &= e^{2\Phi}\partial_\mu C\partial^\mu C - \frac{\hat{g}e^{-\Phi}}{12}H_{\mu\nu\rho}H^{\mu\nu\rho} + \frac{\hat{g}e^\Phi}{12}\tilde{F}_{\mu\nu\rho}\tilde{F}^{\mu\nu\rho}, \\ \nabla^\mu(e^{2\Phi}\partial_\mu C) &= \frac{\hat{g}e^\Phi}{6}H_{\mu\nu\rho}\tilde{F}^{\mu\nu\rho},\end{aligned}\tag{2.41}$$

where it is understood that the indices μ, ν, \dots run in ten dimensions.

Now, considering small perturbations as defined by $\Phi = \Phi_0 + \phi$ and $C = C_0 + \chi$, where Φ_0 and $C_0 = 0$ are the background values given in (2.22), we get the following differential equations in momentum space (after linearizing):

$$\begin{aligned}0 &= f(z)z^2\phi''(z) + [zf'(z) - 3f(z)]z\phi'(z) + \frac{f(z)z^2}{\pi^2T^2}\left[\frac{\omega^2}{f(z)^2} - \frac{k^2}{f(z)h(z)}\right. \\ &\quad + \frac{16\pi^6T^6\theta^2}{z^6f(z)}(1 + 2h(z)) + \frac{h'(z)^2}{h(z)^2}\left(\frac{\pi^6T^6\theta^2}{z^4} - \frac{\pi^2T^2}{2}\right) + \frac{h''(z)}{2h(z)} \\ &\quad \left. + \frac{f'(z)h'(z)}{2f(z)h(z)} - \frac{4h'(z)}{h(z)}\left(\frac{2\pi^6T^6\theta^2}{z^5} + \frac{\pi^2T^2}{z}\right)\right]\phi(z),\end{aligned}\tag{2.42}$$

and

$$\begin{aligned}0 &= f(z)z^2\chi''(z) + \left[zf'(z) + \frac{zh'(z)f(z)}{h(z)} - 3f(z)\right]z\chi'(z) \\ &\quad + \frac{z^2}{\pi^2T^2}\left[\frac{\omega^2}{f(z)} - \frac{k^2}{h(z)}\right]\chi(z),\end{aligned}\tag{2.43}$$

where, as before, we defined $z \equiv u_h/u$ and $k \equiv k_3$.

Close to the horizon, the solutions to both equations behave as

$$\phi, \chi \sim f(z)^{\pm i\omega/(4\pi T)},\tag{2.44}$$

where the $+$ and $-$ signs represent outgoing and ingoing waves, respectively. Thus, we discard the solutions with the $+$ sign. Near the boundary, and for non-vanishing momentum, the solutions take the form

$$\phi, \chi \sim A(\omega, k) z^\lambda e^{k\theta \pi T/z} + B(\omega, k) z^\lambda e^{-k\theta \pi T/z}, \quad (2.45)$$

where $\lambda = 13/2$ for the dilaton and $\lambda = 1/2$ for the axion. Notice that their asymptotic behavior is similar to that of a minimally-coupled scalar field as given in (2.31), although with a different characteristic exponent for z . The first term above blows up near the boundary so we take it to be proportional to the source for the boundary theory dual operator. Equations (2.42) and (2.43) have also three real-valued regular singular points at $z = -1, 1, \infty$ and one irregular singularity at $z = 0$ ⁷. The quasi-normal frequencies of the dilaton and axion fluctuations in the background (2.22) can be computed using the same method we employed in the previous section for the case of a minimally-coupled massless scalar field.

In Figure 2.4 we plotted the behavior of the imaginary part of the dominant quasi-normal frequency as a function of the temperature for $k = 5/100$, $k = 1$ and $k = 10$ (in units of a^{-1}) where we fixed $a = \lambda^{1/4} \sqrt{\theta} = 1$. In each plot, the blue curve shows the result for the dilaton fluctuation while the purple one corresponds to the axion fluctuation. For comparison purposes, we also plotted the commutative result ($\theta = 0$) in black which is same result as

⁷For $k = 0$ the point $z = 0$ is regular in both cases. We do not consider this case here.

for the minimally-coupled massless scalar field in the commutative case⁸. In this case, the results for the best fits are given in the Table II.

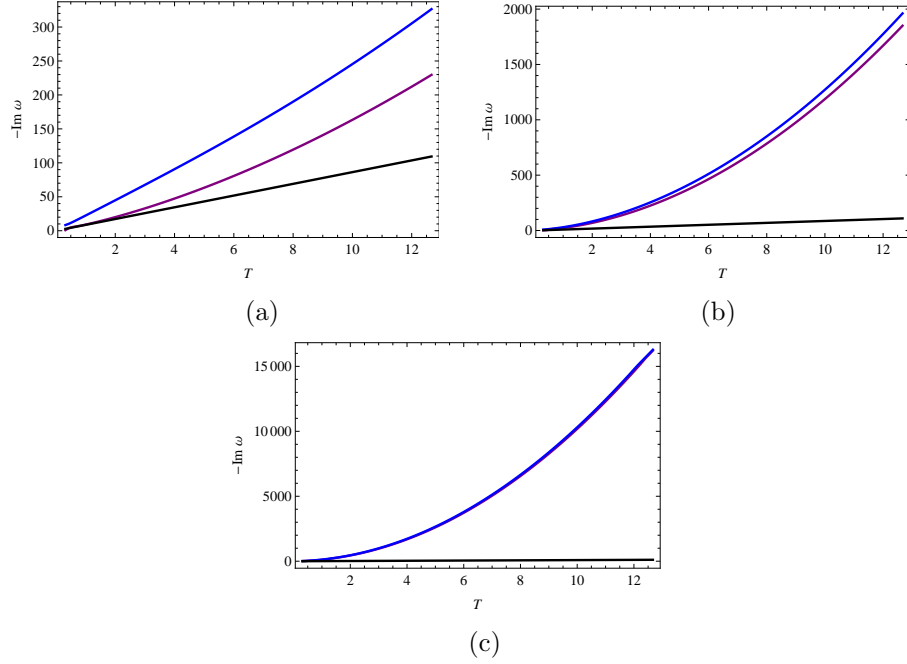


Figure 2.4: Imaginary part of the dominant quasi-normal frequency as a function of T for dilaton and axion.

The behavior of the (negative of the) imaginary part of the dominant quasi-normal frequency as a function of temperature for $k = 5/100$ (a), $k = 1$ (b) and $k = 10$ (c) in units of $1/\sqrt{\theta}$. The blue curves show the behavior for the dilaton fluctuation whereas the purple ones represent the axion fluctuation. For completeness we are also plotting in black the behavior of the same mode for the commutative case. Each point on the plot has been generated with $M = 300$.

These results support the main conclusion found in the previous section: in the regimes at which non-local effects become important, *i.e.* $T \gg \theta^{-1/2}$ and $k \gg \theta^{-1/2}$, the decay rate of a mode with momentum k into the non-

⁸This is because when the background is AdS (Schwarzschild black hole), the equations of motion for the dilaton, the axion and a minimally-coupled massless scalar are all the same.

Dilaton			Axion	
k	α	γ	α	γ
0.05	19.188	1.1094	6.9056	1.3758
1.00	20.691	1.7903	17.047	1.8442
10.00	114.31	1.9552	109.14	1.9703

Table 2.2: Fits of the form $\text{Im } \omega = -\alpha T^\gamma$ for the blue and purple curves shown in Figure 2.4 in the regime of $T \gg \theta^{-1/2}$.

commutative bath is significantly faster in comparison to the decay of the same mode into an ordinary commutative bath.

It is interesting to note that in the regime where $k \gg \theta^{-1/2}$ the behavior of the leading dominant pole (as a function of temperature) is almost the same for the dilaton, the axion, and the minimally-coupled massless scalar field, which leads to a “universal” thermalization time in the UV. This behavior could be attributed to the presence of the open Wilson lines in the definition of the gauge invariant operators in non-commutative gauge theories which, as a result, dominate the UV behavior of the two (and higher) point functions of the gauge invariant operators [74].

2.4 Discussion

In this chapter we showed that strongly coupled non-commutative gauge theories display at high temperature, a fast dissipation rate not seen in local field theory. At the core of this result is the UV-IR connection embodied in the large transverse size of high momenta mode. In order to assess how crucial the strong coupling ingredient is, it is useful to compare the behavior at

high temperature in the weakly coupled regime. An example suggestive of this weakly coupled regime can be found in [36]. Although the model studied there is not a gauge theory, the leading perturbative contributions are similar to the ones found in gauge theories and therefore can be considered exemplary of the behavior at weak coupling. In that work, the authors computed the decay rate of a disturbance of the heat bath and found that the planar contributions to the thermalization rate are always larger than or equal to the contributions from the non-planar diagrams⁹. In Figure (2.5) we show an example of such behavior for $k = 10$ in $1/\sqrt{\theta}$ units and small frequency ω . It is clear from the figure that the enhancement of the thermalization rates found here in strongly coupled non-commutative baths is not present in the corresponding weakly coupled theories.

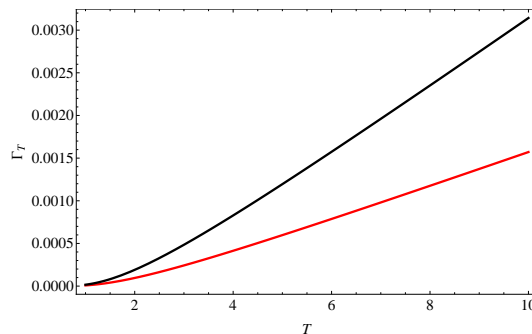


Figure 2.5: Comparison of the thermalization rates for the commutative (black) and noncommutative (red) cases at weak coupling.

It seems, then, that strong coupling is necessary to have faster thermal-

⁹Planar diagrams are the same as in ordinary field theory. Non-planar diagrams have an extra factor that depends on the Moyal tensor $e^{-\frac{i}{2} p_\mu \theta^{\mu\nu} q_\nu}$. For a review of non-commutative quantum field theories, see [127, 60].

ization together with the non-locality inherent of non-commutative theories. We conclude that this provides an important ingredient for the study of fast scramblers. Indeed, there have been studies of the fast scrambling conjecture in the framework of Matrix theory [149, 159, 11], which is known to be related to non-commutative theories [17, 51]. As a final remark, it would be interesting to investigate the decay rates in other non-local theories such as the theory dual to the near horizon limit of a stack of NS5-branes [2], the so-called little string theory, and compare the results with the findings in this work.

Chapter 3

Holographic Brownian Motion in Magnetic Environments

3.1 Preliminaries

In the previous chapter, we introduced the description of non-commutative theories from the point of view of the gravitational background in the context of the gauge/gravity duality. We reviewed how thermal non-commutative field theories emerge in string theory, as the worldvolume theory of D-branes with a constant Neveu-Schwarz B -field provided that one takes a special limit to decouple the open and closed string sectors [59, 10, 148]. In this chapter we continue considering this type of backgrounds to study the dynamics a heavy particle that undergoes Brownian motion.

Various thermal properties of strongly coupled plasmas have been inferred by considering various types of partonic probes and analyzing the way in which the plasma damps their motion. These studies include quarks [90, 75, 39], mesons [137, 120, 48], baryons [46, 110], gluons [46, 77] k-quarks [46] and various types of defects [100]. Although all these probes provide different information regarding the nature of the plasma, here we focus on the dynamics of heavy quarks and their interactions with the thermal bath.

In the context of AdS/CFT, a heavy quark on the boundary theory corresponds to the endpoint of an open string that, at finite temperature, stretches between the boundary and the black hole horizon. The seminal works [90, 75] focused on the energy loss of a quark that is either moving with constant velocity as a result of being pulled by an external force, or is unforced but moving non-relativistically and about to come to rest. Further analyses [76, 40, 47] made it clear that this mechanism of energy loss is closely related with the appearance of a world sheet horizon (not to be confused with the spacetime horizon).

The study of quark fluctuations due to its interaction with the thermal bath involves going beyond the classical description of the string. As customary, small perturbations about the average embedding are described by free scalar fields propagating on the corresponding induced world sheet geometry. These fields can be excited due to Hawking radiation emitted by the world sheet horizon, which in turn populates the various modes of oscillation of the string. It was then found that, once these modes are quantized, the induced motion of the string endpoint is correctly described in terms of Brownian motion and its associated Langevin equation [26, 157]. This result was obtained by two different approaches: the authors of [26] reached this conclusion by assuming (following [114, 69]) that the state of the quantized fields is the usual Hartle-Hawking vacuum, which describes the black hole in equilibrium with its own thermal radiation. The authors of [157] followed a different but equivalent route, employing the relation between the Kruskal

extension of the Schwarzschild-AdS geometry and the Schwinger-Keldysh formalism [122, 91], together with the known connection between the latter and the generalized Langevin equation. These calculations were later elaborated on in [71, 37, 13, 30, 61, 36].

In this chapter, we generalize the original computation of [26] to the case of non-commutative Super-Yang-Mills (NCSYM). Non-commutative theories are known to lead to many qualitatively new phenomena, both classically and quantum mechanically; in particular, the existence of non-local interactions reminiscent of the UV/IR mixing found in string theory[125].

One of the main motivations to study Brownian motion in the presence of non-commutativity is the idea that non-local interactions might lead to significant deviations in the behavior of the thermal properties of the theory [66, 65]. In Chapter 2 and [62] for instance, it was found that the rate of decay of a fluctuation propagating in this thermal bath is remarkably larger than in the case of ordinary SYM, which leads to faster thermalization. Such a property is possibly linked to the connection between the ultraviolet and infrared regimes of the theory, which implies in particular that the transverse size of dipoles grows with their longitudinal momentum [23]. In order to investigate further properties of this non-commutative system, we study in this chapter the holographic realization the Brownian motion of a heavy quark. More specifically, our aim is to formulate a Langevin equation that accounts for the effects of non-commutativity and to study diffusion processes within the plasma.

In section 3.3 of this chapter, we study the case of Brownian motion in ordinary SYM with a magnetic field, which is achieved by the introduction of a gauge field in the open string sector¹. Apart from being an interesting problem in its own right², this exercise helps us to gain some intuition and to set the grounds of our computations. In section 3.4 we turn to the study of Brownian motion in NCSYM. We begin by postulating a Langevin equation for the non-commutative plasma similarly to the one describing the quark in the presence of a magnetic field. We show that this equation correctly captures behavior of Brownian particle. This equation is expressed naturally in terms of matrices and given its structure, it automatically implies that fluctuations along different directions are correlated. We then compute holographically the drag coefficient from the response of the Brownian particle to an external force and, finally, we study the diffusion process of the quark within the plasma, which turns out to be unaffected by non-commutativity.

3.2 Heavy quarks in a magnetic environment and holographic Brownian motion

From the gauge theory perspective, the introduction of an open string sector associated with a stack of N_f D7-branes in the geometry (2.22) is equiv-

¹Here, we should emphasize that we do not expect to recover the non-commutative results in the strong B limit. On one hand, there is a critical magnetic field at which Schwinger pair production is energetically favored [27]. On the other hand, for large magnetic fields the backreaction on the geometry is unsuppressed.

²Indeed, many holographic systems present interesting features when a background magnetic field is turned on. For a recent review on this topic see [20].

alent to the addition of N_f hypermultiplets in the fundamental representation of the gauge group $SU(N)$, and these are the degrees of freedom that we will refer to as quarks. For $N_f \ll N$, we can neglect the backreaction of the D7-branes on the geometry; in the gauge theory perspective, this corresponds to working in a “quenched” approximation that ignores quark loops. For simplicity, we will take $N_f = 1$. The probe brane covers the four gauge theory directions x^μ , and is spread along the radial direction from $u \rightarrow \infty$ to $u = u_m$ where it ends smoothly³.

An isolated quark is dual to an open string that extends radially from the flavor brane at $u = u_m$ to the horizon at $u = u_h$ ⁴. The string couples to both the metric and the B -field so its dynamics follows from the action $S = S_{\text{NG}} + S_{\text{B}}$,⁵

$$S \equiv \int_{\Sigma} d\tau d\sigma \mathcal{L} = \frac{1}{2\pi\alpha'} \int_{\Sigma} d\tau d\sigma \left(\sqrt{-\det g_{ab}} + B_{mn} \partial_{\tau} X^m \partial_{\sigma} X^n \right) \quad (3.1)$$

where $g_{ab} = G_{mn} \partial_a X^m \partial_b X^n$ is the induced metric on the worldsheet Σ . We choose to work in the static gauge, where $\tau = t$, $\sigma = u$. One can easily verify that the embedding $X^m = (t, 0, 0, 0, u)$ is a trivial solution and this correspond to a quark that is in equilibrium in the thermal bath.

Notice that the string is being described in first-quantized language and, as long as it is sufficiently heavy, we are allowed to treat it semiclassically. In

³At this position the $S^3 \subset S^5$ that it is wrapped on shrinks down to zero size.

⁴For a review of quark dynamics in the context of the gauge/gravity correspondence see [49].

⁵The string also couples to the dilaton but this coupling is suppressed by a factor of the string length.

gauge theory language, we are coupling a first-quantized quark to the SYM fields, and then carrying out the full path integral over the strongly-coupled fields, treating the path integral over the quark trajectory in a saddle-point approximation. The mass of the quark m is related to the position of the flavor brane u_m and can be obtained by a straightforward computation:

$$m = \frac{1}{2\pi\alpha'} \int_{u_h}^{u_m} du \sqrt{g_{tt} g_{uu}} = \frac{R^2}{2\pi} (u_m - u_h) \approx \frac{R^2}{2\pi} u_m, \quad \text{for } u_m \gg u_h. \quad (3.2)$$

Now, we want to study fluctuations over the above embedding. In particular, we are interested in motion on the Moyal plane, so our ansatz for the perturbations will be $X^m = (t, 0, X_2(t, u), X_3(t, u), u)$. Using this, the induced metric has the following components:

$$g_{tt} = \alpha' R^2 u^2 \left[-f + h \left(\dot{X}_2^2 + \dot{X}_3^2 \right) \right], \quad (3.3)$$

$$g_{uu} = \alpha' R^2 u^2 \left[h \left(X_2'^2 + X_3'^2 \right) + \frac{1}{u^4 f} \right], \quad (3.4)$$

$$g_{tu} = \alpha' R^2 u^2 h \left(\dot{X}_2 X_2' + \dot{X}_3 X_3' \right), \quad (3.5)$$

where $\dot{X}_i \equiv \partial_t X_i$ and $X_i' \equiv \partial_u X_i$. Up to quadratic order in the perturbations, the action can be written as

$$S \approx \frac{R^2}{4\pi} \int dt du \left[u^4 f h \left(X_2'^2 + X_3'^2 \right) - \frac{h}{f} \left(\dot{X}_2^2 + \dot{X}_3^2 \right) + 2a^2 u^4 h \left(\dot{X}_2 X_3' - \dot{X}_3 X_2' \right) \right]. \quad (3.6)$$

Note that we dropped the constant term that does not depend on X_i . We can consider also the situation in which one has a forced motion due to a

electromagnetic field in the background. This can be easily realized by turning on a world-volume $U(1)$ gauge field on the flavor brane. Since the endpoint of the string is charged, this amounts to add the minimal coupling to the action $S = S_{\text{NG}} + S_{\text{B}} + S_{\text{EM}}$, where

$$S_{\text{EM}} = \int_{\partial\Sigma} \left(A_t + A_i \dot{X}_i \right) dt, \quad (3.7)$$

This will exert the desired force on our heavy quark. However, this coupling is just a boundary term, so it will not play any role for the string dynamics in the bulk, other than modify the boundary condition. We shall ignore this part of the action for now but we will come back to it later on.

Because t is an isometry of the background (2.22), we can set

$$X(t, u) \sim e^{-i\omega t} g_\omega(u) \quad (3.8)$$

and use the frequency ω to label the basis of solutions to the equations of motion. Since the action (3.6) is quadratic in the perturbations, we expect linear differential equations. The solutions are particularly easy to obtain near the horizon limit $u \sim u_h$, where the action reduces to

$$\begin{aligned} S &\approx u_h^2 h(u_h) \frac{R^2}{4\pi} \int dt du_* \left[(X_2'^2 + X_3'^2) - (\dot{X}_2^2 + \dot{X}_3^2) \right. \\ &\quad \left. + 2a^2 u_h^2 (\dot{X}_2 X_3' - \dot{X}_3 X_2') \right] \\ &\approx u_h^2 h(u_h) \frac{R^2}{4\pi} \int dt du_* \left[(X_2'^2 + X_3'^2) - (\dot{X}_2^2 + \dot{X}_3^2) \right]. \end{aligned} \quad (3.9)$$

Here, the primes denote derivatives with respect to the tortoise coordinate u_* , which is defined by

$$du_* = \frac{du}{u^2 f(u)}. \quad (3.10)$$

Note also that the last term drops out because it is a total derivative. Thus, the equations of motion are then

$$(\partial_{u_*}^2 - \partial_t^2)X_i = 0, \quad (3.11)$$

which show that in this region X_i behave like massless Klein-Gordon scalars in flat space. The two independent solutions are

$$X_i^{(\text{out})}(u) = e^{-i\omega t} g_i^{(\text{out})}(u) \sim e^{-i\omega(t-u_*)} \quad (3.12)$$

and

$$X_i^{(\text{in})}(u) = e^{-i\omega t} g_i^{(\text{in})}(u) \sim e^{-i\omega(t+u_*)}, \quad (3.13)$$

corresponding to outgoing and ingoing waves respectively. Near the horizon one finds that

$$u_* \sim \frac{1}{4u_h} \log \left(\frac{u - u_h}{u_h} \right) \quad (3.14)$$

up to an additive numerical constant, so

$$g^{(\text{out/in})}(u) \sim \left(\frac{u}{u_h} - 1 \right)^{\pm i\omega/4u_h}. \quad (3.15)$$

Away from the horizon, these solutions will have a complicate dependence, but it still holds that $g^{(\text{out})} = g^{(\text{in})*}$ (see appendix B.1).

Standard quantization of quantum fields in curved spacetime [25] leads to a mode expansion of the form

$$X_i(t, u) = \int_0^\infty \frac{d\omega}{2\pi} [a_\omega u_\omega(t, u) + a_\omega^\dagger u_\omega(t, u)^*], \quad (3.16)$$

where the functions $u_\omega(x)$ correspond to a basis with positive-frequency modes. These modes can be expressed as a linear combination of outgoing and ingoing waves with arbitrary coefficients, i.e.,

$$u_\omega(t, u) = A [g^{(\text{out})}(u) + B g^{(\text{in})}(u)] e^{-i\omega t}. \quad (3.17)$$

The constant B is fixed through the boundary condition at $u = u_m$ but one generally obtains that it is a pure phase $B = e^{i\theta}$ (see sections 3.3.3 and 3.3.3). The outgoing and ingoing modes have, then, the same amplitude and this implies that the black hole, which emit Hawking radiation, can be in thermal equilibrium [89]. The constant A on the other hand, is obtained by requiring the normalization of the modes through the standard Klein-Gordon inner product.

For any functions $f_i(t, u)$ and $g_j(t, u)$ satisfying the equations of motion, the Klein-Gordon inner product is defined by

$$(f_i, g_j)_\sigma = -\frac{i}{2\pi\alpha'} \int_\sigma \sqrt{\tilde{g}} n^\mu G_{ij} (f_i \partial_\mu g_j^* - \partial_\mu f_i g_j^*), \quad (3.18)$$

where σ is a Cauchy surface in the (t, u) part of the metric, \tilde{g} is the induced metric on σ and n^μ is the future-pointing unit normal to σ . It can be shown that this inner product is independent of the choice of σ [25], but for simplicity we take it as a constant- t surface.

We want to normalize u_ω using (3.18). However the main contribution to the integral comes from the IR region [13], which in terms of the tortoise coordinate is just

$$(f_i, g_j)_\sigma = -i\delta_{ij} \frac{R^2}{2\pi} u_h^2 h(u_h) \int_{u_* \sim -\infty} du_* (f_i \dot{g}_j^* - \dot{f}_i g_j^*). \quad (3.19)$$

Of course, there is a contribution to the inner product from regions away from the horizon, but because the near-horizon region is semi-infinite in the tortoise coordinate u_* , the normalization of solutions is completely determined by this region.

After some algebra, we find that

$$A = \sqrt{\frac{\pi}{\omega R^2 u_h^2 h(u_h)}}, \quad (3.20)$$

so that $(u_\omega, u_\omega) = 1$, ensuring that the canonical commutation relations are satisfied:

$$[a_\omega, a_{\omega'}] = [a_\omega^\dagger, a_{\omega'}^\dagger] = 0, \quad [a_\omega, a_{\omega'}^\dagger] = 2\pi\delta(\omega - \omega'). \quad (3.21)$$

In the semiclassical approximation, the string modes are thermally excited by Hawking radiation emitted by the worldsheet horizon. In particular, they satisfy the Bose-Einstein distribution:

$$\langle a_\omega^\dagger a_{\omega'} \rangle = \frac{2\pi\delta(\omega - \omega')}{e^{\beta\omega} - 1}. \quad (3.22)$$

Using this and the mode expansion given in (3.16), we can derive a general formula for the displacement squared of the Brownian particle.

First of all, let us identify the position of the heavy quark as the string endpoint at the boundary $u = u_m$, i.e.,

$$x_i(t) \equiv X_i(t, u_m) = \int_0^\infty \frac{d\omega}{2\pi} [a_\omega u_\omega(t, u_m) + a_\omega^\dagger u_\omega(t, u_m)^*]. \quad (3.23)$$

Then, it follows that

$$\begin{aligned} \langle x_i(t)x_i(0) \rangle &= \int_0^\infty \frac{d\omega d\omega'}{(2\pi)^2} \left[\langle a_\omega a_{\omega'}^\dagger \rangle u_\omega(t, u_m) u_{\omega'}(0, u_m)^* \right. \\ &\quad \left. + \langle a_\omega^\dagger a_{\omega'} \rangle u_\omega(t, u_m)^* u_{\omega'}(0, u_m) \right]. \end{aligned} \quad (3.24)$$

This has an IR divergence that comes from the zero point energy, which exists even at zero temperature. To avoid this we simply regularize it by implementing the normal ordering $:a_\omega a_\omega^\dagger: \equiv :a_\omega^\dagger a_\omega:$, and after doing so we get⁶

$$\begin{aligned} \langle :x_i(t)x_i(0): \rangle &= \int_0^\infty \frac{d\omega}{2\pi} \frac{1}{e^{\beta\omega} - 1} [u_\omega(t, u_m) u_\omega(0, u_m)^* + u_\omega(t, u_m)^* u_\omega(0, u_m)], \\ &= \int_0^\infty \frac{d\omega}{2\pi} \frac{2|A|^2 \cos(\omega t)}{e^{\beta\omega} - 1} |g^{(\text{out})}(u_m) + B g^{(\text{in})}(u_m)|^2. \end{aligned} \quad (3.25)$$

From this correlator, we can compute the displacement squared of the quark as:

$$\begin{aligned} s_i^2(t) &\equiv \langle :[x_i(t) - x_i(0)]^2: \rangle \\ &= \frac{4}{R^2 u_h^2 h(u_h)} \int_0^\infty \frac{d\omega}{\omega} \frac{\sin^2\left(\frac{\omega t}{2}\right)}{e^{\beta\omega} - 1} |g^{(\text{out})}(u_m) + B g^{(\text{in})}(u_m)|^2, \end{aligned} \quad (3.26)$$

where we have replaced the explicit dependence on A . For future reference we also compute the general form of the momentum correlator,

$$\begin{aligned} \langle :p_i(t)p_i(0): \rangle &= -m^2 \partial_t^2 \langle :x_i(t)x_i(0): \rangle, \\ &= \int_0^\infty \frac{d\omega}{2\pi} \frac{2m^2 \omega^2 |A|^2 \cos(\omega t)}{e^{\beta|\omega|} - 1} |g^{(\text{out})}(u_m) + B g^{(\text{in})}(u_m)|^2. \end{aligned} \quad (3.27)$$

⁶Another way to regularize it is to use the canonical correlator introduced as in [26]. However, this does not change the late-time or low-frequency behavior of the correlator.

3.3 Brownian Motion in SYM with a Magnetic Field

Non-commutative SYM theory has a dual interpretation in terms ordinary SYM with a large and constant magnetic field. We start by studying the Brownian motion in this second system which, aside from being an interesting problem in its own right, helps us to gain some intuition and to set the physical grounds of our computations. Although we find that there are some similarities between these two configurations, our final results show that there are some features that are qualitatively different.

3.3.1 Langevin dynamics in the presence of a magnetic field

The problem of the Brownian motion of a charged particle in an external magnetic field was first investigated almost fifty years ago in the seminal papers [164, 112]. This is an old topic that has originated a lot of interest and it is of great importance in the description of diffusion and transport of plasmas and heavy ions. Nowadays, together with the free Brownian motion, it is widely used as a classic textbook example of how transport properties and correlation functions should be computed in generic situations governed by the Langevin equation.

The discussion of this section will be around the field theory description of Brownian motion in the presence of a magnetic field. Later on, we will show how to realize this phenomenon at strong-coupling, in terms of a probe string living in a black hole background.

Let us consider the Langevin equation of a charged particle of mass m

and unit charge q , in presence of a magnetic field \mathbf{B} :

$$\dot{\mathbf{p}}(t) = -\gamma_o \mathbf{p}(t) + \mathbf{v}(t) \times \mathbf{B} + \mathbf{R}(t), \quad (3.28)$$

where $\mathbf{p}(t) = m \mathbf{v}(t)$ is the momentum of the Brownian particle and $\mathbf{v}(t) = \dot{\mathbf{x}}(t)$ its velocity. The terms in the right-hand side of (3.28) correspond to the friction, lorentz force and random force, respectively, and γ_o is a constant called the friction coefficient. One can think of the particle as moving under the influence of the magnetic field, losing energy to the medium and at the same time, getting random kicks as modeled by the random force.

As a first approximation, we can assume that the random force is white noise, with the following averages:

$$\langle R_i(t) \rangle = 0, \quad \langle R_i(t) R_j(t') \rangle = \kappa_o \delta_{ij} \delta(t - t'), \quad (3.29)$$

and where κ_o is a constant which, due to the fluctuation-dissipation theorem, is related to the friction coefficient through

$$\gamma_o = \frac{\kappa_o}{2mT}. \quad (3.30)$$

This is due to the fact that the frictional and random forces have the same origin at the microscopic level, i.e., collisions with the particles of the thermal bath.

If the magnetic field $\mathbf{B} = B\hat{x}$ is pointing along the x -direction, we can write (3.28) in the matrix form

$$\dot{p}_i(t) = -\Lambda_{ij} p_j(t) + R_i(t), \quad (3.31)$$

where

$$\Lambda_{ij} = \begin{pmatrix} \gamma_o & 0 & 0 \\ 0 & \gamma_o & -\omega_o \\ 0 & \omega_o & \gamma_o \end{pmatrix}. \quad (3.32)$$

Here $\omega_o = B/m$ denotes the Larmor frequency. Since the magnetic field is oriented along the x -direction, it affects the motion in the y and z directions only. Fluctuations along the x -direction decouple and are unaffected by the presence of the magnetic field. We thus restrict our attention to the fluctuations in the transverse plane.

In order to decouple the remaining equations we have to diagonalize the the above matrix. The normal modes are $p_{\pm} = p_2 \pm ip_3$ with corresponding eigenvalues $\lambda_{\pm} = \gamma_o \mp i\omega_o$. Thus, defining $x_{\pm} = x_2 \pm ix_3$ and $R_{\pm} = R_2 \pm iR_3$ we get

$$\dot{p}_{\pm}(t) = -\lambda_{\pm}p_{\pm}(t) + R_{\pm}(t), \quad (3.33)$$

whose formal solution is given by

$$p_{\pm}(t) = e^{-\lambda_{\pm}t}p_{\pm}(0) + \int_0^t e^{-\lambda_{\pm}(t-t')}R_{\pm}(t')dt', \quad (3.34)$$

$$\begin{aligned} x_{\pm}(t) - x_{\pm}(0) = & \frac{1}{m\lambda_{\pm}} \left((1 - e^{-\lambda_{\pm}t})p_{\pm}(0) \right. \\ & \left. + \left[\int_0^t R_{\pm}(t')dt' - \int_0^t e^{-\lambda(t-t')}R_{\pm}(t')dt' \right] \right). \end{aligned} \quad (3.35)$$

Using the above, we can immediately obtain $x_2(t), x_3(t)$ by taking the real and imaginary parts of $x_{\pm}(t)$. $p_2(t)$ and $p_3(t)$ can also be obtained in a similar way. In thermal equilibrium, the two-point correlation functions of

$p_2(t)$ and $p_3(t)$ are given by

$$\langle p_2(t)p_2(0) \rangle = \frac{\kappa_o}{2\gamma_o} e^{-\gamma_o t} \cos(\omega_o t), \quad (3.36)$$

$$\langle p_3(t)p_3(0) \rangle = \langle p_2(t)p_2(t') \rangle, \quad (3.37)$$

$$\langle p_2(t)p_3(0) \rangle = \frac{\kappa_o}{2\gamma_o} e^{-\gamma_o t} \sin(\omega_o t). \quad (3.38)$$

The relevant point here is that, unlike in the case of free Brownian motion, now the components $p_2(t)$ and $p_3(t)$ are correlated. But, the autocorrelator $\langle p_i(t)^2 \rangle$ of each individual component has the same value $\sim \kappa_o/2\gamma_o = mT$ as in the case of zero magnetic field. This can be easily understood by recognizing that $\langle p_i(t)^2 \rangle$ is twice the kinetic energy multiplied by the mass of the particle and that this quantity does not change by application of a magnetic field. Thus, the time scale associated to the energy loss due to drag, $t_{\text{relax}} \sim 1/\gamma_o$, is then independent of the magnetic field.

Another important scale related to the Brownian motion of the quark is the time associated to diffusion. This can be derived by computing the two-point correlation function of $x_2(t)$ and $x_3(t)$, from which one can infer the following late-time behavior for the displacement squared:

$$s_i^2(t) = \langle [x_i(t) - x_i(0)]^2 \rangle \sim 2Dt, \quad \text{for } t \gg 1/\gamma_o. \quad (3.39)$$

where D is called the diffusion constant. In the presence of a magnetic field, the fluctuation-dissipation theorem leads to

$$D = \frac{1}{2m^2} \frac{\kappa_o}{\gamma_o^2 + \omega_o^2} = \frac{T}{m} \frac{\gamma_o}{\gamma_o^2 + \omega_o^2}, \quad (3.40)$$

which decreases with increasing magnetic field. Thus, the relevant time scale for correlations $\sim D$ is smaller in this case and this implies that the diffusion process is more efficient.

The Langevin equation, as presented in (3.28), captures the essential properties of the stochastic processes in Brownian motion, but it fails to give a physically consistent picture for sufficiently short times t , in which the particle suffers only a few or no impacts. It is a general feature of any dynamical system that the dynamical coherence becomes predominant in short time scales, or at high frequencies. Thus, we are led to a natural extension of the Langevin equation in the form [129, 111]

$$\dot{\mathbf{p}}(t) = - \int_{-\infty}^t dt' \gamma(t-t') \mathbf{p}(t') + \mathbf{v}(t) \times \mathbf{B} + \mathbf{R}(t) + \mathbf{E}(t), \quad (3.41)$$

where

$$\langle R_i(t) \rangle = 0, \quad \langle R_i(t) R_j(t') \rangle = \kappa_{ij}(t-t'). \quad (3.42)$$

The main difference between the generalized Langevin equation (3.41) and the usual one (3.28) is that the friction depends now on the past history of the particle through $\gamma(t)$, called the memory kernel, and that the random forces at different times are not independent. Note that we have also included a fluctuating external force $\mathbf{E}(t)$ that can be applied to the system (e.g., an external electric field).

For a magnetic field pointing in the x -direction $\mathbf{B} = B\hat{x}$ and focusing on the transverse fluctuations, we get

$$\dot{p}_{\pm}(t) = - \int_{-\infty}^t dt' \gamma(t-t') p_{\pm}(t') \pm i\omega_o p_{\pm}(t) + R_{\pm}(t) + E_{\pm}(t), \quad (3.43)$$

where $p_{\pm} = p_2 \pm ip_3$, $R_{\pm} = R_2 \pm iR_3$, $E_{\pm} = E_2 \pm iE_3$ and $\omega_o = B/m$.

In frequency domain, the above equation is simply⁷

$$p_{\pm}(\omega) = \frac{R_{\pm}(\omega) + E_{\pm}(\omega)}{\gamma[\omega] - i\omega \mp i\omega_o}, \quad (3.44)$$

and taking the statistical average of the same we get

$$\langle p_{\pm}(\omega) \rangle = \mu_{\pm}(\omega) E_{\pm}(\omega), \quad \text{with} \quad \mu_{\pm}(\omega) \equiv \frac{1}{\gamma[\omega] - i\omega \mp i\omega_o}. \quad (3.45)$$

The quantity $\mu_{\pm}(\omega)$ is known as the admittance. Thus, we can then determine the admittance $\mu_{\pm}(\omega)$, and thereby $\gamma[\omega]$, by measuring the response $\langle p_{\pm}(\omega) \rangle$ to an external fluctuating force. In particular, if the external force is taken to be

$$E_{\pm}(t) = e^{-i\omega t} K_{\pm}, \quad (3.46)$$

then $\langle p_{\pm}(t) \rangle$ is just

$$\langle p_{\pm}(t) \rangle = \mu_{\pm}(\omega) e^{-i\omega t} K_{\pm} = \mu_{\pm}(\omega) E_{\pm}(t). \quad (3.47)$$

For late times (or low frequencies) the generalized Langevin equation reduces to its non-local progenitor, and the timescales associated to the decay of the

⁷Causality imposes that $\gamma(t) = 0$ for $t < 0$ so $\gamma[\omega]$ in this expression denotes the Fourier-Laplace transform,

$$\gamma[\omega] = \int_0^{\infty} dt \gamma(t) e^{i\omega t},$$

while $p_{\pm}(\omega)$, $R_{\pm}(\omega)$, and $E_{\pm}(\omega)$ are Fourier transforms, e.g.,

$$p_{\pm}(\omega) = \int_{-\infty}^{\infty} dt p_{\pm}(t) e^{i\omega t}.$$

two-point function of the momentum as well as the displacement squared are the same as discussed before. In particular, note that

$$\mu_{\pm}(0) \equiv \frac{1}{\gamma_o \mp i\omega_o} \quad (3.48)$$

so

$$\gamma_o = t_{\text{relax}}^{-1} = \mathbf{Re} \left(\frac{1}{\mu_{\pm}(0)} \right). \quad (3.49)$$

For a quantity \mathcal{O} , the power spectrum $I_{\mathcal{O}}(\omega)$ is defined as

$$I_{\mathcal{O}}(\omega) \equiv \int_{-\infty}^{\infty} dt \langle \mathcal{O}(t_0) \mathcal{O}(t_0 + t) \rangle e^{i\omega t}, \quad (3.50)$$

and it is related to the two-point function through the Wiener-Khintchine theorem

$$\langle \mathcal{O}(\omega) \mathcal{O}(\omega') \rangle = 2\pi \delta(\omega + \omega') I_{\mathcal{O}}(\omega). \quad (3.51)$$

For stationary systems (3.50) is independent of t_0 , so one can set $t_0 = 0$ in such situations. When the external force is set to zero, from (3.44) it follows that

$$p_{\pm}(\omega) = \frac{R_{\pm}(\omega)}{\gamma[\omega] - i\omega \mp i\omega_o} = \mu(\omega) R_{\pm}(\omega), \quad (3.52)$$

and, using (3.51) one gets that

$$I_{p_{\pm}}(\omega) = |\mu(\omega)|^2 I_{R_{\pm}}(\omega). \quad (3.53)$$

Therefore, the random force correlator appearing in (3.42) can be evaluated as

$$\kappa_{\pm}(\omega) = I_{R_{\pm}}(\omega) = \frac{I_{p_{\pm}}(\omega)}{|\mu_{\pm}(\omega)|^2}. \quad (3.54)$$

This will be important in the next section, to check the validity of the fluctuation-dissipation theorem.

3.3.2 Bulk dynamics and the drag coefficient

We now turn to the holographic realization of Brownian motion in the presence of a magnetic field. Let us begin by considering the action (3.6), which in the commutative limit $a \rightarrow 0$ reduces to

$$S \approx \frac{R^2}{4\pi} \int dt du \left[u^4 f (X_2'^2 + X_3'^2) - \frac{1}{f} (\dot{X}_2^2 + \dot{X}_3^2) \right]. \quad (3.55)$$

This action describes the dynamics of a string in Schwarzschild-AdS₅ and it is dual to a quark in ordinary SYM at finite temperature. We then turn on a gauge field in the flavor brane of the form

$$\vec{A} = \frac{B}{2} (y\hat{z} - z\hat{y}), \quad (3.56)$$

thus getting the desired magnetic field $\vec{B} = B\hat{x}$. As explained before, this only appears as a boundary term (4.26), so it will not affect the bulk dynamics of the string. The equations of motion coming from the above action are:

$$0 = f \partial_u (u^4 f X_i') - \ddot{X}_i. \quad (3.57)$$

We now proceed by expanding X_i in modes as in (3.8), i.e.,

$$X_i(t, u) = e^{-i\omega t} g_i(u). \quad (3.58)$$

Then the equations of motion (3.57) can be written as

$$0 = g_i''(y) + \frac{4y^3}{y^4 - 1} g_i'(y) + \frac{\nu^2 y^4}{(y^4 - 1)^2} g_i(y) \quad (3.59)$$

where we defined dimensionless quantities

$$y = \frac{u}{u_h}, \quad \nu = \frac{\omega}{u_h}, \quad (3.60)$$

and where primes denote now derivatives with respect to y . The wave equation for the modes (3.59) is independent of the magnetic field and it is exactly the same as the equation considered in [26] for $d = 4$.

We need to find the solutions of the equation (3.59). In general, it is not possible to do this analytically for an arbitrary frequencies ν and hence we employ a low frequency approximation $\nu \ll 1$ by means of the so-called matching technique. Here, we only write down the final result, relegating the details of the computation to appendix B.1. The two solution that correspond to outgoing and ingoing waves at the horizon behave asymptotically as

$$g^{(\text{out/in})}(y) \sim \left(1 \mp \frac{i}{8}\nu(\pi - \log(4))\right) \left(1 + \frac{\nu^2}{2y^2}\right) \mp \frac{i\nu}{3y^3} + \mathcal{O}(1/y^4). \quad (3.61)$$

We now consider the forced motion of our Brownian particle due to a fixed external magnetic field and a fluctuating electric field. As mentioned in section 3.2, this amounts to the addition of the boundary term (4.26) to the action (4.6), which imposes a boundary condition of the form

$$\Pi_i^u|_{\partial\Sigma} \equiv \frac{\partial\mathcal{L}}{\partial X_i'}\Big|_{\partial\Sigma} = F_i. \quad (3.62)$$

Here, $F_i = -(F_{it} + F_{ij}\dot{X}^j)$ is the usual Lorentz force and

$$F_{\mu\nu} \equiv \partial_\mu A_\nu - \partial_\nu A_\mu = \begin{pmatrix} 0 & E_1 & E_2 & E_3 \\ -E_1 & 0 & -B_3 & B_2 \\ -E_2 & B_3 & 0 & -B_1 \\ -E_3 & -B_2 & B_1 & 0 \end{pmatrix}. \quad (3.63)$$

Then, for a magnetic field pointing in the x -direction, $B_1 = B$, and transverse electric fields $E_2 = E_2(t)$ and $E_3 = E_3(t)$ we find a set of boundary conditions

that inevitably mix the fluctuations along the transverse directions:

$$\left. \frac{R^2}{2\pi} u^4 f X'_2 - B \dot{X}_3 \right|_{u=u_m} = E_2, \quad \left. \frac{R^2}{2\pi} u^4 f X'_3 + B \dot{X}_2 \right|_{u=u_m} = E_3, \quad (3.64)$$

where u_m denotes the position of the flavor brane. Our goal is now to compute the thermal expectation value (or one-point function) of the momentum, and then extract the admittance.

The general solution for X_i is the sum of ingoing and outgoing modes at the horizon $X_i = A_i^{(\text{out})} X^{(\text{out})} + A_i^{(\text{in})} X^{(\text{in})}$, where $X^{(\text{out/in})} = e^{-i\omega t} g^{(\text{out/in})}$. In the semiclassical approximation, outgoing modes are always thermally excited because of Hawking radiation, while the ingoing modes can be arbitrary. However, because the radiation is random, the phase of $A_i^{(\text{out})}$ takes random values and, on average $\langle A_i^{(\text{out})} \rangle = 0$. Then, we can write $\langle X_i \rangle = \langle A_i^{(\text{in})} \rangle e^{-i\omega t} g^{(\text{in})}(u)$, where $g^{(\text{in})}(u)$ correspond to the normalized solution given by (3.61). For the remaining part of this section we will denote $\langle A_i^{(\text{in})} \rangle = A_i$ and $g^{(\text{in})} = g$ for simplicity.

In the Brownian motion literature, it is customary to work in a circular basis when an external magnetic field is included. Thus, we define

$$X_{\pm} \equiv X_2 \pm iX_3 = e^{-i\omega t} g_{\pm}(u) \quad \text{and} \quad E_{\pm} \equiv E_2 \pm iE_3 = e^{-i\omega t} K_{\pm}. \quad (3.65)$$

In fact, the equations (3.64) decouple in this basis. After some algebra we get

$$\left. \frac{R^2}{2\pi} u^4 f g' A_{\pm} \pm \omega B g A_{\pm} \right|_{u=u_m} = K_{\pm}, \quad (3.66)$$

where $A_{\pm} = A_2 \pm iA_3$. Inverting this relation we obtain

$$A_{\pm} = \left. \frac{K_{\pm}}{\frac{R^2}{2\pi} u^4 f g' \pm \omega B g} \right|_{u=u_m}, \quad (3.67)$$

from which we can read the average position of the heavy quark, $\langle x_{\pm}(t) \rangle \equiv \langle X_{\pm}(t, u_m) \rangle = e^{-i\omega t} g(u_m) A_{\pm}$,

$$\langle x_{\pm}(t) \rangle = e^{-i\omega t} K_{\pm} \frac{g}{\frac{R^2}{2\pi} u^4 f g' \pm \omega B g} \Big|_{u=u_m}, \quad (3.68)$$

and

$$\langle p_{\pm}(t) \rangle = E_{\pm}(t) \frac{-i\omega m g}{\frac{R^2}{2\pi} u^4 f g' \pm \omega B g} \Big|_{u=u_m}. \quad (3.69)$$

This expression allows us to read the admittance,

$$\mu_{\pm}(\omega) = \frac{-i\omega m g}{\frac{R^2}{2\pi} u^4 f g' \pm \omega B g} \Big|_{u=u_m}. \quad (3.70)$$

In the zero frequency limit, and for a heavy quark $u_m \ll u_h$, we obtain

$$\mu_{\pm}(0) = \frac{2m}{\pi\sqrt{\lambda}T^2 \pm 2iB}, \quad (3.71)$$

from which we can infer

$$\gamma_o = \frac{\pi\sqrt{\lambda}T^2}{2m} \quad \text{and} \quad \omega_o = \pm \frac{B}{m}. \quad (3.72)$$

As expected, the friction coefficient is not modified by the presence of the magnetic field, which is consistent with the fact that the magnetic field does not do work. Also, we find that

$$t_{\text{relax}} = \frac{1}{\gamma_o} = \frac{2m}{\pi\sqrt{\lambda}T^2}. \quad (3.73)$$

This temporal scale dominates the late-time decay of the one-point function of $\mathbf{p}(t)$, for a quark that transverses the plasma, in agreement with the previous works [90, 75]. The late-time⁸ behavior is dominated by the low frequency

⁸There should be a smooth crossover with the early-time regime or high frequency limit. See for example [81].

limit of the generalized Langevin equation, case in which (3.41) reduces to its nonlocal progenitor (3.28). From (3.34) we can thus infer that,

$$\langle p_{\pm}(t) \rangle \sim e^{-\gamma_0 t} e^{\pm i \omega_0 t}. \quad (3.74)$$

This is exactly what is expected for the Brownian motion of a charged particle in the presence of a magnetic field. To obtain the thermal averages of $p_2(t)$ and $p_3(t)$ we can simply take the real and imaginary parts of (3.74).

3.3.3 Diffusion and the fluctuation-dissipation theorem

The purpose of this section is to compute holographically the displacement squared of the heavy quark and to extract from it the diffusion constant D . The upshot of the computation is summarized in equation (3.26), which is valid for an arbitrary background. However, the functions $f_{\omega}^{(\pm)}(u)$ as well as the details for the computation of the constant B vary according to each situation.

Before proceeding with the direct calculation of this quantity, it is useful to understand the boundary conditions we want to impose on the fields. Although we are interested in the world-sheet theory of the probe string, in the static gauge the induced metric on the string inherits the geometric characteristics of the spacetime background. This means that the usual rules for correlators in the gauge/gravity correspondence apply in our case.

First, we need to impose an UV cutoff in order to have a quark with finite mass. The natural place to impose the cutoff is given by the location

of the flavor brane u_m , which can be related to the mass m of the quark through (4.36). The mass of the quark is chosen to be dominant scale of the system, so usually one would push the cutoff up to the boundary $u_m \rightarrow \infty$ and choose normalizable boundary conditions for the modes. However, in our case that would correspond to a infinitely massive quark and there would be no Brownian motion. A Neumann boundary condition at $u = u_m$ also does not work in our case because we would go back to the case of free Brownian motion. Instead, we use a mixed boundary condition in which the external magnetic field is on but the fluctuating electric fields are turned off. According to (3.64) this is,

$$\left. \frac{R^2}{2\pi} u^4 f X'_2 - B \dot{X}_3 \right|_{u=u_m} = 0, \quad \left. \frac{R^2}{2\pi} u^4 f X'_3 + B \dot{X}_2 \right|_{u=u_m} = 0, \quad (3.75)$$

or in terms of the modes X_\pm ,

$$\left. \frac{R^2}{2\pi} u^4 f X'_\pm \pm i B \dot{X}_\pm \right|_{u=u_m} = 0. \quad (3.76)$$

Recall that X_\pm can be expressed as the sum of outgoing modes and ingoing modes found previously, with arbitrary coefficients. Following the convention introduced in (3.17), let us write

$$X_\pm(t, u) = A_\pm [g^{(\text{out})}(u) + B_\pm g^{(\text{in})}(u)] e^{-i\omega t}. \quad (3.77)$$

From (3.76) it follows then that

$$B_\pm = - \frac{\frac{R^2}{2\pi} u^4 f g^{(\text{out})'} \pm \omega B g^{(\text{out})}}{\frac{R^2}{2\pi} u^4 f g^{(\text{in})'} \pm \omega B g^{(\text{in})}} \Big|_{u=u_m} \equiv e^{i\theta_\pm}. \quad (3.78)$$

The fact that B_{\pm} is a pure phase is self-evident, given that $g^{(\text{out})} = g^{(\text{in})*}$. To leading order in frequency one finds that

$$B_{\pm} = \frac{\pi R^2 T^2 (y_m^4 - 1) \mp 2i B y_m^4}{\pi R^2 T^2 (y_m^4 - 1) \pm 2i B y_m^4} + \mathcal{O}(\nu) = \left(\frac{\pi R^2 T^2 \mp 2i B}{\pi R^2 T^2 \pm 2i B} + \mathcal{O}(1/y_m^4) \right) + \mathcal{O}(\nu), \quad (3.79)$$

from which one gets

$$|g^{(\text{out})} + B_{\pm} g^{(\text{in})}|^2 = \frac{4\pi^2 R^4 T^4}{4B^2 + \pi^2 R^4 T^4} + \mathcal{O}(\nu). \quad (3.80)$$

The late-time behavior of the displacement squared can be then inferred from the low-frequency limit of (3.26), i.e.,

$$s_{\pm}^2(t) = \frac{16\sqrt{\lambda}T^3}{4B^2 + \pi^2\lambda T^4} \int_0^\infty d\omega \frac{\sin^2\left(\frac{\omega t}{2}\right)}{\omega^2} \sim \frac{4\pi\sqrt{\lambda}T^3}{4B^2 + \pi^2\lambda T^4} t. \quad (3.81)$$

Thus, as expected, we find that the diffusion constant defined as in (3.39) is given by

$$D = \frac{2\pi\sqrt{\lambda}T^3}{4B^2 + \pi^2\lambda T^4} = \frac{T}{m} \frac{\gamma_o}{\gamma_o^2 + \omega_o^2}. \quad (3.82)$$

Finally, in order to give an explicit check of the fluctuation dissipation theorem (4.33) we compute the random force autocorrelation appearing in (3.54) to extract the coefficient κ_o . From (3.27) we can evaluate the two-point correlator of the momentum p_{\pm} as follows:

$$\begin{aligned} \langle :p_{\pm}(t)p_{\pm}(0): \rangle &= \int_0^\infty \frac{d\omega}{2\pi} \frac{2m^2\omega^2 |A|^2 \cos(\omega t)}{e^{\beta\omega} - 1} |g^{(\text{out})}(u_m) + B_{\pm} g^{(\text{in})}(u_m)|^2, \\ &= \int_{-\infty}^\infty \frac{d\omega}{2\pi} \frac{m^2}{\sqrt{\lambda}\pi T} \frac{\beta|\omega|}{e^{\beta|\omega|} - 1} |g^{(\text{out})}(u_m) + B_{\pm} g^{(\text{in})}(u_m)|^2. \end{aligned} \quad (3.83)$$

Therefore,

$$I_{p_{\pm}}(\omega) = \frac{m^2}{\sqrt{\lambda}\pi T} \frac{\beta|\omega|}{e^{\beta|\omega|} - 1} |g^{(\text{out})}(u_m) + B_{\pm} g^{(\text{in})}(u_m)|^2, \quad (3.84)$$

and combining this with (3.70) one finds that

$$I_{R_{\pm}}(\omega) = \pi\sqrt{\lambda}T^3 + \mathcal{O}(\omega). \quad (3.85)$$

This gives us precisely a coefficient $\kappa_o = \pi\sqrt{\lambda}T^3$ which agrees with (4.33), providing an explicit check of the fluctuation-dissipation theorem in the presence of a magnetic field.

3.4 Brownian Motion in NCSYM

We now turn our attention to the study of Brownian motion in the non-commutative setup. The main difference here is that the closed string sector is modified by the inclusion of an antisymmetric B -field. In this setup, and after the appropriate decoupling limit, the effective field theory is described by a gauge theory living in a noncommutative space. It is interesting to study the similarities and differences with our previous computation when the magnetic field was introduced in the open string sector.

3.4.1 Langevin dynamics in the non-commutative plasma

To start, let us postulate a generalized Langevin equation of a particle in a non-commutative thermal bath:

$$\dot{p}_i(t) = - \int_{-\infty}^t dt' \Gamma_{ij}(t-t') p_j(t') + R_i(t) + E_i(t), \quad (3.86)$$

where

$$\langle R_i(t) \rangle = 0, \quad \langle R_i(t) R_j(t') \rangle = \kappa_{ij}(t-t'). \quad (3.87)$$

In this case, the B -field does not appear explicitly in the Langevin equation, though its effect should be somehow be present through the coefficients Γ and κ . We propose that in this case Γ is a matrix that encodes the effects of the non-commutativity. In particular, for non-commutativity in the (x^2, x^3) -plane, we propose to write

$$\Gamma_{ij}(t) = \begin{pmatrix} \gamma(t) & 0 & 0 \\ 0 & \gamma(t) & -\Omega(t) \\ 0 & \Omega(t) & \gamma(t) \end{pmatrix}. \quad (3.88)$$

In the low frequency limit, the above equation becomes local in time, allowing us to write

$$\dot{p}_i(t) = -\Gamma_{ij}p_j(t) + R_i(t) + E_i(t), \quad (3.89)$$

where $\gamma(t - t') = \gamma_o\delta(t - t')$, $\Omega(t - t') = \Omega_o\delta(t - t')$ and $\kappa(t - t') = \kappa_o\delta(t - t')$. Note that this has exactly the same structure of (3.31), with γ_o being the usual friction coefficient and Ω_o playing the role of the Larmor frequency. Furthermore, if the fluctuation-dissipation theorem applies, we expect that the relation (4.33) is also true for the present configuration. Solutions (3.34) and (3.35) hold in the low frequency limit. This means that the two-point correlators (3.36)-(3.38), as well as the diffusive behavior of the displacement squared (3.39), act in the exact same way, but now with new coefficients γ_o , Ω_o and κ_o which might depend on the noncommutative parameter θ .

The fluctuations along the x^1 -direction are unaffected by the presence of the non-commutativity. We thus restrict our attention to the fluctuations on the Moyal plane. These fluctuations can be decoupled by working in the

circular basis $p_{\pm} = p_2 \pm ip_3$, $R_{\pm} = R_2 \pm iR_3$ and $E_{\pm} = E_2 \pm iE_3$. The eigenvalues of (3.88) are found to be $\lambda_{\pm} = \gamma \mp i\Omega$ so we can rewrite (3.86) as

$$\dot{p}_{\pm}(t) = - \int_{-\infty}^t dt' \lambda_{\pm}(t-t') p_{\pm}(t') + R_{\pm}(t) + E_{\pm}(t). \quad (3.90)$$

In frequency domain this equation can be written as

$$p_{\pm}(\omega) = \frac{R_{\pm}(\omega) + E_{\pm}(\omega)}{\lambda_{\pm}[\omega] - i\omega}, \quad (3.91)$$

and taking the statistical average we obtain

$$\langle p_{\pm}(\omega) \rangle = \mu_{\pm}(\omega) E_{\pm}(\omega), \quad \text{with} \quad \mu_{\pm}(\omega) \equiv \frac{1}{\lambda_{\pm}[\omega] - i\omega}. \quad (3.92)$$

Then, by measuring the response $\langle p_{\pm}(\omega) \rangle$ due to an external force we can determine the admittance $\mu_{\pm}(\omega)$ and thereby $\mu_{\pm}[\omega]$. In particular, if the external force is taken to be

$$E_{\pm}(t) = e^{-i\omega t} K_{\pm}, \quad (3.93)$$

then

$$\langle p_{\pm}(t) \rangle = \mu_{\pm}(\omega) e^{-i\omega t} K_{\pm} = \mu_{\pm}(\omega) E_{\pm}(t). \quad (3.94)$$

With this at hand, one can take the real and imaginary parts of μ_{\pm} to obtain γ and Ω respectively. Note also that in the zero frequency limit

$$\mu_{\pm}(0) \equiv \frac{1}{\lambda_{\pm}[0]} = \frac{1}{\gamma_o \mp i\Omega_o}. \quad (3.95)$$

The analysis of the power spectrum and two-point functions is the same as the one done in section 3.3.1. In particular, the equation (3.54) relating the random force correlations with the momentum correlations should apply in this case, which will be useful to check the validity of the fluctuation-dissipation theorem for the current setup.

3.4.2 Bulk dynamics and the drag coefficient

For the action given by (3.6) we can derive the following equations of motion:

$$0 = \frac{f}{h} \partial_u \left(u^4 f h X'_2 - a^2 u^4 h \dot{X}_3 \right) - \partial_t \left(\dot{X}_2 - a^2 u^4 f X'_3 \right), \quad (3.96)$$

$$0 = \frac{f}{h} \partial_u \left(u^4 f h X'_3 + a^2 u^4 h \dot{X}_2 \right) - \partial_t \left(\dot{X}_3 + a^2 u^4 f X'_2 \right). \quad (3.97)$$

The term with mixed derivatives cancels out in both cases and one ends up with

$$0 = \frac{f}{h} \partial_u \left(u^4 f h X'_2 \right) - 4a^2 u^3 f h \dot{X}_3 - \ddot{X}_2, \quad (3.98)$$

$$0 = \frac{f}{h} \partial_u \left(u^4 f h X'_3 \right) + 4a^2 u^3 f h \dot{X}_2 - \ddot{X}_3. \quad (3.99)$$

These are two coupled partial differential equations. We now proceed by expanding X_i in modes by setting

$$X_2(t, u) = e^{-i\omega t} g_2(u), \quad \text{and} \quad X_3(t, u) = e^{i(\varphi - \omega t)} g_3(u). \quad (3.100)$$

We have introduced a phase difference for reasons that will become clear below.

The equations of motion for the modes are

$$0 = \frac{f}{h} \partial_u \left(u^4 f h g'_2 \right) + 4i\omega a^2 u^3 f h g_3 e^{i\varphi} + \omega^2 g_2, \quad (3.101)$$

$$0 = \frac{f}{h} \partial_u \left(u^4 f h g'_3 \right) - 4i\omega a^2 u^3 f h g_2 e^{-i\varphi} + \omega^2 g_3. \quad (3.102)$$

If we choose $e^{i\varphi} = \pm i$, or equivalently $\varphi = \pm\pi/2$, the two equations of motion turn out to be the same. This motivates to consider the linear combinations $X_{\pm} = X_2 \pm iX_3 = e^{-i\omega t} g_{\pm}(u)$, where

$$g_2 = \frac{g_+ + g_-}{2} \quad \text{and} \quad g_3 = \frac{g_+ - g_-}{2i}. \quad (3.103)$$

Not surprisingly, this is completely equivalent with the circular basis introduced in section 3.3 for the case of Brownian motion in a magnetic field. In this basis the equations of motion decouple, and can be rewritten as:

$$0 = g_{\pm}''(y) + \frac{4(1+b^4)y^3}{(y^4-1)(1+b^4y^4)} g_{\pm}'(y) + \left(\frac{\nu^2 y^4}{(y^4-1)^2} \pm \frac{4\nu b^2 y^3}{(y^4-1)(1+b^4y^4)} \right) g_{\pm}(y) \quad (3.104)$$

where we have defined dimensionless quantities

$$y \equiv \frac{u}{u_h}, \quad \nu \equiv \frac{\omega}{u_h}, \quad b \equiv au_h, \quad (3.105)$$

and the primes denote derivatives with respect to y . The normal modes X_{\pm} correspond to fluctuations with circular polarization, rotating clockwise or counterclockwise, respectively.

Explicit solutions to the above equations can be found in appendix B.1.2. The final expressions for outgoing and ingoing modes are

$$g_{\pm}^{(\text{out})}(y) \sim \frac{ib^2\nu y}{b^2 \mp i} \left(1 - \frac{\nu^2}{2y^2} \right) + \left(1 - \frac{ib^2\nu}{b^2 \mp i} - \frac{1}{8}i\nu(\pi - \log(4)) \right) \left(1 - \frac{\nu^2}{6y^2} \right) + \mathcal{O}(1/y^3),$$

and

$$g_{\pm}^{(\text{in})}(y) \sim -\frac{ib^2\nu y}{b^2 \pm i} \left(1 - \frac{\nu^2}{2y^2} \right) + \left(1 + \frac{ib^2\nu}{b^2 \pm i} + \frac{1}{8}i\nu(\pi - \log(4)) \right) \left(1 - \frac{\nu^2}{6y^2} \right) + \mathcal{O}(1/y^3),$$

respectively.

We now exert an external fluctuating force $\vec{E}(t)$ on the string endpoint by turning on an electric field $F_{ti} = E_i$ on the flavor brane. Variation of the

whole action implies the standard dynamics for all interior points of the string, but now with boundary condition

$$\Pi_i^u|_{\partial\Sigma} \equiv \frac{\partial\mathcal{L}}{\partial X'_i} = E_i, \quad (3.108)$$

where E_i is the external force.

From (3.6), it follows that

$$\frac{R^2}{2\pi} \left(u^4 f h X'_2 - a^2 u^4 h \dot{X}_3 \right) \Big|_{u=u_m} = E_2, \quad \frac{R^2}{2\pi} \left(u^4 f h X'_3 + a^2 u^4 h \dot{X}_2 \right) \Big|_{u=u_m} = E_3, \quad (3.109)$$

where u_m denotes the position of the D7-brane. Our goal is to find the admittance of the system for which we need the one-point function of the momentum.

Again, it is convenient to work in the circular basis, i.e. $X_{\pm} = X_2 \pm iX_3$ and $E_{\pm} = E_2 \pm iE_3$. The general solution for X_{\pm} is the sum of outgoing and ingoing modes $X_{\pm} = A_{\pm}^{(\text{out})} X_{\pm}^{(\text{out})} + A_{\pm}^{(\text{in})} X_{\pm}^{(\text{in})}$. However, as discussed before, the phase of $A_{\pm}^{(\text{out})}$ takes random values and on average $\langle A_{\pm}^{(\text{out})} \rangle = 0$. Then, we can write $\langle X_{\pm} \rangle = \langle A_{\pm}^{(\text{in})} \rangle e^{-i\omega t} g_{\pm}^{(\text{in})}(u)$ and $E_{\pm} = e^{-i\omega t} K_{\pm}$ but, for simplicity, we will denote $\langle A_{\pm}^{(\text{in})} \rangle = A_{\pm}$ and $g_{\pm}^{(\text{in})} = g_{\pm}$ in the remaining part of this section.

In this basis the boundary conditions decouple:

$$\frac{R^2}{2\pi} \left(u^4 f h A_{\pm} g'_{\pm}(u) \pm \omega a^2 u^4 h A_{\pm} g_{\pm}(u) \right) \Big|_{u=u_m} = K_{\pm}, \quad (3.110)$$

or, in terms of the dimensionless quantities y , ν and b as defined previously,

$$A_{\pm} = \frac{2\pi K_{\pm}}{R^2 u_h^3} \frac{1 + b^4 y^4}{(y^4 - 1) g'_{\pm}(y) \pm \nu b^2 y^4 g_{\pm}(y)} \Big|_{y=y_m}. \quad (3.111)$$

The average position of the heavy quark, $\langle x_{\pm}(t) \rangle \equiv \langle X_{\pm}(t, y_m) \rangle$ is then

$$\langle x_{\pm}(t) \rangle = \frac{2\pi}{R^2 u_h^3} \frac{(1 + b^4 y^4) g_{\pm}(y)}{(y^4 - 1) g'_{\pm}(y) \pm \nu b^2 y^4 g_{\pm}(y)} \Big|_{y=y_m} K_{\pm} e^{-i\omega t}, \quad (3.112)$$

and

$$\langle p_{\pm}(t) \rangle = \frac{-2\pi i \omega m}{R^2 u_h^3} \frac{(1 + b^4 y^4) g_{\pm}(y)}{(y^4 - 1) g'_{\pm}(y) \pm \nu b^2 y^4 g_{\pm}(y)} \Big|_{y=y_m} F_{\pm}(t), \quad (3.113)$$

from which we can read the admittance,

$$\mu_{\pm}(\omega) = \frac{-2\pi i \omega m}{R^2 u_h^3} \frac{(1 + b^4 y^4) g_{\pm}(y)}{(y^4 - 1) g'_{\pm}(y) \pm \nu b^2 y^4 g_{\pm}(y)} \Big|_{y=y_m}. \quad (3.114)$$

In the zero frequency limit and for large mass⁹ we get,

$$\mu_{\pm}(0) = \frac{2m(1 + b^4 y_m^4)}{b^2 R^2 \pi T^2} \frac{1 \mp i b^2}{b^2 y_m^4 \pm i} \sim \frac{2m}{R^2 \pi T^2} (1 \mp i b^2) + \mathcal{O}(1/y_m^4). \quad (3.115)$$

As we can see, the real part coincides with the expected value for the commutative case, but now there is an additional part that is imaginary (and independent of the temperature, given that $b = a u_h = a \pi T$). For a quark that transverses the plasma one can read the following evolution at late times:

$$\langle p_{\pm}(t) \rangle \sim e^{-\gamma_o t} e^{\pm i \Omega_o t}, \quad (3.116)$$

where

$$\gamma_o = \frac{\pi \sqrt{\lambda} T^2}{2m(1 + \pi^4 \lambda \theta^2 T^4)} \quad \text{and} \quad \Omega_o = \frac{\pi^3 \lambda \theta T^4}{2m(1 + \pi^4 \lambda \theta^2 T^4)}. \quad (3.117)$$

⁹In the large mass expansion, we set the non-commutative parameter to a fixed value and then take the limit $y_m \rightarrow \infty$.

The friction coefficient is modified by the presence of the non-commutativity, and in this case

$$t_{\text{relax}} = \frac{1}{\gamma_o} = \frac{2m(1 + \pi^4 \lambda \theta^2 T^4)}{\sqrt{\pi \lambda} T^2}. \quad (3.118)$$

This agrees with a previous computation of the drag force in the Maldacena-Russo background [124, 142] (in the non-relativistic regime) and implies that the non-commutative plasma is less viscous in comparison to the commutative one.

3.4.3 Diffusion and the fluctuation-dissipation theorem

Now we turn to the computation of the displacement squared in the Maldacena-Russo background. First of all, we need to understand the boundary conditions we want to impose on the fields. In this case, the effect of non-commutativity is already present in the background itself, so the free Brownian motion is realized by imposing a Neumann boundary condition at $u = u_m$. According to (3.109), this means

$$\left. \frac{R^2}{2\pi} \left(u^4 f h X'_2 - a^2 u^4 h \dot{X}_3 \right) \right|_{u=u_m} = 0, \quad \left. \frac{R^2}{2\pi} \left(u^4 f h X'_3 + a^2 u^4 h \dot{X}_2 \right) \right|_{u=u_m} = 0, \quad (3.119)$$

or simply

$$\left. f X'_\pm \pm i a^2 \dot{X}_\pm \right|_{u=u_m} = 0, \quad (3.120)$$

where again, we defined $X_\pm = X_2 \pm i X_3$. The general solution is then written as a linear combination of outgoing and ingoing modes,

$$X_\pm(t, u) = A_\pm \left[g_\pm^{(\text{out})}(u) + B_\pm g_\pm^{(\text{in})}(u) \right] e^{-i\omega t}, \quad (3.121)$$

and from the boundary condition (3.120) we get that

$$B_{\pm} = -\frac{f g_{\pm}^{(\text{out})'} \pm \omega a^2 g_{\pm}^{(\text{out})}}{f g_{\pm}^{(\text{in})'} \pm \omega a^2 g_{\pm}^{(\text{in})}} \Big|_{u=u_m} \equiv e^{i\theta_{\pm}}. \quad (3.122)$$

Here, B_{\pm} is also a pure phase given that, in this case, it still holds that $g_{\pm}^{(\text{out})} = g_{\pm}^{(\text{in})*}$. To leading order in frequency, we obtain

$$B_{\pm} = -\frac{(1 \mp ib^2)(1 \pm ib^2 y_m^4)}{(1 \pm ib^2)(1 \mp ib^2 y_m^4)} + \mathcal{O}(\nu). \quad (3.123)$$

With this at hand, we can also compute

$$\left| g_{\pm}^{(\text{out})} + B_{\pm} g_{\pm}^{(\text{in})} \right|^2 = \left(\frac{4}{(1 + b^4)} + \mathcal{O}(1/y_m^4) \right) + \mathcal{O}(\nu), \quad (3.124)$$

and finally, by taking the low-frequency limit of (3.26) we compute the late-time behavior of the displacement squared:

$$s_{\pm}^2(t) = \frac{16}{\pi^2 \sqrt{\lambda} T} \int_0^{\infty} d\omega \frac{\sin^2\left(\frac{\omega t}{2}\right)}{\omega^2} \sim \frac{4}{\pi \sqrt{\lambda} T} t. \quad (3.125)$$

Note that the factor that depends on b exactly cancels with the $h(u_h)$ term that appears in the normalization constant A . We find that, surprisingly, the diffusion constant is not affected by non-commutativity, but the relation with respect to γ_o and Ω_o is still the same

$$D = \frac{2}{\pi \sqrt{\lambda} T} = \frac{T}{m} \frac{\gamma_o}{\gamma_o^2 + \Omega_o^2}. \quad (3.126)$$

This suggests that the fluctuation-dissipation theorem holds even in the presence of non-commutativity. In order to explicitly check this, we compute the random force correlator in to extract the coefficient κ_o . From (3.27) it follows

that

$$\langle :p_{\pm}(t)p_{\pm}(0): \rangle = \int_{-\infty}^{\infty} \frac{d\omega}{2\pi} \frac{m^2(1+b^4)}{\sqrt{\lambda}\pi T} \frac{\beta|\omega|}{e^{\beta|\omega|}-1} |g^{(\text{out})}(u_m) + B_{\pm} g^{(\text{in})}(u_m)|^2 e^{-i\omega t}, \quad (3.127)$$

and hence

$$I_{p_{\pm}}(\omega) = \frac{m^2(1+b^4)}{\sqrt{\lambda}\pi T} \frac{\beta|\omega|}{e^{\beta|\omega|}-1} |g^{(\text{out})}(u_m) + B_{\pm} g^{(\text{in})}(u_m)|^2. \quad (3.128)$$

At leading order, we find through (3.54) that

$$\kappa_o = \frac{\pi\sqrt{\lambda}T^3}{1 + \pi^4\lambda\theta^2T^4}. \quad (3.129)$$

This agrees with (4.33), thus providing an explicit check of the fluctuation-dissipation theorem for the non-commutative plasma.

3.5 Discussion

In this chapter we carried out an analytical study of the dynamics of a heavy quark in two strongly-coupled systems at finite temperature: SYM in the presence of a magnetic field and NCSYM. The former was realized by studying the fluctuations of a string living in an AdS black hole background and turning on a gauge field in the open string sector. The latter was achieved by replacing the background for one that incorporates the effects of non-commutativity through the introduction of an antisymmetric B -field in the closed string sector.

For both systems, we found that the Langevin equation that describes the dynamics of such a quark has matrix coefficients and this fact induces

correlations along the relevant directions. This is in complete agreement with the classical theory of Brownian motion in a magnetic field [164, 112]. We then displayed the basic properties of these equations by computing holographically the admittance and the random force autocorrelator and we showed that these two quantities are related through the usual fluctuation-dissipation theorem. The existence of such theorem is due to the fact that, at the microscopic level, friction and random forces have the same origin, i.e., interactions with the degrees of freedom of the thermal bath. Finally, we studied the diffusion of the quark in both systems and we showed that, although the non-commutative plasma is less viscous, the late-time behavior of the displacement squared is unaffected by the non-commutativity.

As explained in the introduction, one of the main motivations that led to this work was to establish whether the fast thermalization found in [62] holds for more general situations or not. An important difference between the approach of this chapter and the previous one is that here we studied the non-commutative plasma with a local probe. In the previous work, on the other hand, we considered composite non-local operators that are obtained by smearing the usual gauge covariant operators over open Wilson lines¹⁰. The fast thermalization and large decay rates of the modes are then possibly related to the non-local character of the probes¹¹. It would be interesting to further

¹⁰In non-commutative field theories, this modification makes the operators gauge-invariant. In fact, this class of operators are known to couple to the linearized supergravity fields [55, 119].

¹¹It is well known that the presence of the open Wilson lines dominate the UV behavior

explore this question by probing the theory with probes of different ‘size’ and study the associated timescales for the approach to thermal equilibrium. Two interesting possibilities to consider are Wilson loops and entanglement entropy.

It is important to emphasize that all of our computations were performed in the low frequency limit of the theory, in which case the analytical computations were under control. Going beyond the hydrodynamical regime might also offer new insights but it requires a numerical approach. For example, in [28] it was shown that a large class of holographic quantum liquids exhibit novel collective excitations that appear due to the presence of a magnetic field. At high frequency, the dominant peak in the spectral function is associated to sound mode similar to the zero sound mode in the collisionless regime of a Landau Fermi liquid. The study of Brownian motion within this regime is beyond the scope of this thesis, but it is also left for future works.

In conclusion, the results obtained in this chapter shed additional light on the thermal nature of non-commutative gauge theories and suggest future directions of research. The present study constitutes yet another illustration of the usefulness of the gauge/gravity correspondence.

of the two (and higher) point functions of the gauge invariant operators [74].

Chapter 4

Quantum Fluctuations in Holographic Theories with Hyperscaling Violation

4.1 Preliminaries

Generalizing the notion of holography for gravitational theories in non-asymptotically AdS backgrounds is of great interest. Such generalizations are not only interesting in their own right where one might hope to obtain a better understanding of quantum gravity in spacetimes other than AdS, but also from a practical point of view in terms of engineering toy models resembling the real-world non-relativistic condensed matter systems. In the latter approach, the hope is that holography would shed light on some strongly-correlated features of these systems which would normally be impossible to understand using the conventional field theoretical methods.

Indeed, starting from the original works [154, 16, 102], various holographic setups have already been constructed in the literature where the boundary theory is scale, but not conformally, invariant. These boundary theories typically have either Schrödinger or Lifshitz symmetries. A variant of such setups where the gravity solution is not only characterized by a dynamical exponent z (as in the Lifshitz case) but also by the so-called hyperscaling

violation exponent θ , has recently gained some attention [73, 135, 96, 150, 58, 52, 105, 34, 4, 29, 146, 145, 57, 5, 22, 8, 106, 33, 138, 56, 152, 104, 132]; some earlier studies include [80, 45, 151, 97]. The interest in these solutions partly stems from the observation that the entanglement entropy computed holographically using these gravity solutions exhibits a logarithmic violation of the area law in the boundary theory for some values of θ [135, 96]. Since entanglement entropy computed for theories with Fermi surfaces also shows a logarithmic violation [171, 72, 161, 162, 172], these bulk solutions have been proposed as potential gravity duals of field theories with Fermi surfaces even though there are no explicit fermions in the bulk¹.

In this chapter, we consider zero-temperature gravity solutions with hyperscaling violation parameter and assume that they represent in the boundary a class of quantum critical points characterized by two parameters, z and θ . Our objective here is to compute the response of these quantum critical points to a disturbance caused by coupling them to a massive charged particle (which is represented in the bulk by a long fundamental string). We give analytical expressions for the two-point functions of the zero-temperature (quantum) fluctuations of the massive charged probe for arbitrary values of z and θ . This enables us to show the existence of a crossover in the late-time behavior of these two-point functions in the two-dimensional parameter space of z and θ . More concretely, in the range $z + 2\theta/d > 2$, where d de-

¹See also [84] for a discussion of the issues which plague identifying the gravity solutions with hyperscaling violation exponent as gravity duals for field theories with Fermi surfaces.

notes the spatial dimension of the boundary theory, the two-point functions become independent of the mass of the probe at late times. We also verify the fluctuation-dissipation theorem for the quantum fluctuations of the probe. As a check, we show that our results for $\theta = 0$ reduce to the ones in [167] for holographic quantum critical points with Lifshitz scaling. Moreover, our results also apply to the recently constructed holographic theories [104] which are supposed to represent in the boundary a class of quantum critical points with hyperscaling violation but with Schrödinger symmetries. In addition, we study the zero-temperature fluctuations of the charged probe in quantum critical points dual to the Reissner-Nordström AdS background and verify that the results agree with the late-time behavior of the two-point functions when the $z \rightarrow \infty$ limit is taken.

This chapter is organized as follows. In the next section we briefly review some facts about the gravity solutions with hyperscaling violation exponent especially their regime of validity and the allowed values of z and θ imposed by the null energy condition. In section 4.3 we present analytical results for the two-point functions of the zero-temperature fluctuation of the massive probe and analyze their late-time behavior as a function of z and θ , followed by the verification of the fluctuation-dissipation theorem in section 4.4. In section 4.5 we do the analysis for holographic quantum critical points with $z = \infty$ by taking the extremal Reissner-Nordström AdS black hole as the background. We conclude with some remarks and open questions for future directions.

4.2 Bulk metric

Our starting point is the following $(d + 2)$ -dimensional line element

$$\begin{aligned} ds^2 &\equiv G_{\mu\nu} dx^\mu dx^\nu \\ &= \frac{1}{r^{2\theta/d}} \left(-r^{2z} dt^2 + \frac{dr^2}{r^2} + r^2 d\vec{x}^2 \right). \end{aligned} \quad (4.1)$$

where d denotes the number of spatial dimensions and z and θ are the dynamical critical and the hyperscaling violation exponents, respectively. Such a metric could be obtained, for example, as a solution (in the IR) to the equations of motion coming from a system of Einstein-Maxwell-dilatonic scalar with Lagrangian density given by [135, 96]

$$\mathcal{L} = \frac{1}{2\kappa^2} \left[\mathcal{R} - L^2 Z(\Phi) F^2 - 2(\partial\Phi)^2 - \frac{V(\Phi)}{L^2} \right], \quad (4.2)$$

where

$$Z(\Phi) = Z_0^2 e^{\alpha\Phi}, \quad V(\Phi) = -V_0^2 e^{\delta\Phi}. \quad (4.3)$$

with α and δ being some constants determining z and θ . Also, the constants Z_0 and V_0 are related to the effective coupling of the gauge field and the cosmological constant, respectively. The solutions for the gauge field $A = A_t(r)dt$ and the dilatonic scalar $\Phi(r)$ will not play any significant role in our following discussions, hence, we will not write them here. The metric (4.1) is the most general one that is spatially homogeneous and covariant under the scale transformations

$$t \rightarrow \zeta^z t, \quad \vec{x} \rightarrow \zeta \vec{x}, \quad r \rightarrow \zeta^{-1} r, \quad ds \rightarrow \zeta^{\theta/d} ds. \quad (4.4)$$

Some comments on the allowed values of z and θ are in order. On the gravity side, the null energy condition implies important consequences for theories that admit a consistent gravity dual [135, 58]. These conditions can be summarized as²

$$\begin{aligned}(d - \theta) [d(z - 1) - \theta] &\geq 0, \\ (z - 1)(d + z - \theta) &\geq 0.\end{aligned}\tag{4.5}$$

In a Lorentz invariant theory, $z = 1$ and then the first inequality above implies that $\theta \leq 0$ or $\theta \geq d$. On the other hand, for a scale invariant theory, $\theta = 0$ and one recovers the known result $z \geq 1$ [102, 107]. Notice that, if $\theta \neq 0$ the null energy condition can be satisfied for $z < 1$. In particular, $z < 0$ together with $\theta > d$ gives a consistent solution to (5.11), as well as $0 < z < 1$ along with $\theta \geq d + z$. However, as discussed in [58], $\theta > d$ leads to instabilities on the gravity side. Hence, we will not consider the case of $\theta > d$ here.

The metric (4.1), together with the solutions for the gauge field and the dilatonic scalar, is assumed to holographically describe a quantum field theory at a strongly-coupled quantum critical point with a dynamical critical exponent z and a hyperscaling violation exponent θ . As is well known in holography, the radial direction is mapped into the energy scale in the boundary field theory. For $\theta < d$, in the coordinates we have chosen in (4.1), $r \rightarrow \infty$ and

²As we alluded to earlier, theories with some special values of θ , namely for $\theta = d - 1$, are of interest since they have been argued in [135, 96] to give holographic realizations of theories with Fermi surfaces. The null energy condition then requires that the dynamical critical exponent satisfies $z \geq 2 - 1/d$ in order to have a consistent gravity description.

$r \rightarrow 0$ then describe, respectively, the UV and IR of the field theory. However, it is important to emphasize that the gravity background provides a good description of the aforementioned quantum critical point only in a certain range of r as the solution could get significantly modified as the two regions $r \rightarrow \infty$ and $r \rightarrow 0$ are approached. If the dual field theory under consideration flows from a UV fixed point to a quantum critical point which violates hyperscaling relation, then the background (4.1) is only valid up to a scale of order $r \sim r_F$ beyond which it ceases to exist as a valid solution to the equations of motion coming from the action (4.2) (Figure 4.1 depicts the regime of validity of our solution). The region $r > r_F$ in this case is drastically modified and the scale r_F then appears in the metric as an overall factor $ds^2 \propto L^2/r_F^{2\theta/d}$ (with L being the AdS radius) which is indeed responsible for restoring the canonical dimensions in the presence of hyperscaling violation³. In the deep IR, on the other hand, the theory may flow to some other fixed points, develop a mass gap and so forth, resulting in the metric (4.1) not being valid in this regime either [58]. Relatedly, in the deep IR, the background seems to have a genuine null singularity [150] for generic values of z and θ allowed by the null energy condition, which may require stringy effects for it to be resolved. For now, we will simply ignore these issues while being cognizant of the fact that the results we present in the following sections may only be valid in a certain range of energies.

³For example, in models with a Fermi surface, r_F is set by the Fermi momentum [135]. In addition, see [58] for an example of UV completions of these models.

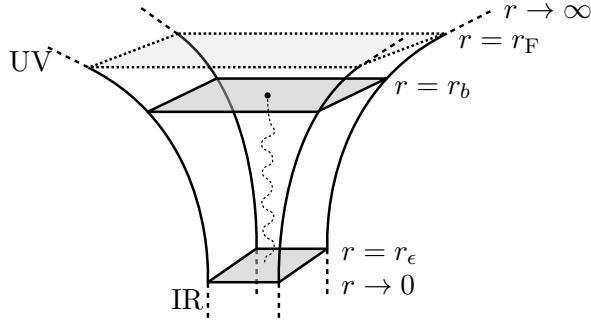


Figure 4.1: Schematic picture of the fluctuating string dual to a charged heavy particle coupled to a quantum critical point. The string stretches in the bulk between a D-brane at $r = r_b$ and the IR region of the geometry at $r = r_\epsilon$.

4.3 Quantum fluctuations and the two-point function

A charged heavy particle on the boundary theory can be realized as the endpoint of an open string that stretches between a D-brane and the IR region, $r = r_\epsilon \rightarrow 0$, of the geometry. The brane is treated in the probe approximation. It covers the directions parallel to the boundary and spreads along the radial direction from $r \rightarrow \infty$ to $r = r_b$ where it ends smoothly. For the validity of our computations, we will assume that $r_b < r_F$, so that the above-mentioned issues regarding the validity of the gravity solution does not affect our analysis.

The classical dynamics of a fundamental string is governed by the Nambu-Goto action

$$S_{\text{NG}} = -\frac{1}{2\pi\alpha'} \int d^2\sigma \sqrt{-\det g_{ab}}, \quad (4.6)$$

where $g_{ab} = G_{\mu\nu} \partial_a X^\mu \partial_b X^\nu$ denotes the induced metric on the worldsheet. We choose to work in the static gauge, namely, we set $\tau = t$ and $\sigma = r$. Our string

embedding is then given by $X^\mu(t, r) = \{t, r, \vec{x}(t, r)\}$. One can then easily check that $\vec{x}(t, r) = \vec{c}$ is a trivial solution with \vec{c} being a constant vector which we take, without loss of generality, to be zero. This solution is dual to a static particle whose energy is given by

$$E = \frac{1}{2\pi\alpha'} \int_0^{r_b} dr \sqrt{-g_{tt}g_{rr}} = \frac{1}{2\pi\alpha'} \frac{r_b^{z-2\theta/d}}{z-2\theta/d}. \quad (4.7)$$

It is worth mentioning that for $z \neq 1$, the energy E is not the same as the inertial mass m of the particle. The precise form of the dependence of E on m will be given below, after the computation of the response function.

Now, we would like to study the fluctuations over this static embedding (see Figure 4.1 for a schematic picture of the fluctuating string). Since the fluctuations along the various directions decouple from each other we restrict our attention to a single direction and take $X^\mu(t, r) = \{t, r, x(t, r), 0, \dots\}$. Up to quadratic order in the perturbations $x(t, r)$, the Nambu-Goto action (4.6) takes the form

$$S_{\text{NG}} \approx -\frac{1}{4\pi\alpha'} \int dt dr \left(r^{z+3-2\theta/d} \dot{x}'^2 - r^{1-z-2\theta/d} \dot{x}^2 \right), \quad (4.8)$$

where $\dot{x} \equiv \partial_t x$ and $x' \equiv \partial_r x$. Note that we dropped a constant term in (4.8) that neither depends on x nor on its derivatives. The resulting equation of motion is

$$\frac{\partial}{\partial r} \left(r^{z+3-2\theta/d} \frac{\partial x}{\partial r} \right) - r^{1-z-2\theta/d} \frac{\partial^2 x}{\partial t^2} = 0. \quad (4.9)$$

Now, because t is an isometry of the background (4.1), we Fourier transform $x(t, r)$:

$$x(t, r) \sim e^{-i\omega t} g_\omega(r). \quad (4.10)$$

Substituting (4.10) into (4.9), the equation for the Fourier modes $g_\omega(r)$ becomes

$$\frac{d}{dr} \left(r^{z+3-2\theta/d} \frac{dg_\omega}{dr} \right) + \omega^2 r^{1-z-2\theta/d} g_\omega = 0, \quad (4.11)$$

whose general solution can be written in the following form

$$g_\omega(r) = \frac{A_\omega}{r^{1+z/2-\theta/d}} \left[J_{\frac{1}{2}+\frac{1}{z}-\frac{\theta}{zd}} \left(\frac{\omega}{zr^z} \right) + B_\omega Y_{\frac{1}{2}+\frac{1}{z}-\frac{\theta}{zd}} \left(\frac{\omega}{zr^z} \right) \right]. \quad (4.12)$$

Here A_ω , and B_ω are the two constants of integration and J and Y are Bessel functions of the first and second kind, respectively.

To fix the first constant we normalize the solution in the following way. For functions $u_1(t, r), u_2(t, r)$ satisfying the equation of motion (4.9), we can define a Klein-Gordon inner product [25]

$$(u_1, u_2)_\Sigma = -\frac{i}{2\pi\alpha'} \int_\Sigma \sqrt{\tilde{g}} n^\mu G_{xx} (u_1 \partial_\mu u_2^* - \partial_\mu u_1 u_2^*), \quad (4.13)$$

where Σ is a Cauchy surface in the (t, r) part of the metric, \tilde{g} is the induced metric on Σ and n^μ is the future-pointing unit normal to Σ . This inner product is independent of the choice of Σ , but for simplicity we take Σ to be a constant- t surface.

We want a normalized basis of solutions such that for functions $u_\omega(t, r) = e^{-i\omega t} g_\omega(r)$, one has $(u_\alpha, u_\beta^*) = 0$ and $(u_\alpha, u_\beta) = (u_\alpha^*, u_\beta^*) = \delta_{\alpha\beta}$. The reason is that, if this normalization is satisfied, it can be shown that the usual canonical commutation relations hold once the theory is quantized [26]. In this context one would write

$$x(t, r) = \int_0^\infty d\omega g_\omega(r) [a(\omega) e^{-i\omega t} + a^\dagger(\omega) e^{i\omega t}], \quad (4.14)$$

with $a^\dagger(\omega), a(\omega)$ being the creation and annihilation operators .

The first normalization condition is satisfied due to the properties of Bessel functions. The second one implies that,

$$\begin{aligned} (u, u) &= \frac{1}{2\pi\alpha'}(\omega' + \omega) \int \frac{dr}{r^{z-1+\frac{2\theta}{d}}} g_\omega(r) g_{\omega'}(r) \\ &= \delta(\omega - \omega'). \end{aligned} \quad (4.15)$$

Using (4.12) and defining $\xi = 1/r^z$, one obtains

$$\begin{aligned} \frac{e^{-i(\omega-\omega')t}}{2\pi\alpha'z}(\omega + \omega')A_\omega A'_\omega \int d\xi \left\{ \xi \left[J_\nu\left(\frac{\omega}{z}\xi\right) + B_\omega Y_\nu\left(\frac{\omega}{z}\xi\right) \right] \right. \\ \left. \times \left[J_\nu\left(\frac{\omega'}{z}\xi\right) + B_{\omega'} Y_\nu\left(\frac{\omega'}{z}\xi\right) \right] \right\} = \delta(\omega - \omega'), \end{aligned} \quad (4.16)$$

with $\nu = 1/2 + 1/z - \theta/zd$. The last integral can be performed using various properties of Bessel functions⁴. Finally, using the identity $\delta(ax) = \delta(x)/a$, we arrive at

$$A_\omega = \sqrt{\frac{\pi\alpha'}{z(1+B_\omega^2)}}. \quad (4.17)$$

Note the particular dependence of A_ω on B_ω , which itself remains to be fixed by the UV boundary condition. This is in stark contrast with the finite temperature case, in which case the overall normalization turns out to be sensible only to the IR part of the geometry [13, 68].

⁴In particular, one needs to use the following properties

$$\begin{aligned} \int d\xi \xi J_\nu(u\xi) Y_\nu(v\xi) &= 0, \\ \int d\xi \xi J_\nu(u\xi) J_\nu(v\xi) &= \int d\xi \xi Y_\nu(u\xi) Y_\nu(v\xi) = \frac{1}{u} \delta(u - v). \end{aligned}$$

To fix the constant B_ω , we impose Neumann boundary condition at the cut-off surface [26], *i.e.* $x'(r_b) = 0$. A straightforward computation then yields

$$B_\omega = -\frac{J_{\frac{1}{z}-\frac{1}{2}-\frac{\theta}{zd}}\left(\frac{\omega}{zr_b^z}\right)}{Y_{\frac{1}{z}-\frac{1}{2}-\frac{\theta}{zd}}\left(\frac{\omega}{zr_b^z}\right)}. \quad (4.18)$$

Thus, the solution (4.12) takes the form

$$g_\omega(r) = \sqrt{\frac{\pi\alpha'}{z(1+B_\omega^2)}} \frac{1}{r^{1+z/2-\theta/d}} \left[J_{\frac{1}{2}+\frac{1}{z}-\frac{\theta}{zd}}\left(\frac{\omega}{zr^z}\right) + B_\omega Y_{\frac{1}{2}+\frac{1}{z}-\frac{\theta}{zd}}\left(\frac{\omega}{zr^z}\right) \right], \quad (4.19)$$

with the constant B_ω given in (4.18).

To calculate the two-point function, we use canonical commutation relations for the creation and annihilation operators, $[a(\omega), a^\dagger(\omega')] = \delta(\omega - \omega')$, and define the vacuum state such that $a(\omega)|0\rangle = 0$. Then, using equations (4.14) and (4.19), we obtain⁵

$$\langle X(t)X(0) \rangle = \int_0^\infty \frac{d\omega}{2\pi} e^{-i\omega t} \langle X(\omega)X(0) \rangle, \quad (4.20)$$

where

$$\langle X(\omega)X(0) \rangle = \frac{8z\alpha' r_b^{-2+z+2\theta/d}}{\omega^2} \left[J_{\frac{1}{z}-\frac{1}{2}-\frac{\theta}{zd}}\left(\frac{\omega}{zr_b^z}\right)^2 + Y_{\frac{1}{z}-\frac{1}{2}-\frac{\theta}{zd}}\left(\frac{\omega}{zr_b^z}\right)^2 \right]^{-1}. \quad (4.21)$$

⁵In order to write the correlators in terms of the boundary theory data, one must specify the relation between r_b and the mass m of the charged particle. This can be obtained through the computation of the response function and is given at the end of section 4.4. Additionally, α' needs to be written in terms of the 't Hooft coupling λ . However, this last step depends on the UV completion of the effective gravitational model we are considering here. We leave our results for the correlators in terms of α' , while keeping in mind that this relation is implicit.

The case of $z = 1, \theta = 0$ is the only one for which $\langle X(t)X(0) \rangle$ can be computed from $\langle X(\omega)X(0) \rangle$ analytically using (4.20). For these special values of the parameters, the two-point function reads [167]

$$\langle X(t)X(0) \rangle = -\frac{1}{4\pi^2\alpha'E^2}(\log|t| + \gamma_E), \quad (4.22)$$

where γ_E is the Euler-Mascheroni constant. For other values of the parameters an estimate for the behavior of $\langle X(t)X(0) \rangle$ at late times can be obtained as follows. At low frequencies, $\omega \ll r_b^z$, the leading order behavior of $\langle X(\omega)X(0) \rangle$ reads

$$\langle X(\omega)X(0) \rangle \sim \begin{cases} E^{\frac{2(z-2+2\theta/d)}{z-2\theta/d}} \omega^{-3+\frac{2}{z}-\frac{2\theta}{zd}} & z + \frac{2\theta}{d} \leq 2, \\ \omega^{-1-\frac{2}{z}+\frac{2\theta}{zd}} & z + \frac{2\theta}{d} \geq 2. \end{cases} \quad (4.23)$$

Assuming that at late times the dominant contribution to the two-point function comes from the low frequency limit of $\langle X(\omega)X(0) \rangle$ as given in (4.23), we find that

$$\langle X(t)X(0) \rangle \sim \begin{cases} E^{\frac{2(z-2+2\theta/d)}{z-2\theta/d}} |t|^{2-\frac{2}{z}+\frac{2\theta}{zd}} & z + \frac{2\theta}{d} \leq 2, \\ |t|^{\frac{2}{z}-\frac{2\theta}{zd}} & z + \frac{2\theta}{d} \geq 2. \end{cases} \quad (4.24)$$

Depending on the values of z and θ the two-point function at late times shows markedly different behaviors. In particular, notice that for $z + 2\theta/d > 2$, the long-time correlation of the particle is independent of the mass. (Note, in particular, that theories with $\theta = d - 1$ belong to this category.) A similar change in behavior of the two-point function was recently shown in [167] for holographic theories with Lifshitz scaling but without hyperscaling violation. Indeed, our results for $\theta = 0$ perfectly agree with the analysis presented in [167]. Sitting exactly at the line $z + 2\theta/d = 2$, one can show that the two-point function grows linearly with t at late times, which is its maximum rate of

growth. The minimum, on the other hand, can be realized in various situations: I) $\theta = d(1 - z)$, II) $\theta = d$ with arbitrary z or III) $z = \infty$ with arbitrary θ , all of which give a logarithmic behavior in time for the late-time behavior of the two-point function.

The third situation deserves further attention. For any fixed θ , taking the $z \rightarrow \infty$ limit, the second line in (4.23) implies that at low frequencies $\langle X(\omega)X(0) \rangle \sim \omega^{-1}$ regardless of the values of θ and d . Indeed, in section 4.5 we verify this behavior independently by considering the extremal Reissner-Nordström AdS black hole. Since the near horizon geometry of an extremal Reissner-Nordström AdS black hole contains an AdS_2 factor, the boundary field theory flows in the IR to a quantum critical point with $z = \infty$ (which is holographically dual to AdS_2).

4.4 Response function and the fluctuation-dissipation theorem

We now turn to the computation of the response of the system due to an external force $F(t)$. From the point of view of the field theory, for $F(t) \sim e^{-i\omega t}F(\omega)$, the linear response of the particle is

$$\langle x(\omega) \rangle = \chi(\omega)F(\omega), \quad (4.25)$$

where $\chi(\omega)$ is the retarded Green's function (also known as admittance). This can be easily realized from the gravity side by turning on a gauge field on the D-brane. Since the endpoint of the string is charged, this amounts to adding

a minimal coupling to the action $S = S_{\text{NG}} + S_{\text{EM}}$, where

$$S_{\text{EM}} = \int dt \left(A_t + \vec{A} \cdot \dot{\vec{x}} \right) \Big|_{r=r_b}. \quad (4.26)$$

This will exert the desired force on the fluctuating particle. However, this coupling is just a boundary term, so it will not play any role for the dynamics of the string in the bulk. The UV boundary condition for the string is now replaced by

$$\frac{\partial \mathcal{L}_{\text{NG}}}{\partial x'} \Big|_{r=r_b} = -\frac{r_b^{3+z-2\theta/d}}{2\pi\alpha'} x'(r_b, t) = F(t), \quad (4.27)$$

whereas in the IR region we impose ingoing boundary condition which is the appropriate one for the computation of the retarded Green's function $\chi(\omega)$ [155]. In order to identify the desired combination of J 's and Y 's, notice that near $r \sim 0$,

$$S \sim \int dt dr_* (x'^2 - \dot{x}^2), \quad (4.28)$$

where we have defined the ‘tortoise’ coordinate $r_* = r^{-z}/z$, such that the (t, r_*) part of the metric is conformally flat. In (4.28), prime denotes the derivative with respect to r_* . In this coordinate system, the equation of motion near the horizon $r_* \rightarrow \infty$ behaves just like the wave equation in flat space, with solutions given by

$$\begin{aligned} x^{(\text{out})}(t, r) &\sim e^{-i\omega(t+r_*)} \sim e^{-i\omega(t+r^{-z}/z)}, \\ x^{(\text{in})}(t, r) &\sim e^{-i\omega(t-r_*)} \sim e^{-i\omega(t-r^{-z}/z)}. \end{aligned} \quad (4.29)$$

Thus, from the IR behavior of the Bessel functions, we select the first Hankel function $H^{(1)} = J + iY$ as the combination that satisfies ingoing boundary

condition at the horizon. Up to a constant, we then have

$$x(t, r) = e^{-i\omega t} \frac{A_\omega}{r^{1+z/2-\theta/d}} H_{\frac{1}{2}+\frac{1}{z}-\frac{\theta}{zd}}^{(1)} \left(\frac{\omega}{zr^z} \right). \quad (4.30)$$

Given the boundary condition (4.27) we get

$$F(t) = e^{-i\omega t} \frac{r_b^{1-z/2-\theta/d}}{2\pi\alpha'} \omega A_\omega H_{-\frac{1}{2}+\frac{1}{z}-\frac{\theta}{zd}}^{(1)} \left(\frac{\omega}{zr_b^z} \right), \quad (4.31)$$

from which we can read off the admittance,

$$\chi(\omega) = \frac{2\pi\alpha'}{\omega r_b^{2-2\theta/d}} \frac{H_{\frac{1}{2}+\frac{1}{z}-\frac{\theta}{zd}}^{(1)} \left(\frac{\omega}{zr_b^z} \right)}{H_{-\frac{1}{2}+\frac{1}{z}-\frac{\theta}{zd}}^{(1)} \left(\frac{\omega}{zr_b^z} \right)}. \quad (4.32)$$

It is straightforward to show that the fluctuation-dissipation theorem holds in the present setup at zero temperature. In particular, this theorem relates the two-point function to the imaginary part of the admittance,

$$\langle X(\omega) X(0) \rangle = 2 [n_B(\omega) + 1] \text{Im } \chi(\omega) \quad (4.33)$$

where $n_B(\omega) = (e^{\beta\omega} - 1)^{-1}$ is the Bose-Einstein distribution. Of course, at zero temperature (where $\beta \rightarrow \infty$) one ends up only with the last term in the above equation. On the other hand, from (4.32) and using properties of Bessel functions it follows that

$$\text{Im } \chi(\omega) = \frac{4z\alpha' r_b^{-2+z+2\theta/d}}{\omega^2} \left[J_{\frac{1}{z}-\frac{1}{2}-\frac{\theta}{zd}} \left(\frac{\omega}{zr_b^z} \right)^2 + Y_{\frac{1}{z}-\frac{1}{2}-\frac{\theta}{zd}} \left(\frac{\omega}{zr_b^z} \right)^2 \right]^{-1}, \quad (4.34)$$

thus providing an explicit check of the fluctuation-dissipation theorem in the presence of hyperscaling violation in our holographic setup.

Finally, for low frequencies this response function can be written as

$$\chi(\omega) \sim \frac{1}{m (i\omega)^2 + \gamma (-i\omega)^{1+2/z-2\theta/zd} + \dots}, \quad (4.35)$$

where

$$m = \frac{r_b^{2-z-2\theta/d}}{2-z-2\theta/d},$$

$$\gamma = \frac{\pi \left[1 - i \tan\left(\frac{\pi}{z} - \frac{\pi\theta}{zd}\right)\right]}{(2iz)^{2/z-2\theta/zd} \Gamma\left(\frac{1}{2} + \frac{1}{z} - \frac{\theta}{dz}\right)^2}. \quad (4.36)$$

The constants m and γ are interpreted as the inertial mass and the self-energy of the particle. For $z + 2\theta/d > 2$, the self-energy dominates over the inertial mass at low frequencies, which is consistent with the change in the behavior of the two point function found in the previous section. (Recall that for $z + 2\theta/d > 2$ the two-point function was independent of mass.) More explicitly, from (4.36) one observes that under the scale transformations given in (4.4), m transform as

$$m \rightarrow \zeta^{z+2\theta/d-2} m, \quad (4.37)$$

implying that for $z + 2\theta/d > 2$, m is an irrelevant coupling in the boundary theory, which should not affect the dynamics at low energies.

4.5 Quantum Fluctuations in Holographic QCPs with $z = \infty$

Consider a $(d+2)$ -dimensional Einstein-Maxwell system with negative cosmological constant $2\Lambda = -d(d+1)/L^2$

$$S = \frac{1}{2\kappa^2} \int d^{d+2}x \sqrt{-g} \left[\mathcal{R} - 2\Lambda - L^2 F_{\mu\nu} F^{\mu\nu} \right]. \quad (4.38)$$

The $(d+2)$ -dimensional Reissner-Nordström AdS black hole background (hereafter denoted by RN-AdS $_{d+2}$) is a solution [141, 44] to the Einstein-Maxwell equations of motion coming from the above action with the metric and gauge field given by

$$ds^2 = -\frac{r^2}{L^2}f(r)dt^2 + \frac{L^2}{r^2}\frac{dr^2}{f(r)} + \frac{r^2}{L^2}d\vec{x}^2, \quad (4.39)$$

$$A = \mu\left(1 - \frac{r_0^{d-1}}{r^{d-1}}\right)dt, \quad (4.40)$$

where

$$f(r) = 1 - \frac{M}{r^{d+1}} + \frac{Q^2}{r^{2d}}, \quad M = r_0^{d+1} + \frac{Q^2}{r_0^{d-1}}, \quad (4.41)$$

with r_0 being the radius of the horizon given by the largest positive root of $f(r)$. The Hawking temperature of the black hole (4.39) is given by

$$T = \frac{(d+1)r_0}{4\pi L^2} \left[1 - \frac{(d-1)Q^2}{(d+1)r_0^{2d}}\right]. \quad (4.42)$$

The RN-AdS $_{d+2}$ background is assumed to holographically describe a $(d+1)$ -dimensional boundary field theory at finite temperature T , given by (4.42), and finite chemical potential μ which is determined by the asymptotic ($r \rightarrow \infty$) value of the bulk gauge field $A_t(r)$. The chemical potential is related to the charge density Q through

$$\mu = \sqrt{\frac{d}{2(d-1)}} \frac{Q}{L^2 r_0^{d-1}}. \quad (4.43)$$

For the present computation, however, we are interested in the case where the boundary theory is at zero temperature, *i.e.* when the RN-AdS $_{d+2}$

is extremal. In this case, the near horizon geometry becomes $\text{AdS}_2 \times \mathbb{R}^d$. The holographic interpretation is that the boundary theory flows in the IR to a dimensional CFT (dual to AdS_2) which describes a quantum critical point in which only the time coordinate scales, namely it is a QCP with $z = \infty$. Nonetheless, similar to the theories with hyperscaling violation, the holographic description is not valid in the deep IR and should only be thought of as an effective description up to some IR scale below which it flows to another fixed point. This could be traced back to the fact that the black hole has indeed a finite horizon area at zero temperature, suggesting a large ground state degeneracy. While keeping in mind the possible limitations of our results, we will not be concerned with such issues here.

Setting $T = 0$ in (4.42) yields

$$Q^2 = \frac{d+1}{d-1} r_0^{2d}, \quad (4.44)$$

which upon being substituted in (4.41)-(4.43) results in

$$f(r) = 1 - \frac{2d}{d-1} \left(\frac{r_0}{r}\right)^{d+1} + \frac{d+1}{d-1} \left(\frac{r_0}{r}\right)^{2d}, \quad (4.45)$$

$$M = \frac{2d}{d-1} r_0^d, \quad (4.46)$$

$$\mu = \sqrt{\frac{d(d+1)}{2}} \frac{r_0}{L^2(d-1)}. \quad (4.47)$$

One can easily check that a static string is again a trivial solution to the equations of motion coming from the Nambu-Goto action. For a such a string, one has

$$E = \frac{1}{2\pi\alpha'} \int_{r_0}^{r_b} dr \sqrt{-g_{tt}g_{rr}} \approx \frac{r_b}{2\pi\alpha'}, \quad \text{for } r_b \gg r_0, \quad (4.48)$$

where r_b is the radial location of the probe D-brane from which the string hangs. Now, similar to our discussion in previous sections, we take an ansatz of the form $X^\mu = \{t, r, x(t, r), 0, \dots\}$ for the fluctuations around the static solution. Up to quadratic order, the Nambu-Goto action becomes

$$S_{\text{NG}} \approx -\frac{L^2}{4\pi\alpha'} \int dt dr \left[\frac{r^4 f(r)}{L^4} x'^2 - \frac{\dot{x}^2}{f(r)} \right], \quad (4.49)$$

where $\dot{x} \equiv \partial_t x$ and $x' \equiv \partial_r x$. The resulting equation of motion is then

$$\frac{\partial}{\partial r} \left(r^4 f(r) \frac{\partial x}{\partial r} \right) - \frac{L^4}{f(r)} \frac{\partial^2 x}{\partial t^2} = 0. \quad (4.50)$$

We now proceed by expanding $x(t, r)$ in Fourier modes, *i.e.* $x(t, r) \sim e^{-i\omega t} g_\omega(r)$. Equation (5.15) then yields

$$\frac{d}{d\rho} \left(\rho^4 f(\rho) \frac{dg_\omega}{d\rho} \right) + \frac{\mathbf{w}^2}{f(\rho)} g_\omega = 0, \quad (4.51)$$

where, for convenience, we have defined dimensionless quantities

$$\rho = \frac{r}{r_0}, \quad \mathbf{w} = \frac{L^2 \omega}{r_0}. \quad (4.52)$$

Hereafter, primes will denote derivatives with respect to ρ in our expressions. Also, we set $L = 1$.

The next step is to find the solutions of the equation (4.51). For general d one finds that, near the boundary, $g_\mathbf{w}(\rho)$ has the following expansion

$$g_\mathbf{w}(\rho) = C_1 \left(1 + \frac{\mathbf{w}^2}{2\rho^2} \right) + C_2 \frac{i\mathbf{w}^3}{3\rho^3} + \mathcal{O}\left(\frac{1}{\rho^4}\right). \quad (4.53)$$

Note that C_1 and C_2 are functions of \mathbf{w} . To determine the constants of integration, C_1 and C_2 , we have to study the behavior of (4.53) in the IR, but

since we are interested only in the solution at low energies, *i.e.* $\mathfrak{w} \ll 1$, we perform a series expansion in \mathfrak{w} and make use of a matching technique which can be found, for example, in [26, 13, 68]. For simplicity, and to reduce clutter in our expressions, we now focus on the case where $d = 2$ (however, we expect our results to hold for general d , and in the appendix we explicitly verify that this is indeed the case for $d = 3$.) Here, we only write down the final results, relegating the details of the computations to the appendix. For $d = 2$ the constants of integration C_1 and C_2 take the form

$$\begin{aligned} C_1^{(\text{out/in})} &= 1 \pm \frac{i\mathfrak{w}}{36} \left(\frac{\sqrt{2}}{2} \pi - \sqrt{2} \tan^{-1} \sqrt{2} - 2 \log 6 \right), \\ C_2^{(\text{out/in})} &= \mp \frac{1}{\mathfrak{w}^2}, \end{aligned} \tag{4.54}$$

where the indices “out” and “in” correspond to outgoing and ingoing modes respectively.

To compute the two-point function $\langle X(\omega)X(0) \rangle$, we proceed differently compared to what we did in the previous sections. Namely, we first compute the response to an external force

$$\langle X(\omega) \rangle \equiv \langle x(\omega, r_b) \rangle = \chi(\omega) F(\omega), \tag{4.55}$$

and then relate it to the two-point function, assuming that the fluctuation-dissipation theorem holds true

$$\langle X(\omega)X(0) \rangle = 2 \text{Im} \chi(\omega). \tag{4.56}$$

We impose ingoing boundary condition in the IR, namely $x(t, \rho) = A_\omega e^{-i\omega t} g_\nu^{(\text{in})}(\rho)$, where A_ω is an arbitrary constant that might have a frequency dependence.

Using the UV boundary condition (evaluated at $\rho_b = r_b/r_0$)

$$\left. \frac{r_0^3}{2\pi\alpha'} \rho^4 f(\rho) x' \right|_{\rho_b} = F(t), \quad (4.57)$$

and the solution (4.53), we obtain

$$F(\omega) = \frac{r_b}{2\pi\alpha'} A_\omega f(\rho_b) \omega^2 \left(C_1^{(\text{in})} + \frac{i\omega}{r_b} C_2^{(\text{in})} \right). \quad (4.58)$$

In the limits $\omega/r_0 \ll 1$ and $r_b/r_0 \gg 1$, the imaginary part of the admittance scales in ω as

$$\text{Im } \chi(\omega) \sim \frac{1}{\omega}. \quad (4.59)$$

Notice that this expression does not depend on the mass of the charged particle. (A similar result holds for the case of $d = 3$ as shown in the appendix.) Consequently, at low frequencies, the scaling behavior of two-point function reads

$$\langle X(\omega) X(0) \rangle \sim \frac{1}{\omega}. \quad (4.60)$$

Note that the correct dimensions in the above expression can trivially be restored by including powers of the chemical potential μ . Some comments are in order here. First note that the low energy scaling of the two-function above, and the fact that the two-point function is also independent of mass, agrees with our previous results in the limit $z \rightarrow \infty$ (for arbitrary θ). Such an agreement is not surprising given that geometries with Lifshitz scaling go over to $\text{AdS}_2 \times R^d$ in the limit of $z \rightarrow \infty$.

4.6 Final remarks

In this chapter we studied the fluctuations of a heavy charged particle in a class of strongly-coupled quantum critical points with dynamical exponent z and hyperscaling violation exponent θ . The late-time behavior of the two-point function for the zero-temperature fluctuations of the particle exhibits a crossover in the (z, θ) parameter space. In a specific region, namely for $z + 2\theta/d > 2$, the two-point function is found to be independent of the mass.

Furthermore, we studied quantum critical points with $z = \infty$. Even though we focused on the cases $d = 2$ and $d = 3$, we expect that our results remain valid for arbitrary d . The reason is that the near horizon limit of RN- AdS_{d+2} geometries have a universal behavior that goes over to $\text{AdS}_2 \times \mathbb{R}^d$. This implies that at low energies the dual field theory exhibits emergent quantum critical behavior controlled by a CFT which could be thought of representing a quantum critical point with $z = \infty$. Our results in this case are in agreement with the $z \rightarrow \infty$ limit of the behavior of the two-point function for the quantum fluctuation of a massive charged particle in theories with hyperscaling violation, that, at late times, the two-point function grows logarithmically with time and is independent of the mass.

As a final remark, one might wonder if this markedly different behavior in the space of z and θ holds true for other kind of operators. In [58], for instance, the authors considered massive scalars in the bulk and they found a transition in the two-point function from a universal power law at short distances (for $\theta > 0$) to a nontrivial exponential behavior at long distances

(where the WKB approximation is valid). It would be interesting to investigate this issue further in order to identify more precisely the behavior in the full space of parameters (z, θ) and compare the results with our findings.

Chapter 5

Strong Subadditivity, Null Energy Condition and Charged Black Holes

5.1 Introduction

Black holes have become, to a modern day's theoretical physicist, an instructive toy to play with: the “harmonic oscillator” *à la mode*. The very nature of black hole entropy, which states that the number of degrees of freedom in a theory of quantum gravity scales as the area, gave birth to the idea of holography[158, 17]. As we have said in the introduction, AdS/CFT is a particular realization of this idea. In this context, it is possible to realize ideas that are natural in quantum information theory: one such example is entanglement entropy. Entanglement entropy, defined as the von-Neumann entropy with respect to a reduced density matrix, measures the quantum entanglement of a system, and thus becomes an interesting quantity to analyze specially for systems described by strongly coupled quantum field theories. For large N gauge theories, whose gravity duals are described by Einstein gravity (with a negative cosmological constant) in the presence of a suitable matter field, entanglement entropy can be computed using the Ryu-Takayanagi (RT) conjectured formula[143] for static backgrounds, and later generalized in the Hubeny-Rangamani-Takayanagi (HRT) formula[95] for time-dependent

backgrounds. The conjectured RT formula has passed various non-trivial checks[88, 87] known in quantum information theory and has also found numerous intriguing applications; see *e.g.* [163] for a recent review.

One important property satisfied by the entanglement entropy is known as the strong sub-additivity, henceforth abbreviated as SSA. A quantum system can be described by the density matrix, usually denoted by ρ , which is a self-adjoint, positive semi-definite, trace class operator. The entropy of the corresponding system can be described by the von-Neumann formula: $S = -\text{tr}[\rho \log \rho]$.

Let us imagine a quantum field theory on a Lorentzian manifold and further imagine a Cauchy surface that divides the entire system in two sub-systems: A and A^c respectively.¹ We can now define a “reduced” density matrix for the sub-system A by tracing over A^c : $\rho_A = \text{tr}_{A^c} [\rho]$, and subsequently define a von-Neumann entropy: $S_A = -\text{tr} [\rho_A \log \rho_A]$ as the entanglement entropy. We can now imagine partitioning the Hilbert space by more than one Cauchy surfaces. Specifically, if we have three sub-systems A_1 , A_2 and A_3 , then SSA is defined as

$$S_{A_1 \cup A_2} + S_{A_2 \cup A_3} - S_{A_2} - S_{A_1 \cup A_2 \cup A_3} \geq 0 , \quad (5.1)$$

$$S_{A_1 \cup A_2} + S_{A_2 \cup A_3} - S_{A_1} - S_{A_3} \geq 0 . \quad (5.2)$$

This property was originally proved in [9, 117], for a recent expository account

¹Note that there can be multiple Cauchy surfaces resulting in the same partitioning of the Hilbert space. Thus the Hilbert subspace is specified by the (future) Cauchy horizon rather than the Cauchy surface itself[41].

see *e.g.* [133]. This inequality, that stands as a cornerstone of quantum information theory, can be viewed as a crucial ingredient in characterizing the von-Neumann entropy[1, 134].

In AdS/CFT correspondence, in a $(d + 1)$ -dimensional bulk theory the RT formula to compute entanglement entropy of a region A is given by

$$S_A = \frac{1}{4G_N^{(d+1)}} \min [\text{Area}(\gamma_A)], \quad (5.3)$$

where $G_N^{(d+1)}$ is the bulk Newton’s constant, γ_A denotes the $(d - 1)$ -dimensional minimal area surface that satisfies $\partial\gamma_A = \partial A$. For backgrounds with time dependence this proposal is generalized to, *via* the HRT formula, considering extremal surfaces rather than a minimal one.² In [88], a simple geometric proof was constructed showing that the RT formula obeys the SSA condition, further substantiating the validity of the RT formula itself.

On the other hand, time-dependent backgrounds do provide a more non-trivial check of the SSA condition. The prototypical example is the so called AdS-Vaidya background, which describes the collapse of a null dust and the formation of a black hole in an asymptotically AdS-space. In the dual field theory this corresponds to a “global quench” process³ corresponding to the time evolution from a “low temperature” state to a thermalized state at a higher temperature. In such a time-dependent background, it was shown in

²In case there are more than one extremal surfaces, one chooses the surface with the minimum area.

³Strictly speaking we are not really studying a quench process –where a sudden change in a parameter of the Hamiltonian is followed by a unitary evolution.

[6, 35] that violation of SSA is strongly tied to the violation of null energy condition (NEC) from the bulk point of view.⁴ For this example, the background is characterized by a time-dependent mass function and the NEC imposes a condition on this function.

Before proceeding further, let us mull over a curious aside. Within AdS/CFT, the importance of the NEC has been realized elsewhere: in constructing a monotonically decreasing central charge function along an RG-flow[130, 153, 131] for a CFT living in arbitrary dimensions. For a $(1+1)$ -dim CFT, it can be shown that the SSA condition indeed implies the Zamolodchikov c -theorem[42]; for more recent developments in higher dimensions see *e.g.* [43]. Thus, fundamental “inequalities” in a large N gauge theory, *e.g.* a monotonically decreasing central charge along an RG-flow or the SSA condition, seem to be stemming from the NEC condition in the bulk description.

In this chapter, we intend to sharpen the connection of the SSA condition with the NEC condition by studying the formation of a charged black hole in AdS-space. In the dual field theory, this will correspond to a global thermalization process in the presence of a chemical potential[31, 70, 3]. The corresponding background is a Reissner-Nordström-Vaidya background in AdS-space, henceforth abbreviated as AdS-RN-Vaidya background. This background is characterized by time-dependent mass and charge functions and the

⁴A violation of the NEC violates the bound in (5.1), whereas (5.2) remains satisfied. Thus, from a holographic perspective, there is a clear distinction between the inequalities in (5.1) and (5.2).

corresponding null energy condition has subtle implications. For a given mass and a given charge function, the null energy condition yields a critical surface, denoted by z_c , that separates the entire spacetime in two regimes: for $z < z_c$, the NEC is satisfied and for $z > z_c$ it is violated.⁵ Therefore, a violation of the NEC depends on whether the regime $z > z_c$ is accessible to an asymptotic observer.

It was argued in [99, 136] that for arbitrary⁶ mass and charge functions, time-like and null geodesics cannot penetrate the critical surface and hence from a gravitational perspective the NEC is protected by having a no-go constraint on these geodesics. However, in AdS/CFT correspondence, space-like geodesics⁷ are also relevant since they carry the information about non-local operators in the dual field theory such as a 2-point function, Wilson loop or entanglement entropy. In this chapter, we will discuss various examples where space-like geodesics can or cannot penetrate this critical surface depending on the choices for the mass and the charge functions. In the dual field theory, this penetration is perceived as a violation of the SSA condition. Thus, we cannot conspire to have a large N gauge theory with certain choices for the mass and the charge functions: entanglement entropy *knows it all*. However, we will merely discuss generic and instructive examples rather than attempting for a general characterization of these functions.

⁵We are working in a coordinate where the boundary of the spacetime is located at $z \rightarrow 0$.

⁶The functions are not completely arbitrary; namely, we need to still impose the same condition on the mass function that the NEC imposes in the uncharged AdS-Vaidya case.

⁷Through this work, when we mention geodesics, we actually mean extremal area surfaces.

This chapter is divided in the following parts: We begin with a short review about the SSA and the NEC condition in the AdS-Vaidya background in section 2. Then, we discuss in details the AdS-RN-Vaidya background in section 3. We also discuss generic examples relating the physics of the NEC condition with the SSA condition based on our numerical explorations. We provide examples for asymptotically AdS₄ and AdS₅-backgrounds. Finally, we conclude in section 4.

5.2 A brief review of known results

We begin by briefly reviewing the results that are already known in the literature, specially in [6, 35].

5.2.1 Strong subadditivity, concavity and monotone-increasing

Let us begin by demonstrating the relation of concavity and monotone-increasing with the SSA conditions. We will follow closely the discussion in [35]. Let us consider three adjacent single intervals A_1 , A_2 and A_3 , whose lengths are denoted by a_1 , a_2 and a_3 . By symmetry of the construction, $S(A_i) = S(a_i)$. Now, let us assume that S is a concave function. By definition

$$S(yx_1 + (1 - y)x_2) \geq yS(x_1) + (1 - y)S(x_2) , \quad 0 < y < 1 . \quad (5.4)$$

Now, let us choose $y = a_3/(a_1 + a_3)$

$$x_1 = a_2, x_2 = \sum_i a_i, \implies S(a_1 + a_2) \geq y s(a_2) + (1 - y) S\left(\sum_i a_i\right) \quad (5.5)$$

$$x_2 = a_2, x_1 = \sum_i a_i, \implies S(a_2 + a_3) \geq (1 - y) s(a_2) + y S\left(\sum_i a_i\right) \quad (5.6)$$

Adding (5.5) and (5.6) we get (5.1).

On the other hand, the condition of monotone-increasing yields

$$S(a_1 + a_2) \geq S(a_1) , \quad S(a_2 + a_3) \geq S(a_3) , \quad (5.7)$$

adding which we get (5.2). Thus the SSA conditions are equivalent to concavity and monotone-increasing conditions on entanglement entropy.

5.2.1.1 AdS-Vaidya background and entanglement entropy

The AdS-Vaidya metric in a $(d + 1)$ spacetime is given by

$$ds^2 = \frac{L^2}{z^2} [-f(z, v) dv^2 - 2dzdv + d\vec{x}^2] , \quad f = 1 - m(v)z^d , \quad (5.8)$$

which describes the formation of a black holes as a shell of null dust collapses. Here, $m(v)$ is a function that interpolates between empty AdS and an AdS-Schwarzschild background as a function of v . Also, L is the radius of curvature, \vec{x} is a $(d - 1)$ -dimensional vector. We have expressed the above background in the Eddington-Finkelstein coordinates, where the coordinate v is defined as

$$dv = dt - \frac{dz}{f(z, v)} , \quad (5.9)$$

and t denotes the boundary time. In this coordinate system, the boundary is located at $z \rightarrow 0$.

The energy-momentum tensor that sources this metric has only one non-vanishing component:

$$T_{vv} = \frac{d-1}{2} z^{d-1} \partial_v m(v) . \quad (5.10)$$

The null energy condition imposes the following constraint on $m(v)$:

$$T_{\mu\nu} n^\mu n^\nu \geq 0 \quad \implies \quad \partial_v m(v) \geq 0 , \quad (5.11)$$

where n^μ is a null vector.

We now use the HRT formula (5.3) to compute the entanglement entropy for a spatial region A . Let's assume A to be a $(d-1)$ -dimensional “rectangle” in the boundary such that $x^1 \in (-\ell/2, \ell/2)$ and $x^2, \dots, x^{d-1} \in (0, \ell_\perp)$ at some fixed boundary time t_b . The HRT prescription establishes that S_A is proportional to the area of the extremal surface γ_A , parametrized by $v(x)$ and $z(x)$, and whose boundary coincides with the boundary of A at $z = 0$.

Thus, we extremize the area

$$\text{Area}(\gamma_A) = L^{d-1} \mathcal{V} \int_{-\ell/2}^{\ell/2} dx \frac{1}{z^{d-1}} \sqrt{1 - [1 - m(v)z^d](v')^2 - 2v'z'}, \quad ' \equiv d/dx, \quad (5.12)$$

where $\mathcal{V} \equiv \ell_\perp^{d-2}$. We also impose the boundary conditions

$$v(-\ell/2) = v(\ell/2) = t_b , \quad z(-\ell/2) = z(\ell/2) = 0 . \quad (5.13)$$

The two equations of motion that follow from (5.12) are

$$0 = [1 - m(v)z^d]v'' + z'' - \frac{\partial_v m(v)}{2} z^d (v')^2 - dm(v) z^{d-1} z' v' , \quad (5.14)$$

$$0 = z v'' - \frac{d-2}{2} m(v) z^d (v')^2 + (d-1)[(v')^2 + dv'z' - 1] , \quad (5.15)$$

and the momentum conservation corresponding to the cyclic coordinate x results in the equation

$$1 - [1 - m(z)z^d](v')^2 - 2v'z' = \left(\frac{z_*}{z}\right)^{2(d-1)}, \quad z_* \equiv z(0). \quad (5.16)$$

It can be shown that only two of the above three equations are independent. Thus, we can solve one of the equations of motion together with the conservation equation by imposing appropriate boundary conditions. It is more practical to use the infra-red boundary conditions $z(0) = z_*$, $v(0) = v_*$ ⁸ to solve the equations and, then, read off the values of t_b and l from (5.13). Once we solve the system, the extremal area can be computed by simplifying (5.12) using (5.16):

$$S(\ell) = \text{Area}(\gamma_A) = 2L^{d-1}\mathcal{V} \int_0^{\ell/2} dx \frac{z_*^{d-1}}{z^{2(d-1)}}. \quad (5.17)$$

This area contains the usual divergent pieces and we will focus on the finite part only.

5.2.1.2 Strong subadditivity and the null energy condition

In order to illustrate the results found in [6, 35] about the relationship between SSA and NEC, we consider two explicit forms of the function $m(v)$

⁸Note that these boundary conditions are guaranteed because of the symmetry of our construction under $x^1 \rightarrow -x^1$. The smoothness of the surface at z_* also imposes: $z'(0) = 0$ and $v'(0) = 0$. Thus, we have sufficient number of boundary conditions altogether.

in equation (5.8):

$$m_1(v) = \frac{M}{2} \left(1 + \tanh \left(\frac{v}{v_0} \right) \right) , \quad (5.18)$$

$$m_2(v) = \frac{M}{2} \left(1 - \tanh \left(\frac{v}{v_0} \right) \right) , \quad (5.19)$$

which depicted in Fig (5.1). It is, then, easy to realize that the null energy condition in equation (5.11) is obeyed by (5.18) and violated by (5.19). We

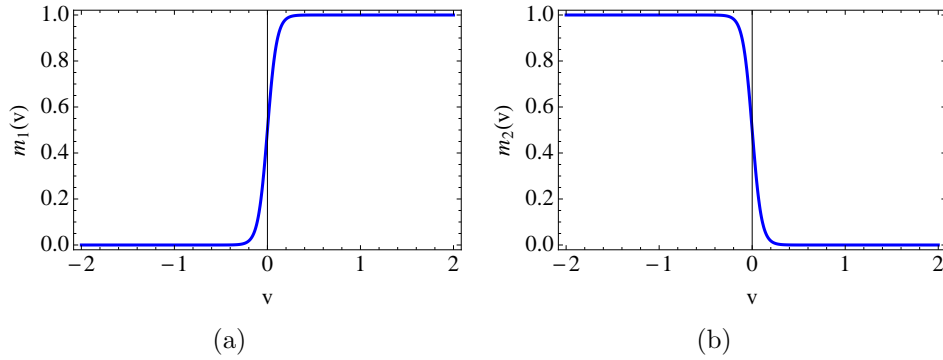


Figure 5.1: Examples of two functions $m(v)$ where (a) NEC is obeyed, and (b) NEC is violated.

now specialize in the case $d = 3$ and solve equations (5.15) and (5.16) for both functions $m(v)$ using $M = 1.0$, $v_0 = 0.01$. Then, we plot the entropy function in equation (5.17) for different values of the boundary time. It is found that for the case obeying NEC, $S(\ell)$ is a monotonically increasing function that is also concave; whereas for the NEC violating function, $S(\ell)$ is still increasing monotonically but it is not a concave function. These results are shown in Figure 5.2. The fact that $S(\ell)$ is not a concave function leads to conclude that SSA is violated, which establishes a direct connection between SSA and NEC.

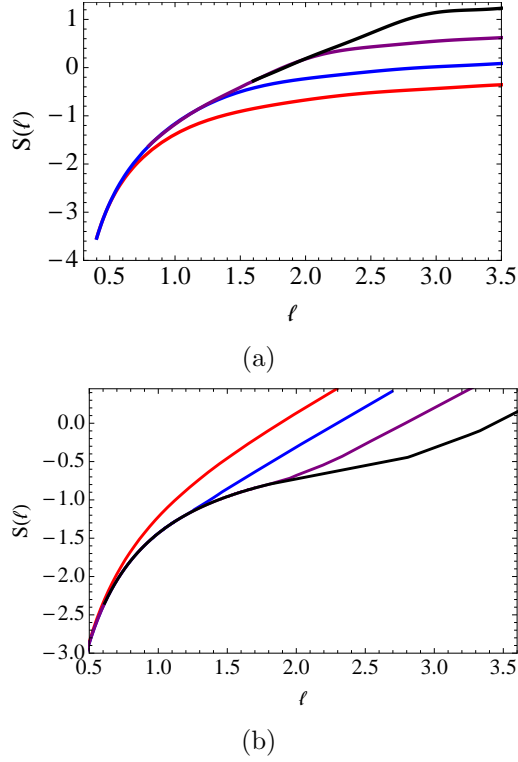


Figure 5.2: Entropy function for the cases where (a) NEC is obeyed, and (b) NEC is violated.

The different colors correspond to boundary times $t_b = 0.3$ (red), $t_b = 1.0$ (blue), $t_b = 1.5$ (purple), and $t_b = 2.0$ (black). Notice that the curves in (b) are not concave and, thus, SSA is violated.

5.3 The AdS-RN-Vaidya background

We will now delve into discussing how this connection of SSA and NEC manifests itself when there is a non-zero background charge. Here we will flesh out all details in their full glory.

5.3.1 The bulk action and the backgrounds

Our initial goal is to write down a metric which describes the formation of a charged Reissner-Nordström (RN) black hole in AdS-space. One such time-dependent background that smoothly interpolates between pure AdS to AdS-RN background is given by the so called AdS-RN-Vaidya background. In $(d+1)$ -bulk dimensions, this background is given by⁹

$$ds^2 = \frac{L^2}{z^2} (-f(z, v)dv^2 - 2dzdv + d\vec{x}^2) \ , \quad A_v = q(v)z^{d-2} \ , \quad (5.20)$$

$$f(z, v) = 1 - m(v)z^d + \frac{(d-2)q(v)^2}{(d-1)L^2}z^{2(d-1)} \ , \quad \Lambda = -\frac{d(d-1)}{2L^2} \quad (5.21)$$

where L is the radius of curvature, z is the AdS-radial coordinate, \vec{x} is a $(d-1)$ -dimensional vector, A_v is the gauge field and $m(v)$ and $q(v)$ are the mass and the charge functions that depend on time. As before, we are working with the Eddington-Finkelstein coordinates. The mass and the charge functions, denoted by $m(v)$ and $q(v)$, are hitherto unconstrained.

The background in (5.20) can be obtained as a solution to the Einstein-Hilbert-Maxwell action with a negative cosmological constant coupled to an external source

$$S = S_0 + \kappa S_{\text{ext}} \ , \quad (5.22)$$

$$S_0 = \frac{1}{8\pi G_N^{(d+1)}} \left[\frac{1}{2} \int d^{d+1}x \sqrt{-g} (R - 2\Lambda) - \frac{1}{4} \int d^{d+1}x \sqrt{-g} F_{\mu\nu} F^{\mu\nu} \right] \quad (5.23)$$

⁹We are considering the case $d > 2$. The case of $d = 2$ is somewhat special, which we will briefly comment on later.

where S_0 denotes the Einstein-Hilbert-Maxwell term, S_{ext} denotes the external source and κ is some coupling.

The equations of motion resulting from this action are given by

$$\begin{aligned} R_{\mu\nu} - \frac{1}{2}(R - 2\Lambda)g_{\mu\nu} - g^{\alpha\rho}F_{\rho\mu}F_{\alpha\nu} + \frac{1}{4}g_{\mu\nu}F_{\alpha\beta}F^{\alpha\beta} \\ = 2\left(8\pi G_N^{(d+1)}\kappa\right)T_{\mu\nu}^{\text{ext}} , \end{aligned} \quad (5.24)$$

$$\partial_\rho(\sqrt{-g}g^{\mu\rho}g^{\nu\sigma}F_{\mu\nu}) = \left(8\pi G_N^{(d+1)}\kappa\right)J_{\text{ext}}^\sigma , \quad (5.25)$$

where the external energy-momentum tensor $T_{\mu\nu}^{\text{ext}}$ and the external current J_μ^{ext} are contained within the action S_{ext} . More precisely, in order for the equations of motion to be satisfied, we have

$$2\kappa T_{\mu\nu}^{\text{ext}} = \left(\frac{d-1}{2}z^{d-1}\frac{dm}{dv} - \frac{d-2}{L^2}z^{2d-3}q(v)\frac{dq}{dv}\right)\delta_{\mu\nu}\delta_{\nu\nu} , \quad (5.26)$$

$$\kappa J_{\text{ext}}^\mu = (d-2)L^{d-3}\frac{dq}{dv}\delta^{\mu z} . \quad (5.27)$$

In the special case for $d = 2$, we get

$$ds^2 = \frac{L^2}{z^2}(-f(z, v)dv^2 - 2dv dz + dx^2) , \quad A_v = q(v)\log z , \quad (5.28)$$

$$f(z, v) = 1 - m(v)z^2 + \frac{q(v)^2}{L^2}z^2\log z , \quad \Lambda = -\frac{1}{L^2} . \quad (5.29)$$

The above background is sourced by the following energy-momentum tensor and vector current

$$2\kappa T_{\mu\nu}^{\text{ext}} = \frac{z}{2}\left(\frac{dm}{dv} - \frac{2}{L^2}q(v)\frac{dq}{dv}\log z\right)\delta_{\mu\nu}\delta_{\nu\nu} , \quad \kappa J_{\text{ext}}^\mu = \frac{1}{L}\frac{dq}{dv}\delta^{\mu z} . \quad (5.30)$$

There is a subtlety in the identification of the source and the VEV in this case and the chemical potential should be identified with the sub-leading term

rather than the leading term of the gauge field as one approaches the boundary. For a detailed discussion on this, see [101]. However, we will not discuss this case.

The energy-momentum tensor presented in equations (5.26) and (5.30) corresponds to the energy-momentum tensor of a charged null dust. The easiest way to understand this is to note that

$$T_{\mu\nu}^{\text{ext}} \sim k_\mu k_\nu , \quad \text{with} \quad k^2 = 0 , \quad (5.31)$$

where we have chosen the vector $k_\mu = \delta_{\mu\nu}$, which is a lightlike vector.

Now, NEC — which a reasonable energy-momentum tensor should obey — is given by the following inequality: $T_{\mu\nu}^{\text{ext}} n^\mu n^\nu \geq 0$, where n^μ is lightlike, *i.e.* $n^\mu n_\mu = 0$. There are two solutions to the null normal equation $n^\mu n_\mu = 0$. Without any loss of generality we can write them as

$$n_{(1)}^\mu = (0, 1, \vec{0}) , \quad n_{(2)}^\mu = \left(1, -\frac{1}{2}f, \vec{0}\right) , \quad (5.32)$$

where $\vec{0}$ denotes the components along the \vec{x} -directions, which we have chosen to set to zero. The null vector $n_{(1)}^\mu$ imposes a trivial constraint, and the null vector $n_{(2)}^\mu$ imposes

$$\frac{d-1}{2} z^{d-1} \frac{dm}{dv} - \frac{d-2}{L^2} z^{2d-3} q(v) \frac{dq}{dv} \geq 0 , \quad \text{for} \quad d > 2 , \quad (5.33)$$

$$\frac{dm}{dv} - \frac{2}{L^2} q(v) \frac{dq}{dv} \log z \geq 0 , \quad \text{for} \quad d = 2 . \quad (5.34)$$

Clearly, NEC is obeyed for all $z > z_c$, where z_c denotes the radial position beyond which the null energy condition is violated. This critical surface is

given by

$$z_c^{d-2} = \frac{d-1}{d-2} \frac{L^2}{2} \frac{m'}{qq'} , \quad \text{for } d > 2 , \quad (5.35)$$

$$\log z_c = \frac{L^2}{2} \frac{m'}{qq'} , \quad \text{for } d = 2 . \quad (5.36)$$

Here $' \equiv d/dv$.

A few comments are in order. Note that for the neutral case, we have $q(v) = 0 = q'(v)$ identically. In that case, the critical surface does not exist. In turn, the null energy condition then imposes a condition on the mass function: $m'(v) \geq 0$. In [6, 35], this condition was related to the strong subadditivity property of entanglement entropy, which we reviewed in the previous section. In the absence of charge, however, the null energy condition seems to be correlated with other simple observations as well. We will discuss these momentarily.

Before proceeding further, let us introduce the apparent horizon for the backgrounds in (5.20) and (5.28) following the notations in [64]. The apparent horizon is given by the null hypersurface which has vanishing expansion of the outgoing null geodesics. For these backgrounds, the tangent vectors to the ingoing and the outgoing null geodesics are

$$\ell_- = -\partial_z , \quad \ell_+ = -\frac{z^2}{L^2} \partial_v + \frac{z^2}{2L^2} f \partial_z \quad (5.37)$$

such that we satisfy

$$\ell_- \cdot \ell_- = 0 = \ell_+ \cdot \ell_+ , \quad \ell_- \cdot \ell_+ = -1 . \quad (5.38)$$

The codimension 2 spacelike hypersurface, which is orthogonal to the above null geodesics, has an area: $\Sigma = (L/z)^{d-1}$. The expansion parameters associated with this hypersurface are

$$\theta_{\pm} = \mathcal{L}_{\pm} \log \Sigma = \ell_{\pm}^{\mu} \partial_{\mu} (\log \Sigma) , \quad (5.39)$$

where \mathcal{L}_{\pm} denotes the Lie derivatives along the null directions ℓ_{\pm} . The location of the apparent horizon is then obtained by solving $\Theta = 0$, where $\Theta = \theta_- \theta_+$. In this particular case, the equation $\Theta = 0$ implies $f(z, v) = 0$.

In the absence of any charge, we write down a general treatment including the $d = 2$ case. The equation for determining the apparent horizon then yields

$$1 - m(v)z^d = 0 \quad \implies \quad z_{\text{ah}} = m(v)^{-1/d} . \quad (5.40)$$

Here z_{ah} denotes the apparent horizon. Note that in the future infinity, *i.e.* $v \rightarrow \infty$, the apparent horizon coincides with the actual event-horizon.

Note that, during the time-evolution, a global event-horizon exists in the background. This is generated by null geodesics in the background and is the boundary of a causal set. Since the background in (5.20) has $(d-1)$ Killing vectors $(\partial/\partial x)^a$, the location of the event-horizon is given by a curve $z(v)$. The null geodesic equation in the background (5.20) is given by

$$\frac{dz_{\text{eh}}(v)}{dv} = -\frac{1}{2}f(z_{\text{eh}}(v), v) , \quad (5.41)$$

where z_{eh} denotes the location of the event-horizon. In the limit $v \rightarrow +\infty$, we have $z_{\text{ah}} = z_{\text{eh}}$; however, this is not true in the $v \rightarrow -\infty$ limit, *i.e.* the event-horizon lies above the apparent horizon.

It was argued in [64] that, during a time-evolution, it is the apparent horizon rather than the event-horizon that can define a “thermodynamics”. Based on an analogy, we can define a “temperature function” and an “entropy function” in terms of the apparent horizon

$$T(v) = - \frac{1}{4\pi} \frac{d}{dz} f(z, v) \Big|_{z_{\text{ah}}} = \frac{d}{4\pi} m(v)^{1/d} , \quad (5.42)$$

$$S(v) = (V_{\mathbb{R}^{d-1}}) m(v)^{-(d-1)/d} . \quad (5.43)$$

Here $V_{\mathbb{R}^{d-1}}$ denotes the volume of the \vec{x} -directions. The temperature function is obtained by computing the surface gravity at the apparent horizon and the entropy function is obtained as the area of the apparent horizon. Clearly, $T(v)$ and $S(v)$ have well-defined thermodynamic meaning in the limit $v \rightarrow +\infty$.

Now, taking derivative of these functions with respect to v , we get

$$\frac{dT(v)}{dv} \sim \frac{dS(v)}{dv} \sim \frac{dm}{dv} \geq 0 , \quad (5.44)$$

where we have used the constraint coming from the null energy condition in (5.11). From the perspective of the boundary theory, if it makes sense to talk about a “temperature function” or an “entropy function” as defined above, the null energy condition implies that these must be monotonically increasing. We already remarked that the null energy condition was demonstrated in [6, 35] to imply the strong sub-additivity property of entanglement entropy. Thus, either all the above observations are physically equivalent or we are unable to separate them for the example we are considering here.

Before proceeding in to the actual computations, let us make some more observations here. If we introduce a charge in the system, the null en-

ergy condition no longer imposes a simple constraint on the mass or the charge function. Instead, it seems to give rise to a critical surface z_c , above which the energy condition is violated. It was argued in [136] that, for such charged backgrounds, null geodesics never penetrate the critical surface z_c and thus the apparent pathology is not relevant. Within the context of AdS/CFT correspondence, spacelike geodesics are also relevant since they contain informations about non-local operators, such as 2-point function or the entanglement entropy itself. Our goal here will be to analyze further what choices of mass and charge functions actually violate the null energy condition and how this is perceived from the perspective of the boundary theory as a violation of SSA. For now, we will discuss the case when $m' \geq 0$, which will smoothly connect to the known results when the charge vanishes.

5.3.2 Tests of strong subadditivity

We now proceed to study entanglement entropy and the SSA inequality in holographic theories dual to $(d+1)$ -dimensional AdS-RN-Vaidya spacetimes. As mentioned before, $d = 2$ is somehow special so in this section we will restrict our attention to the cases with $d \geq 3$.

Our starting point is the metric given in (5.20)-(5.21). For simplicity, we consider that the region A in the boundary theory is an infinite “rectangular strip” with $x_1 \in (-\ell/2, \ell/2)$ and $x_i \in (-\infty, \infty)$, $\forall i \neq 1$. We will call $x_1 \equiv x$ given that this is the only relevant direction and we will denote the transverse directions collectively as \vec{x}_\perp . According to the covariant prescription for en-

tanglement entropy, we have to find the surface γ_A living in a constant- t slice that extremizes the proper area functional $\text{Area}(\gamma_A)$. This surface is invariant under translation in \vec{x}_\perp . Thus, without loss of generality, we can parameterize it with functions $z(x)$, $v(x)$ and boundary conditions

$$z(\pm\ell/2) = 0 \quad \text{and} \quad v(\pm\ell/2) = t. \quad (5.45)$$

These boundary conditions impose that the boundary of γ_A coincides with the boundary of A along the boundary temporal evolution. The area of this surface is given by the following functional

$$S(\ell) = \text{Area}(\gamma_A) = \mathcal{V} L^{d-1} \int_{-\ell/2}^{\ell/2} \frac{dx}{z^{d-1}} (1 - f v'^2 - 2v' z')^{1/2}, \quad (5.46)$$

where \mathcal{V} is the volume that result from integrating over the \vec{x}_\perp directions. Since there is no explicit x -dependence in the Lagrangian, the corresponding conservation equation is given by

$$1 - f v'^2 - 2v' z' = \left(\frac{z_*}{z}\right)^{2(d-1)}, \quad (5.47)$$

where z_* is defined through $z(0) = z_*$. The two equations of motion obtained by extremizing the area functional are

$$z'' + v'' f + z' v' \frac{\partial f}{\partial z} + \frac{1}{2} v'^2 \frac{\partial f}{\partial v} = 0, \quad (5.48)$$

$$z v'' + (d-1) (v'^2 f + 2z' v' - 1) - \frac{1}{2} z v'^2 \frac{\partial f}{\partial z} = 0. \quad (5.49)$$

In particular, note that the first equation is independent of the dimensions. By taking the derivative of the conservation equation (5.47) with respect to

x and using one of these two equations of motion, one obtains the other one. Thus, it is sufficient to consider only (5.47) and *e.g.* (5.48) to find $z(x)$ and $v(x)$. We, then, solve numerically these two equations subject to the boundary conditions

$$z(0) = z_*, \quad z'(0) = 0, \quad v(0) = v_*, \quad v'(0) = 0. \quad (5.50)$$

In practice, however, we start the integration at some arbitrarily small $x = \epsilon$ to avoid possible numerical issues. Also, due to the symmetry of the problem, it is sufficient to integrate only for positive values of x .

So far, z_* and v_* are two free parameters that generate the numerical solutions for $z(x)$ and $v(x)$. The boundary data $\{\ell, t_b\}$ can be obtained from these numerical solutions through $z(\ell/2) = z_0$ and $v(\ell/2) = t_b$, where z_0 is a UV cutoff. This cutoff is needed because, the area functional (5.46) is divergent and one needs to regularize. The divergence comes from the fact that the volume of any asymptotically AdS background is infinite and the spatial surface A we are considering reaches the boundary.

The divergence term can be isolated by studying the same problem in AdS_{d+1} in the standard way [144]. Parameterizing with functions $x(z)$ and $v(z)$, it is clear that near the boundary $x'(z \rightarrow 0) = 0$, $v'(z \rightarrow 0) = 0$ and therefore

$$S_{\text{div}}(\ell) = \mathcal{V} L^{d-1} \int_{z \sim z_0} \frac{dz}{z^{d-1}} = \frac{2\mathcal{V} L^2}{(d-2)z_0^{d-2}}. \quad (5.51)$$

Subtracting this divergence, we obtain the finite term of the area which is the

main quantity we are interested in,

$$S_{\text{reg}}(\ell) = 2\mathcal{V}L^{d-1} \int_{z_0}^{\ell/2} \frac{dx}{z^2} (1 - fv'^2 - 2v'z')^{1/2} - \frac{2\mathcal{V}L^2}{(d-2)z_0^{d-2}}. \quad (5.52)$$

In order to find numerical solutions to the system (5.47)-(5.48), we employ a “shooting” method. First, we give initial values $z(0) = z_*$, $v(0) = v_*$ and integrate until the functions hit the boundary. Once we have the profiles $z(x)$ and $v(x)$, we read the boundary values and extract ℓ and t_b . The numerical implementation of (5.52) is straightforward.

In the remaining part of this section, we will consider specific functions for $m(v)$ and $q(v)$ in $d = 3, 4$. As advertised in the introduction, we will find that, although there is always a critical surface above which the null energy condition is violated, for some appropriate choices of mass and charge functions the extremal surfaces attached to the boundary never cross into that region and SSA is satisfied.

5.3.3 Thin shells and junction conditions

Before proceeding to specific examples, let us gain some insight into the properties of the critical surface (5.35). To this effect we consider the particular case of a thin null shell located at $v = 0$ which is the boundary of two static spaces. The conditions to join space-like or time-like hypersurfaces demand that the two spacetimes induce the same metric on the hypersurface and relate the surface stress energy tensor S_{ab} to the jump of the normal extrinsic curvature K_{ab} across the hypersurface. The issue is more subtle

for null shells since the extrinsic curvature no longer carries any transverse geometrical information. For null hypersurfaces, the extrinsic curvature is given by tangential derivatives of the metric and is, thus, necessarily continuous across the shell and cannot be related to the stress energy tensor of the shell S_{ab} . A general formalism applicable to null hypersurfaces was developed in [19].

For simplicity, consider $d = 3$. The spacetime metric is given by

$$ds^2 = \frac{L^2}{z^2} (-f(z, v)dv^2 - 2dzdv + d\vec{x}^2). \quad (5.53)$$

Consider two static backgrounds \mathcal{M}^- and \mathcal{M}^+ , with mass and charge parameters M_i, Q_i and M_f, Q_f respectively. Let \mathcal{M}^- and \mathcal{M}^+ be bounded by hypersurfaces Σ_- and Σ_+ . We glue the two spaces by identifying $\Sigma_- = \Sigma_+ = \Sigma$. In the present case, we take Σ to be the hypersurface $v = 0$. We are interested in the case when \mathcal{M}^- and \mathcal{M}^+ are vacuum solutions with,

$$M(v) = M_i + \Theta(v)(M_f - M_i), \quad Q(v) = Q_i + \Theta(v)(Q_f - Q_i), \quad (5.54)$$

$$f(z, v) = 1 - M(v)z^3 + \frac{1}{2}Q(v)^2z^4 \quad (5.55)$$

$$= 1 - (M_i + \Theta(v)(M_f - M_i))z^3 + \frac{1}{2}(Q_i^2 + \Theta(v)(Q_f^2 - Q_i^2))z^4, \quad (5.56)$$

where $\Theta(v)$ is the Heaviside step function. Note that (5.54) allows for the initial and final backgrounds to be AdS, AdS-Schwarzschild or AdS-RN. The

stress energy tensor (5.26) is,

$$\begin{aligned}
2\kappa T_{\mu\nu} &= z^2 \left(\frac{dM}{dv} - zQ(v) \frac{dQ}{dv} \right) \delta_{\mu\nu} \delta_{\nu\nu} \\
&= \delta(v) z^2 \left((M_f - M_i) - z(Q_f - Q_i)(Q_i + \Theta(v)(Q_f - Q_i)) \right) \delta_{\mu\nu} \delta_{\nu\nu} .
\end{aligned} \tag{5.57}$$

Note that (5.57) identically vanishes in \mathcal{M}^- and \mathcal{M}^+ and is non-zero only at $v = 0$. This discontinuity comes with a sound physical interpretation; it is associated with the presence of a thin distribution of matter at $v = 0$. The only non-zero component of the surface stress energy tensor is T^{zz} ,

$$2\kappa T_{\Sigma}^{\mu\nu} = \delta(v) z^2 \left((M_f - M_i) - z(Q_f - Q_i)(Q_i + \Theta(v)(Q_f - Q_i)) \right) k^{\mu} k^{\nu} \tag{5.58}$$

$$\equiv \delta(v) \sigma(z) \delta^{\mu z} \delta^{\nu z} . \tag{5.59}$$

Since there is no rest frame for a null shell, we cannot formally identify σ as *the* surface density. However, σ can be used to determine the results of measurements by any specified observer. This involves introducing an arbitrary congruence of timelike geodesics intersecting Σ associated with the different families of observers making measurements on the shell. An observer with four-velocity $u^{\alpha} = dx^{\alpha}/d\tau$, will measure an energy density associated with the shell $T_{\Sigma}^{\mu\nu} u_{\mu} u_{\nu} = \delta(v) \sigma(z) (k^{\mu} u_{\mu})^2$. Thus, the arbitrariness of the choice of congruence is limited to an overall factor and the quantity $\sigma(z)$ is independent of this choice. It is in this sense that we interpret $\sigma(z)$ as the shell's surface density.

From (5.35), we see that for this type of backgrounds the critical surface

is located at $v = 0$ and

$$z_c = \frac{M_f - M_i}{(Q_f - Q_i)(Q_i + \Theta(0)(Q_f - Q_i))} = \frac{2(M_f - M_i)}{Q_f^2 - Q_i^2} , \quad (5.60)$$

where we have used $\Theta(0) = 1/2$ as is conventional in distribution theory.

Evaluating σ at the critical surface we obtain,

$$\sigma(z_c) = 0 .$$

Thus, the critical surface is the locus where the shell's surface density becomes zero.

Our main interest is to study extremal spacelike surfaces in the backgrounds described above. From the point of view of the spacelike surface, there is a discontinuity in the dz/dv when the surface crosses the shell. This can easily be seen from the equations of motion. As in the previous section, consider a rectangular strip in the boundary theory. Extremizing the area functional (5.46) we obtain the equations of motion (5.48-5.49) which for $d = 3$ read,

$$zv'' + 4v'z' + (2f - \frac{z}{2} \frac{df}{dz})v'^2 = 0 , \quad (5.61)$$

$$z'' + fv'' + \frac{df}{dz}z'v' + \frac{1}{2} \frac{df}{dv}v'^2 = 0 . \quad (5.62)$$

The $z(x)$ and $v(x)$ coordinates are continuous across the shell while f and $\frac{df}{dz}$ present a finite jump. From (5.61) we see that z', v' and v'' remain finite. On the other hand,

$$\begin{aligned} \frac{df}{dv} &= z^3[(M_f - M_i) - z(Q_f - Q_i)(Q_i + \Theta(v)(Q_f - Q_i))]\delta(v) \\ &\equiv -\tilde{f}(z, v)\delta(v) \end{aligned} \quad (5.63)$$

diverges at $v = 0$. Thus, the behavior of (5.62) across the shell is,

$$z'' \sim -\frac{1}{2}\tilde{f}(z, v)\delta(v)v'^2 \quad (5.64)$$

and z' has a finite jump. Indeed,

$$(z')^+ - (z')^- = \int_{0^-}^{0^+} z'' dx = \int_{0^-}^{0^+} \frac{z''}{v'} dv \sim -\frac{1}{2}\tilde{f}(z, 0)v' \quad (5.65)$$

and the jump of $\frac{dz}{dv}$ across the shell is,

$$\Delta\left(\frac{dz}{dv}\right) \equiv \left(\frac{dz}{dv}\right)^+ - \left(\frac{dz}{dv}\right)^- = -\frac{1}{2}\tilde{f}(z, 0)$$

where $+$ and $-$ refer to quantities evaluated in \mathcal{M}^+ and \mathcal{M}^- respectively. Using (5.60) we find that the critical surface corresponds to the surface at which the jump on $\frac{dz}{dv}$ vanishes,

$$\Delta\left(\frac{dz}{dv}\right)\Big|_{z_c} = -\frac{1}{2}\tilde{f}(z_c, 0) = 0. \quad (5.66)$$

Intuitively this makes sense; we know that at z_c the mass of the shell goes to zero, the shell has disappeared and there is no reason for a jump in $\frac{dz}{dv}$.

5.3.4 Examples in $d = 3$

Let us begin our discussion for the $(3 + 1)$ -dimensional bulk theory, where the dual field theory is a $(2 + 1)$ -dimensional conformal field theory in the presence of a chemical potential. Presumably the corresponding UV-completion is given by an S^7 -reduction of 11-dimensional supergravity, which leads to an $SO(8)$ gauged supergravity in $(3 + 1)$ -dimensions. Therefore,

the boundary theory should correspond to an ABJM-like, *i.e.* Chern-Simons-matter theory in the presence of a chemical potential.¹⁰

5.3.4.1 Backgrounds that respect SSA

We will begin with the examples that do not violate SSA. A good starting point is to use the functions analyzed in [31] that were used to address scaling properties of the thermalization time with respect to the temperature and the chemical potential of the thermalized state. These are:

$$m(v) = \frac{1}{2} \left(1 + \tanh \left(\frac{v}{0.01} \right) \right) \quad \text{and} \quad q(v) = 0.9 m(v)^{2/3} . \quad (5.67)$$

It is clear from Figure 5.3 that there is no change in concavity of the entan-

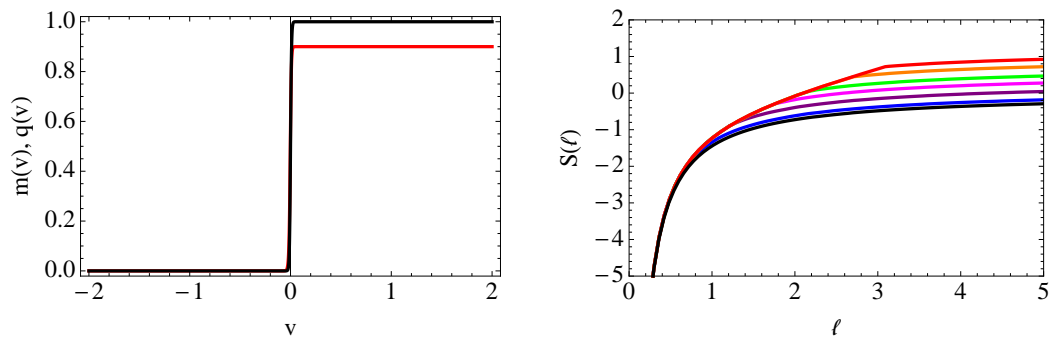


Figure 5.3: $m(v)$, $q(v)$ and $S(\ell)$ functions.

Left panel: $m(v)$ (black) and $q(v)$ (red). Right panel: $S(\ell)$, for $t_b = 0.01$ (black), 0.5 (blue), 1 (purple), 1.5 (magenta), 2 (green), 3 (orange) and 5 (red).

glement entropy function as ℓ grows for a given boundary time t_b .

¹⁰We should note that while this is a very plausible scenario, we are making an assumption that the Vaidya-type backgrounds can be embedded within gauged supergravity consistently *at least* in some well-defined limit.

According to equation (5.35), there exists a critical surface in the bulk geometry beyond which NEC is violated. It is thus instructive to analyze whether the space-like geodesics, which eventually determine the entanglement entropy, can penetrate this critical surface or not. In Figure 5.4, we show a representative family (characterized by the length of the entangling region) of geodesics corresponding to function (5.67). We also display the critical surface (5.35) and the location of the apparent horizon.

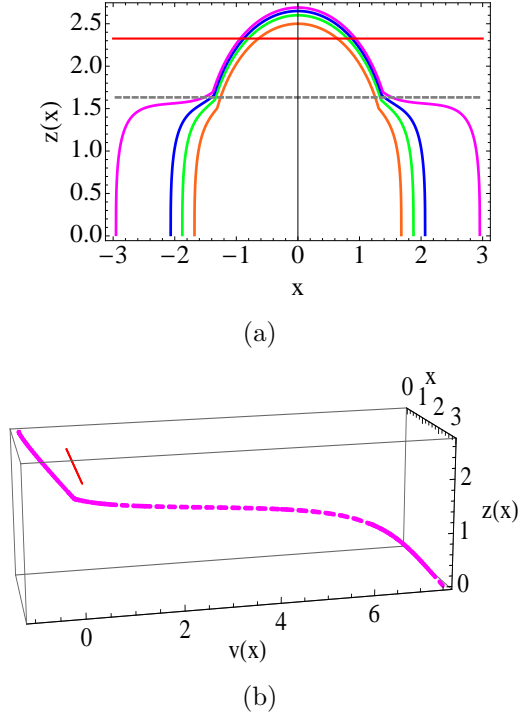


Figure 5.4: Profiles of a family of geodesics when SSA is obeyed. The dashed gray line represents the apparent horizon at $v = 0$ and the red line represents the critical surface. This family is parametrized by ℓ , the length of the entangling region at the boundary. Note that right panel shows that the geodesics do not intersect the critical surface as explained in text.

Before going further we should note that the critical surface, in the thin-shell limit, exists within a tiny¹¹ region around $v = 0$. Also, we note that the coordinate v evolves along each geodesics independently and at $v = 0$ these geodesics cross the shell, which in the thin-shell limit coincides with the apparent horizon. Figure 5.4 therefore compares the location of the critical surface to the location of the geodesics at $v = 0$.

There are two key features that stand out from Figure 5.4: First, the critical surface lies above the apparent horizon¹²; in other words, it is cloaked by the apparent horizon. Second, although the space-like surfaces cross the apparent horizon, they do not probe the *forbidden region* beyond the critical surface irrespective of how large ℓ becomes. At this point we would like to stress that the above observations seem very robust against a substantial amount of test cases. One might imagine designing a situation where the critical surface comes arbitrarily close to the apparent horizon, thus encouraging the geodesics to cross it. However, we have verified that this does not seem to happen.

Let us now illustrate a couple of more examples where the SSA condition is satisfied.

$$m(v) = 1 + \frac{1}{2} \left(1 + \tanh \left(\frac{v}{0.01} \right) \right) \quad \text{and} \quad q(v) = \frac{0.9}{2} \left(1 - \tanh \left(\frac{v}{0.01} \right) \right) . \quad (5.68)$$

¹¹The width of this region is characterized by the shell thickness parameter v_0 .

¹²*i.e.* $z_c > z_{ah}$.

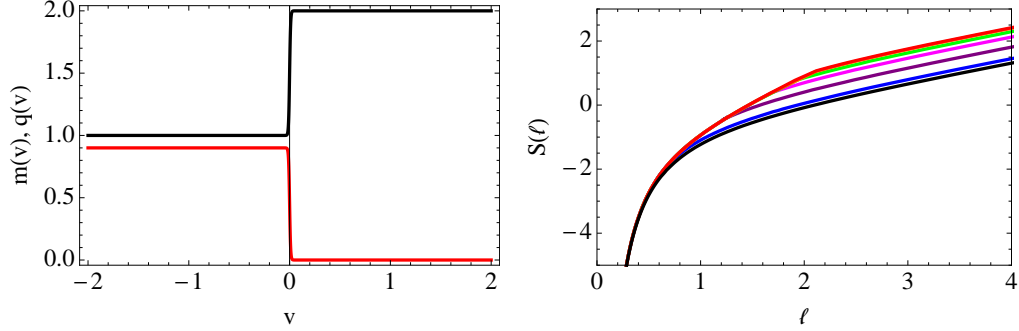


Figure 5.5: $m(v)$, $q(v)$ given in (5.68) and $S(\ell)$.
Left panel: $m(v)$ (black) and $q(v)$ (red) given in (5.68). Right panel: $S(\ell)$, for $t_b = 0.01$ (black), 0.5 (blue), 1 (purple), 1.5 (magenta), 2 (green), 3 (orange) and 5 (red).

$$m(v) = \frac{1}{2} \left(1 + \tanh \left(\frac{v}{0.01} \right) \right) \quad \text{and} \quad q(v) = \frac{0.9}{2} \left(\tanh \left(\frac{v}{0.01} \right) - \tanh \left(\frac{v-1}{0.01} \right) \right). \quad (5.69)$$

The choice functions are given in equations (5.68) and (5.69) and the corresponding figures are shown in Figure 5.5 and 5.6 respectively.

Before concluding this section, let us offer some remarks. In view of (5.44), it can be verified that the condition $dT(v)/dv \geq 0$ is not satisfied for all v with the choices made in (5.69). Thus the SSA condition is an independent constraint which is not related to the rate of change of surface gravity at the apparent horizon in the dynamical geometry. As far as the corresponding physical processes are concerned, the choices in (5.67) represents a situation in the dual field theory, where both temperature and chemical potential are increasing from a “low value” to a higher non-zero value. On physical grounds, this is perhaps the most “reasonable” process.

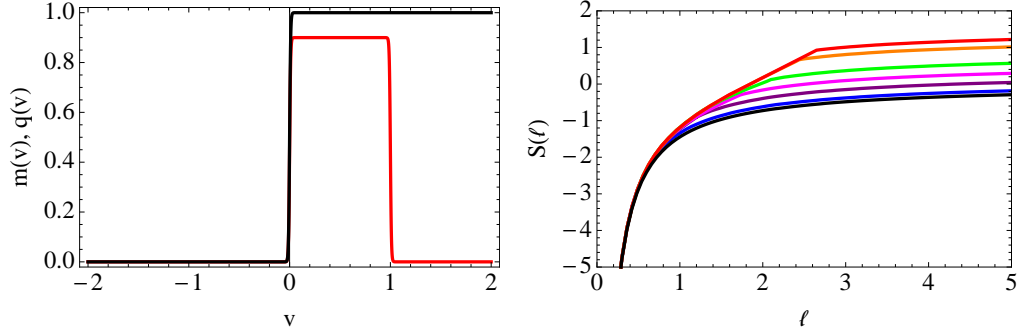


Figure 5.6: $m(v)$, $q(v)$ given in (5.69) and $S(\ell)$.
Left panel: $m(v)$ (black) and $q(v)$ (red) given in (5.69). Right panel: $S(\ell)$, for $t_b = 0.01$ (black), 0.5 (blue), 1 (purple), 1.5 (magenta), 2 (green), 3 (orange) and 5 (red).

The choices in (5.68) takes a low temperature, high chemical potential initial state to a high temperature, low chemical potential final state. Finally, the choices in (5.69) are rather exotic, which takes a low temperature, vanishing chemical potential initial state to a high temperature vanishing chemical potential final state; but does not obey $dT(v)/dv \geq 0$, $\forall v$. As far as NEC or SSA is considered, there is nothing preventing these two choices; however, whether they are realizable as solutions of gravity with a reasonable matter field is an issue we will not address here.

5.3.4.2 Backgrounds that violate SSA

Now let us illustrate a few examples where SSA is violated. One such choice is:

$$m(v) = 0.95 + \frac{0.05}{2} \left(1 + \tanh \left(\frac{v}{0.01} \right) \right) \quad \text{and} \quad q(v) = \frac{0.9}{2} \left(1 + \tanh \left(\frac{v}{0.01} \right) \right) . \quad (5.70)$$

The corresponding illustration is shown in Figure 5.7. The corresponding geodesic is shown in Figure 5.8. Once again, the critical surface exists only around a small neighbourhood of $v = 0$ and the geodesics reach the shell at $v = 0$. Note here that both the features alluded to in the previous subsection are gone: First, the critical surface lies outside the apparent horizon at $v = 0$; second, the minimal area surface *brings news* from the *forbidden region* in the bulk by probing the region beyond the critical surface. This is perceived as the violation of SSA condition in the boundary theory. At this point we emphasize that these observations seem rather generic and hence we will not pictorially illustrate a similar behaviour of the geodesics for other representative cases, whenever SSA is violated.

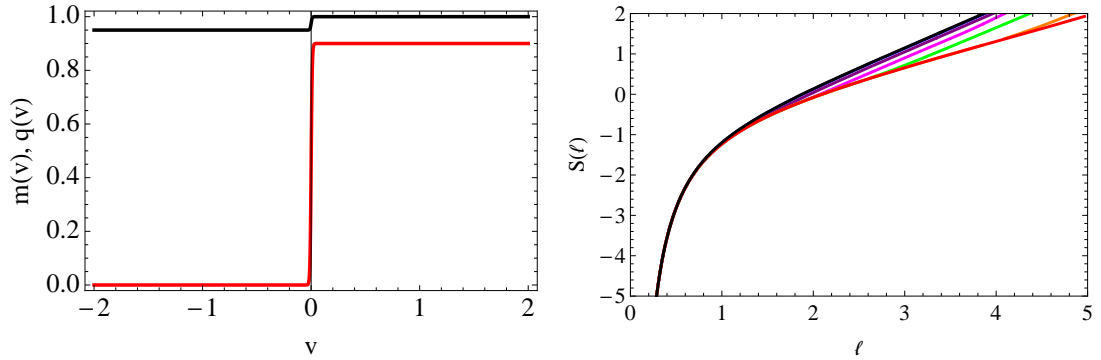


Figure 5.7: $m(v)$, $q(v)$ given in (5.70) and $S(\ell)$.
Left panel: $m(v)$ (black) and $q(v)$ (red) given in (5.70). Right panel: $S(\ell)$, for $t_b = 0.01$ (black), 0.5 (blue), 1 (purple), 1.5 (magenta), 2 (green), 3 (orange) and 5 (red).

Let us now take a second example where the violation of SSA is ob-

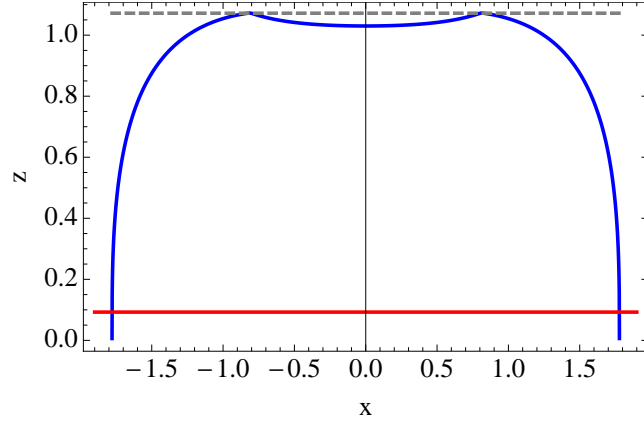


Figure 5.8: Profile of geodesic when SSA is violated corresponding to the choice (5.70).

The dashed line represents the apparent horizon or the position of the shell at $v = 0$ and the red line depicts the critical surface at $v = 0$. Clearly the geodesic probes the region behind the critical surface at $v = 0$.

served:

$$m(v) = \frac{1}{2} \left(1 + \tanh \left(\frac{v}{0.01} \right) \right) \text{ and } q(v) = \frac{0.9}{2} \left(1 + \tanh \left(\frac{v-1}{0.01} \right) \right) . \quad (5.71)$$

In this case also the minimal area surface probes the region beyond the critical surface. The corresponding plots showing the violation of SSA are presented in Figure 5.9.

Once again, a few comments are in order. First, it can be checked that for the choices in (5.71) we will get $dT(v)/dv \geq 0$ and $dS(v)/dv \geq 0$ and still a violation of SSA. Thus, the SSA condition is indeed independent of these. Intuitively, the process in (5.71) is not very meaningful since it seems to allow for the black hole to accumulate charges keeping its mass fixed. On the other hand, there is no such *a priori* objection to the process in (5.70), and still

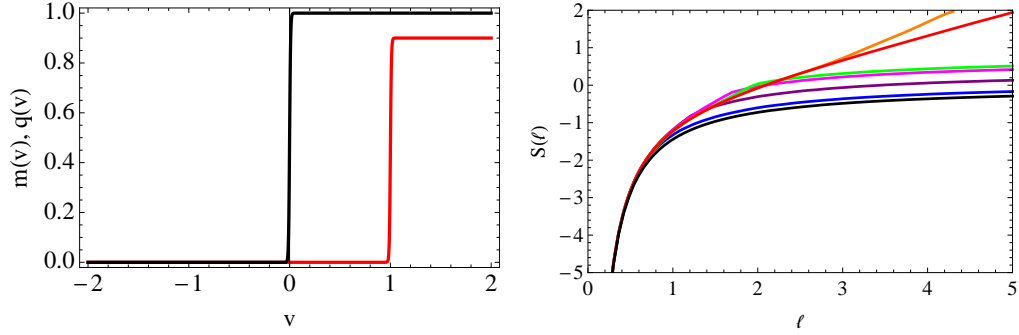


Figure 5.9: $m(v)$, $q(v)$ given in (5.71) and $S(\ell)$.
Left panel: $m(v)$ (black) and $q(v)$ (red) given in (5.71). Right panel: $S(\ell)$, for $t_b = 0.01$ (black), 0.5 (blue), 1 (purple), 1.5 (magenta), 2 (green), 3 (orange) and 5 (red).

SSA is violated. This indicates that SSA is a rather non-trivial condition on the allowed trajectories a thermalization process might take for a given field theory.

5.3.5 Examples in $d = 4$

We will now move up by one dimension and consider a (3+1)-dimensional conformal field theory. The dual geometry will correspond to the formation of a charged black hole in five-dimensional AdS-space. In this case, the possible UV-completion will be given by an S^5 -reduction (or a reduction on a Sasaki-Einstein five-manifold) of type IIB supergravity truncated to the $\mathcal{N} = 2$ sector with an $U(1)^3$ symmetry (or at least one $U(1)$). Thus the dual field theory is presumably a cousin of the prototype $\mathcal{N} = 4$ super Yang-Mills (SYM) theory

in the presence of a chemical potential.¹³

5.3.5.1 Backgrounds that respect SSA

We will discuss similar processes as in the case for $d = 3$. The qualitative features are very similar here, and hence we will limit ourselves in terms of the details. The analogous choices that preserve SSA are pictorially represented in Figure 5.10 and 5.11. Note that, Figure 5.10 corresponds to the choices used in [31] to analyze the scaling of the thermalization time with temperature and chemical potential of the system.

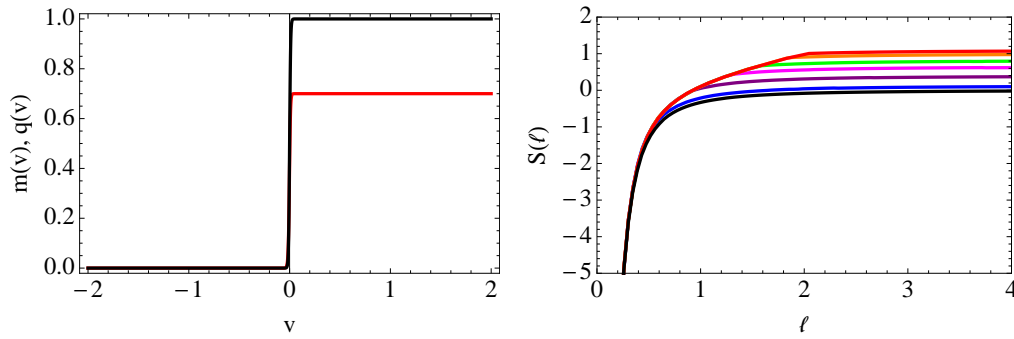


Figure 5.10: Example 1 of $m(v)$, $q(v)$ and $S(\ell)$ in $d = 4$. Left panel: $m(v)$ (black) and $q(v)$ (red). Right panel: $S(\ell)$, for $t_b = 0.01$ (black), 0.5 (blue), 1 (purple), 1.5 (magenta), 2 (green), 3 (orange) and 5 (red).

¹³Once again we note that this claim needs to be rigorously demonstrated, which we will not attempt here.

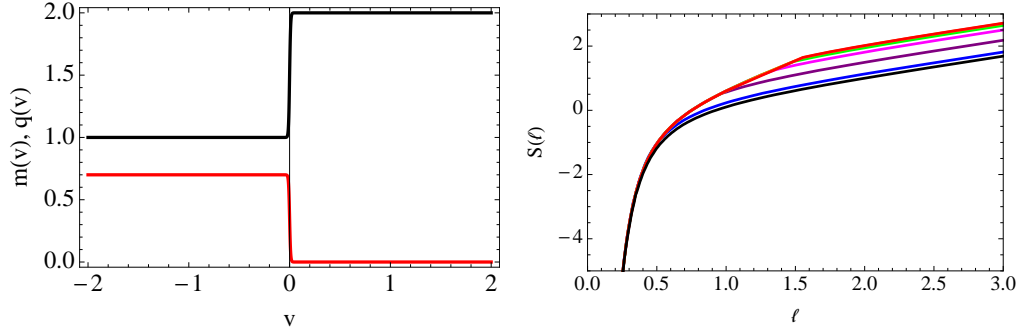


Figure 5.11: Example 2 of $m(v)$, $q(v)$ and $S(\ell)$ in $d = 4$.

Left panel: $m(v)$ (black) and $q(v)$ (red). Right panel: $S(\ell)$, for $t_b = 0.01$ (black), 0.5 (blue), 1 (purple), 1.5 (magenta), 2 (green), 3 (orange) and 5 (red).

5.3.5.2 Backgrounds that violate SSA

Once more, we will keep our discussion very brief and present the examples that violate SSA. These are shown in Figure 5.13 and Figure 5.14). The choices are analogous to the ones made in (5.70) and (5.71). In Figure 5.14 the change in concavity is not as clear from the graph as in the other examples but it is easy to verify it numerically¹⁴. This physics can also be observed by studying the geodesics, which penetrate the critical surface whenever there is a violation of SSA but not otherwise.

¹⁴Since the curves are initially concave we just have to verify that after certain value of $l = l_0$ they become convex. Namely, we verify that if we take any two points $x_1, x_2 > l_0$ and we will have $S(yx_1 + (1 - y)x_2) \leq yS(x_1) + (1 - y)S(x_2)$ where $0 < y < 1$.

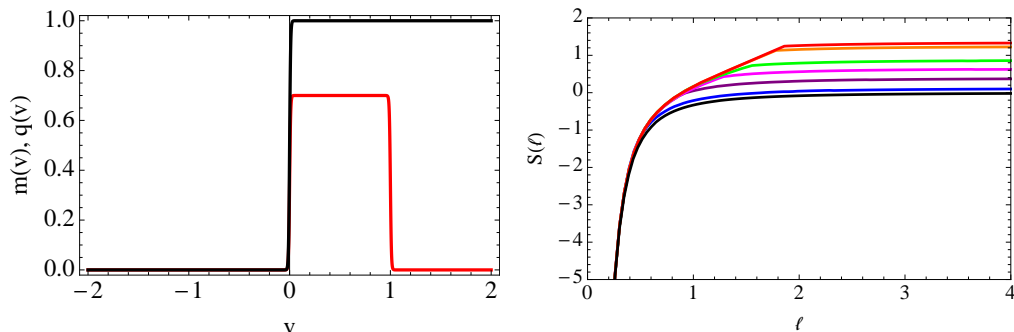


Figure 5.12: Example 3 of $m(v)$, $q(v)$ and $S(\ell)$ in $d = 4$.
Left panel: $m(v)$ (black) and $q(v)$ (red). Right panel: $S(\ell)$, for $t_b = 0.01$ (black), 0.5 (blue), 1 (purple), 1.5 (magenta), 2 (green), 3 (orange) and 5 (red).

5.4 Discussion and conclusions

In this chapter we have explored and demonstrated an interesting pictorial realization of the strong sub-additivity condition in terms of the bulk gravitational description. In the presence of charge, the dynamical evolution from a low temperature, low chemical potential pure state to a thermalized state with a non-zero value of the chemical potential does indeed sharpen the connection between the bulk null energy condition constraint and the strong sub-additivity of entanglement entropy in the boundary field theory, which was alluded to in [6, 35].

Our investigations suggest that the dual field theory disallows specific choices of the mass and the charge functions for which it is possible to penetrate the critical surface. However, as we have learned now, the nature of the violation of the NEC depends on the class of examples we choose; such as

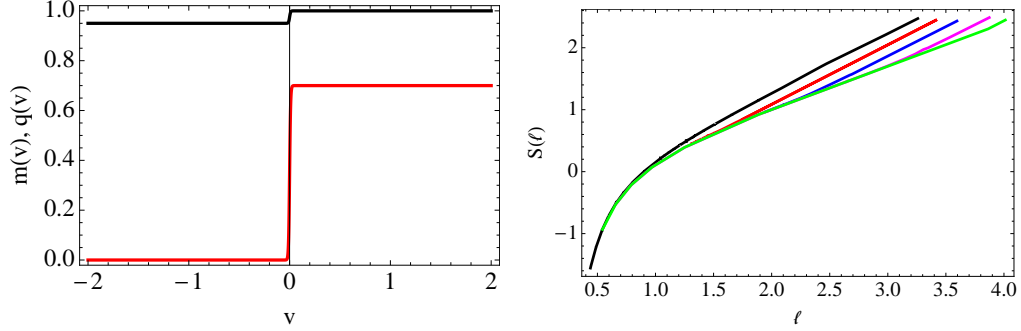


Figure 5.13: Example 1 of violation of SSA in $d = 4$. $m(v)$ (black) and $q(v)$ (red). Right panel: $S(l)$ for $t_b = 0.5$ (black), 1.5 (red), 2.0 (blue), 2.5 (magenta) and 3.0 (green).

the details which have qualitatively distinct behaviours for the charged case and the uncharged one. Generally, the NEC is an algebraic constraint on the bulk energy-momentum tensor, which — should a general result exist — may correspond to an algebraic constraint in the boundary theory as well. Strong sub-additivity depends crucially on the concavity property of the entropy function and thus it is an intriguing possibility to consider establishing a direct *equivalence* between the bulk null energy condition and the concavity property of the entropy function at the boundary. See [168] for some recent progress towards a *proof*; however, it does not necessarily apply for backgrounds where a black hole eventually forms.

Coming back to our case, it is perhaps surprising how SSA can be obeyed for some examples, specially since the critical surface always exists for any generic mass and charge functions. Unlike the time-independent cases, where no extremal surface can penetrate the black hole event horizon, the

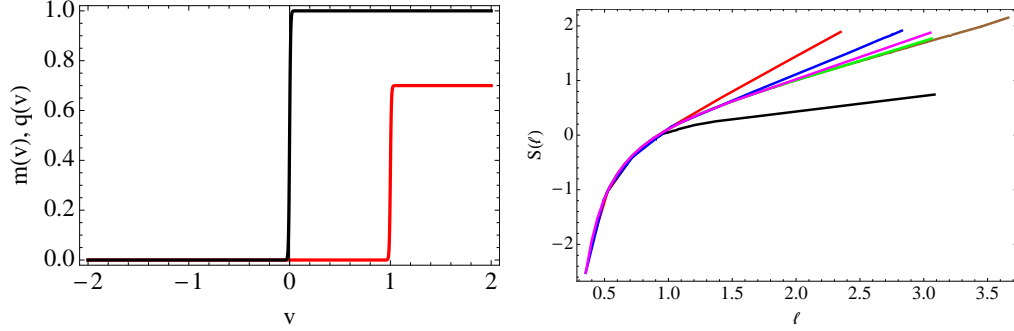


Figure 5.14: Example 2 of violation of SSA in $d = 4$. $m(v)$ (black) and $q(v)$ (red). Right panel: $S(l)$ for $t_b = 1.0$ (black), 1.5 (red), 2.5 (blue), 3.0 (magenta) and 3.5 (green). For the blue and magenta curves we have numerically verified the change in concavity.

Vaidya backgrounds give rise to an apparent horizon that can be penetrated by a space-like surface. The critical surface may lie above or below this apparent horizon. If it is below ($z_c < z_{\text{ah}}$) there is violation of NEC and SSA; If it is above ($z_c > z_{\text{ah}}$) NEC and SSA are respected. Let us emphasize that there is no *a priori* criterion that prohibits the minimal surface to penetrate the critical surface when it is cloaked by the apparent horizon. Nevertheless, this is what we observe. It would be interesting to understand how general this feature is. We can also ask if the analysis changes if we consider extremal black holes. If the initial state is the vacuum and the final state is extremal (mass and charge functions similar to Figure 5.10), the critical surface is cloaked by the apparent horizon ($z_c > z_{\text{ah}}$) and NEC and SSA are obeyed, in agreement with our observations. On the other hand, if the initial state is extremal and the final state is an arbitrary thermal state we cannot conclude something general.

However, we do not see new features emerging in the analysis.

Therefore, based on our observations we can venture a *naïve* characterization for the choice functions. Let us assume that $m'(v) \geq 0$. This is required by continuity with the results known in $q(v) \rightarrow 0$ limit. Given this, we can characterize a charge function $q(v)$ to be *good* if $z_c > z_{\text{ah}}$ for all times and *bad* if $z_c < z_{\text{ah}}$ for any time. Of course, we also need to impose a constraint on the maximum magnitude of the mass and the charge functions in order to avoid the *naked*. Such a characterization, at present, is only a plausibility.

It is intriguing that the SSA condition seems to constrain the global time-evolution process but does not say anything about the initial conditions. In general, it is possible that given an *arbitrary but reasonable* initial condition the dual field theory undergoes time-evolution, but never thermalizes or obtains a steady-state phase. Such a process, once obtained by solving Einstein gravity with a reasonable matter field in the bulk, will surely preserve NEC and hence SSA. It will thus be interesting to investigate whether the SSA condition plays a similar role for more conventional systems rather than large N gauge theories having a gravity dual. We hope to address these issues in details in future.

Chapter 6

Conclusions

The last two decades have brought lots of interesting ideas to theoretical physics, particularly as a result of the gauge/gravity correspondence. The applications of this approach to the study of strongly coupled theories have branched out to many subfields in high energy theory and condensed matter and remarkable phenomena have been explored through such formalism.

The studies presented in this thesis are some examples of such program. We have shown investigations on different techniques to probe the dissipation and thermalization of perturbations in a variety of systems. These included systems near and far from thermodynamic equilibrium, dissipation in the presence of magnetic fields and systems close to a critical point. These studies have shed some light about different features of strongly coupled theories, such as fast thermalization of fluctuations in non-commutative geometries, universal properties of two-point functions in theories at a quantum critical point and a direct correlation between the null energy condition in the bulk and the strong subadditivity property of entanglement entropy on the boundary.

There are several open issues that are not investigated in this work. One of such issues is the lack of a complete microscopic description of the

degrees of freedom at the black hole horizon that could show directly the non-local character of such system. There are other properties of non-commutative SYM theories that are not included here; for instance, the calculation of entanglement entropy and expectation value of Wilson loops in this system. Those computations, however, have been presented in [67]. One could also extend the investigations of Chapter 4 to more general operators in order identify more precisely the behavior in the full space of parameters (z, θ) . And, finally, a definite proof of the prescription for entanglement entropy in time-dependent systems is still lacking; a further step in that direction is given in this work by uncovering the equivalence between the bulk null energy condition and the concavity of the entropy function at the boundary. It will be interesting to investigate whether the strong subadditivity condition plays a similar role for more conventional systems rather than large N gauge theories.

Appendices

Appendix A

Appendix to Fast Scrambling in NCSYM

In this appendix, we show that the poles in the retarded Green's function of the boundary theory operator which is dual to a minimally-coupled massless scalar field in the bulk, are all in the lower half of the complex frequency plane. This then implies that the non-commutative field theory under consideration is stable against the small perturbations caused by turning on the aforementioned operator. Our analysis here follows the argument given in [93] where it was shown that the quasi-normal frequencies of a minimally-coupled massless scalar field in the Schwarzschild AdS background are all located in the lower half of the complex frequency plane.

The equation of motion for a minimally-coupled massless scalar in the non-extremal background (2.22) is given in (2.27). Defining the tortoise coordinate u_* by

$$\frac{du_*}{du} = \frac{1}{u^2 f(u)}, \quad (\text{A.1})$$

the equation (2.27) can be put in the form of a Schrödinger equation

$$\Psi''(u_*) + [\omega^2 - V(u_*)]\Psi(u_*) = 0, \quad (\text{A.2})$$

where $\Psi(u) = u^{3/2}\varphi(u)$ and

$$V(u_*) = f(u) \left[\frac{k^2}{h(u)} + \frac{3}{2}u^3 f'(u) + \frac{15}{4}u^2 f(u) \right]. \quad (\text{A.3})$$

In the above expression, it is understood that u is a function of u_* . Note that the potential blows up in the asymptotic boundary ($u_* \rightarrow 0$) and vanishes exponentially at the horizon where $u_* \rightarrow -\infty$.

Suppose now that Ψ is a quasi-normal mode with the associated quasi-normal frequencies ω_n . Since, by definition, the quasi-normal mode Ψ is in-falling near the horizon, we isolate its near horizon behavior and define

$$\Psi(u_*) \sim e^{-i\omega_n u_*} \psi(u_*). \quad (\text{A.4})$$

Note that $\psi(u_*)$ vanishes in the asymptotic $u_* \rightarrow 0$ region. Substituting (A.4) into (A.2), and changing back to the u -coordinate, one easily obtains

$$\partial_u [u^2 f(u) \partial_u \psi(u)] - 2i\omega_n \partial_u \psi(u) + U(u) \psi(u) = 0, \quad (\text{A.5})$$

with

$$U(u) = \frac{k^2}{u^2 h(u)} + \frac{3}{2}u f'(u) + \frac{15}{4}f(u). \quad (\text{A.6})$$

Now, multiplying (A.5) by $\bar{\psi}$ and integrating the result, we obtain

$$\int_1^\infty du \left[u^2 f(u) |\psi'(u)|^2 + 2i\omega_n \bar{\psi}(u) \psi'(u) + U(u) |\psi(u)|^2 \right] = 0, \quad (\text{A.7})$$

where we have also performed an integration by parts. Subtracting (A.7) from its complex conjugate yields

$$\int_1^\infty du \left[\omega_n \bar{\psi}(u) \psi'(u) + \bar{\omega}_n \psi(u) \bar{\psi}'(u) \right] = 0, \quad (\text{A.8})$$

which, after an integration by parts, results in

$$(\operatorname{Im} \omega_n) \int_1^\infty \bar{\psi}(u) \psi'(u) du = -\frac{i}{2} \bar{\omega}_n |\psi(u=1)|^2. \quad (\text{A.9})$$

Note that, from the above equation, for $\operatorname{Re} \omega_n \neq 0$, one obtains $\operatorname{Im} \omega_n \neq 0$.

Substituting (A.9) into (A.7), one obtains

$$\int_1^\infty du \left[u^2 f(u) |\psi'(u)|^2 + U(u) |\psi(u)|^2 \right] + \frac{1}{\operatorname{Im} \omega_n} |\omega_n|^2 |\psi(u=1)|^2 = 0. \quad (\text{A.10})$$

Since the potential $U(u)$, given in (A.6), is positive definite for all (real) values of k and a in the range $u \in [1, \infty)$, one deduces from (A.10) that $\operatorname{Im} \omega_n < 0$.

Appendix B

Appendix to Brownian motion in NCSYM

B.1 Solutions for the string embedding

In this appendix we will derive explicitly the solutions to the equations of motion considered in sections 3.3.2 and 3.4.2. At low frequencies, the solutions can be obtained by means of the matching technique [26, 13] (see also [82]). To find these solutions, consider three regimes: (A) the near horizon solution ($y \sim 1$) for arbitrary ν , (B) the solution for arbitrary y but $\nu \ll 1$, and (C) the asymptotic solution ($y \rightarrow \infty$) for arbitrary ν . The idea is to find the approximate solutions for each of the three regimes, and to match these to leading order in ν .

B.1.1 Solution for the AdS-Schwarzschild black hole

Here we will solve the equation (3.59), by considering the three regimes alluded above.

(A) In this regime we can focus on the equation as $y \rightarrow 1$:

$$0 = g''(y) + \frac{1}{y-1}g'(y) + \frac{\nu^2}{16(y-1)^2}g(y). \quad (\text{B.1})$$

We have dropped the subindex i because the equations of motion are the same

for both $i = 2, 3$. The general solution in this regime is

$$g^A(y) = A^{(\text{out})}(y-1)^{i\nu/4} + A^{(\text{in})}(y-1)^{-i\nu/4}, \quad (\text{B.2})$$

where the coefficients $A^{(\text{out})}$ and $A^{(\text{in})}$ correspond to outgoing and ingoing modes respectively. Normalizing each solution according to (3.15) and expanding for low frequencies, we obtain

$$g^{A(\text{out/in})}(y) = (y-1)^{\pm i\nu/4} \sim 1 \pm \frac{i\nu}{4} \log(y-1) + \mathcal{O}(\nu^2). \quad (\text{B.3})$$

(B) For the regime of low frequencies we proceed to expand the solution as a series of the form

$$g^B(y) = g_0(y) + \nu g_1(y) + \nu^2 g_2(y) + \dots \quad (\text{B.4})$$

The first function can be obtained analytically by solving the equation

$$0 = g_0''(y) + \frac{4y^3}{y^4 - 1} g_0'(y). \quad (\text{B.5})$$

The general solution goes as follows:

$$g_0(y) = B_1 + B_2 \left(\tan^{-1}(y) + \tanh^{-1}(y) \right), \quad (\text{B.6})$$

where, in order to have a reliable expansion in frequencies, we have to assume that the constants B_1 and B_2 are independent of ν . In order to find the appropriate coefficients B_1 and B_2 to obtain the ingoing and outgoing modes we expand around the horizon and match with the first term in (B.3). After doing so we obtain $B_1^{(\text{out/in})} = 1$ and $B_2^{(\text{out/in})} = 0$, so

$$g_0^{(\text{out/in})}(y) = 1. \quad (\text{B.7})$$

The equation for $g_1(y)$ turns out to be the same as for $g_0(y)$, but now the matching has to be done with the second term in (B.3). At the end we get

$$\begin{aligned} g_1^{(\text{out/in})}(y) &= \pm \frac{1}{8} ((2+i)\pi + 2i \log(2)) \mp \frac{i}{2} (\tan^{-1}(y) + \tanh^{-1}(y)) \\ &\sim \pm \frac{i}{4} \log(y-1) \text{ as } y \rightarrow 1. \end{aligned} \quad (\text{B.8})$$

Then, up to this order we can write

$$g^{B(\text{out/in})}(y) = 1 \pm \frac{1}{8} \nu ((2+i)\pi + 2i \log(2)) \mp \frac{i}{2} \nu (\tan^{-1}(y) + \tanh^{-1}(y)) + \mathcal{O}(\nu^2). \quad (\text{B.9})$$

Asymptotically, these solutions behave as

$$g^{B(\text{out/in})}(y) \sim \left[1 \mp \frac{i}{8} \nu (\pi - \log(4)) + \mathcal{O}(\nu^2) \right] \mp \frac{1}{y^3} \left[\frac{i}{3} \nu + \mathcal{O}(\nu^2) \right] + \mathcal{O}(1/y^4). \quad (\text{B.10})$$

(C) The general solution in region C can be found perturbatively, as a series expansion in $1/y$. The leading order terms go as follows:

$$g^C(y) = C_1 \left[1 + \frac{\nu^2}{2y^2} + \mathcal{O}(1/y^4) \right] + \frac{C_2}{y^3} \left[1 - \frac{\nu^2}{10y^2} + \mathcal{O}(1/y^4) \right]. \quad (\text{B.11})$$

Again, comparing this with (B.10), in the low frequency limit, we obtain

$$C_1^{(\text{out/in})} = 1 \mp \frac{i}{8} \nu (\pi - \log(4)), \quad \text{and} \quad C_2^{(\text{out/in})} = \mp \frac{i}{3} \nu. \quad (\text{B.12})$$

Thus, the *normalized* asymptotic solutions for modes corresponding to outgoing and ingoing waves at the horizon, can be written as

$$g^{C(\text{out/in})}(y) \sim \left(1 \mp \frac{i}{8} \nu (\pi - \log(4)) \right) \left(1 + \frac{\nu^2}{2y^2} \right) \mp \frac{i\nu}{3y^3} + \mathcal{O}(1/y^4). \quad (\text{B.13})$$

This agrees with the solutions reported in [26]. Note in particular that $g^{(\text{out})}(y) = g^{(\text{in})}(y)^*$.

B.1.2 Solution for the Maldacena-Russo background

Next, we solve (4.9) following a similar procedure as the one used for the commutative case.

(A) In this regime we can focus on the equation as $y \rightarrow 1$:

$$0 = g_{\pm}''(y) + \frac{1}{y-1}g_{\pm}'(y) + \frac{\nu^2}{16(y-1)^2}g_{\pm}(y), \quad (\text{B.14})$$

which is equivalent to (B.1). As expected, the IR is not affected by the non-commutativity. The general solution in this regime is

$$g_{\pm}^A(y) = A_{\pm}^{(\text{out})}(y-1)^{i\nu/4} + A_{\pm}^{(\text{in})}(y-1)^{-i\nu/4}, \quad (\text{B.15})$$

where the coefficients $A_{\pm}^{(\text{out})}$ and $A_{\pm}^{(\text{in})}$ correspond to outgoing and ingoing modes respectively. Normalizing these solution and expanding for low frequencies, we obtain

$$g_{\pm}^{A(\text{out/in})}(y) = (y-1)^{\pm i\nu/4} \sim 1 \pm \frac{i\nu}{4} \log(y-1) + \mathcal{O}(\nu^2). \quad (\text{B.16})$$

(B) In this regime we start by expanding the solution as a series in ν :

$$g_{\pm}^B(y) = g_{0\pm}(y) + \nu g_{1\pm}(y) + \nu^2 g_{2\pm}(y) + \dots \quad (\text{B.17})$$

The first function can be obtained analytically by solving the equation

$$0 = g_{0\pm}''(y) + \frac{4(1+b^4)y^3}{(y^4-1)(1+b^4y^4)}g_{0\pm}'(y). \quad (\text{B.18})$$

The general solution goes as follows:

$$g_{0\pm}(y) = B_{\pm 1} + B_{\pm 2} \left[b^4 y - \frac{1}{2}(1+b^4) \left(\tan^{-1}(y) + \tanh^{-1}(y) \right) \right], \quad (\text{B.19})$$

where, in order to have a reliable expansion in frequencies, we have to assume that the constants $B_{\pm 1}$ and $B_{\pm 2}$ are independent of ν . We then expand near the horizon and match the above solution with the first term in (B.16) to obtain the outgoing and ingoing modes. We find that $B_{\pm 1}^{(\text{out/in})} = 1$ and $B_{\pm 2}^{(\text{out/in})} = 0$, so

$$g_{0\pm}^{(\text{out/in})}(y) = 1. \quad (\text{B.20})$$

Plugging (B.17) into the equation of motion and using (B.20) we can derive the following equation for the next leading order term of the normalized modes:

$$0 = g_{1\pm}''(y) + \frac{4(1+b^4)y^3}{(y^4-1)(1+b^4y^4)}g_{1\pm}'(y) \pm \frac{4b^2y^3}{(y^4-1)(1+b^4y^4)}. \quad (\text{B.21})$$

The solution to this equation is

$$g_{1\pm}(y) = B_{\pm 1} + B_{\pm 2} \left[b^4 y - \frac{1}{2}(1+b^4) (\tan^{-1}(y) + \tanh^{-1}(y)) \right] \mp \frac{1}{2b^2} (\tan^{-1}(y) + \tanh^{-1}(y)), \quad (\text{B.22})$$

and after expanding around the horizon and matching with the second term in (B.16) we obtain

$$B_{\pm 1}^{(\text{out})} = \pm \frac{(1-2i)\pi \pm b^2((2+i)\pi - i(8 - \log(4))) + \log(4)}{8(b^2 \mp i)}, \quad B_{\pm 2}^{(\text{out})} = \frac{i}{b^2(b^2 \mp i)}, \quad (\text{B.23})$$

and

$$B_{\pm 1}^{(\text{in})} = \pm \frac{(1-2i)\pi \mp b^2((2+i)\pi - i(8 - \log(4))) + \log(4)}{8(b^2 \pm i)}, \quad B_{\pm 2}^{(\text{in})} = -\frac{i}{b^2(b^2 \pm i)}. \quad (\text{B.24})$$

Asymptotically, the solutions $g_{\pm}^{B(\text{out/in})}(y) = g_{0\pm}^{(\text{out/in})}(y) + \nu g_{1\pm}^{(\text{out/in})}(y) + \mathcal{O}(\nu^2)$

behave as

$$g_{\pm}^{B(\text{out})}(y) \sim \left[\frac{ib^2\nu}{b^2 \mp i} y + \left(1 - \frac{ib^2\nu}{b^2 \mp i} - \frac{1}{8}i\nu(\pi - \log(4)) \right) + \mathcal{O}(\nu^2) \right] + \mathcal{O}(1/y), \quad (\text{B.25})$$

and

$$g_{\pm}^{B(\text{in})}(y) \sim \left[-\frac{ib^2\nu}{b^2 \pm i} y + \left(1 + \frac{ib^2\nu}{b^2 \pm i} + \frac{1}{8}i\nu(\pi - \log(4)) \right) + \mathcal{O}(\nu^2) \right] + \mathcal{O}(1/y). \quad (\text{B.26})$$

(C) The general solution in region C can be found as a series expansion in $1/y$. The leading order terms are:

$$g_{\pm}^C(y) = C_{\pm 1} y \left[1 - \frac{\nu^2}{2y^2} + \mathcal{O}(1/y^3) \right] + C_{\pm 2} \left[1 - \frac{\nu^2}{6y^2} + \mathcal{O}(1/y^3) \right]. \quad (\text{B.27})$$

Comparing this with (B.25) and (B.26) we obtain

$$C_{\pm 1}^{(\text{out})} = \frac{ib^2\nu}{b^2 \mp i}, \quad C_{\pm 2}^{(\text{out})} = 1 - \frac{ib^2\nu}{b^2 \mp i} - \frac{1}{8}i\nu(\pi - \log(4)), \quad (\text{B.28})$$

and

$$C_{\pm 1}^{(\text{in})} = -\frac{ib^2\nu}{b^2 \pm i}, \quad C_{\pm 2}^{(\text{in})} = 1 + \frac{ib^2\nu}{b^2 \pm i} + \frac{1}{8}i\nu(\pi - \log(4)). \quad (\text{B.29})$$

Thus, the *normalized* asymptotic solutions, in the low frequency limit, and for modes corresponding to outgoing and ingoing waves at the horizon, can be written as

$$g_{\pm}^{C(\text{out})}(y) \sim \frac{ib^2\nu y}{b^2 \mp i} \left(1 - \frac{\nu^2}{2y^2} \right) + \left(1 - \frac{ib^2\nu}{b^2 \mp i} - \frac{1}{8}i\nu(\pi - \log(4)) \right) \left(1 - \frac{\nu^2}{6y^2} \right) + \mathcal{O}(1/y^3), \quad (\text{B.30})$$

and

$$g_{\pm}^{C(\text{in})}(y) \sim -\frac{ib^2\nu y}{b^2 \pm i} \left(1 - \frac{\nu^2}{2y^2}\right) + \left(1 + \frac{ib^2\nu}{b^2 \pm i} + \frac{1}{8}i\nu(\pi - \log(4))\right) \left(1 - \frac{\nu^2}{6y^2}\right) + \mathcal{O}(1/y^3). \quad (\text{B.31})$$

It is clear that $g_{\pm}^{(\text{out})}(y) = g_{\pm}^{(\text{in})}(y)^*$ as was found for the case analyzed in appendix B.1.1.

Appendix C

Appendix to Quantum Fluctuations in Theories with Hyperscaling Violation

In this appendix we will derive the solutions to the equation of motion (4.51) given the boundary conditions to be discussed below. At low frequencies, the solutions can be obtained by means of a matching technique [26, 13, 68]. To find the solutions, consider three regimes: (I) the near horizon solution ($\rho \sim 1$) for arbitrary \mathfrak{w} , (II) the solution for arbitrary ρ in the limit $\mathfrak{w} \ll 1$, and (III) the asymptotic $\rho \rightarrow \infty$ solution for arbitrary \mathfrak{w} . The idea is to find the approximate solutions for each of the three regimes and to match them to leading order in \mathfrak{w} . We implement the above matching method and write down the solutions only for the two cases of $d = 2$ and $d = 3$.

Before focusing on these two cases, let us make some remarks that are valid for arbitrary d . In terms of the ‘tortoise coordinate’ defined by

$$dr_* = \frac{dr}{r^2 f(r)}, \quad (\text{C.1})$$

with the following behavior near the horizon

$$r_* \sim \frac{1}{d(d+1)(r-r_0)} + \cdots, \quad (\text{C.2})$$

we expect two solutions in the regime (I) of the form

$$x^{(\text{out})}(t, r) \sim e^{-i\omega(t+r_*)} \sim e^{-i\omega t} e^{-\frac{i\omega}{d(d+1)(r-r_0)}}, \quad (\text{C.3})$$

$$x^{(\text{in})}(t, r) \sim e^{-i\omega(t-r_*)} \sim e^{-i\omega t} e^{\frac{i\omega}{d(d+1)(r-r_0)}}, \quad (\text{C.4})$$

corresponding to outgoing and ingoing modes, respectively. The reason being is that, in this coordinate system, the (t, r_*) part of the metric is conformally flat and the equation of motion near $r \rightarrow r_0$ (or $r_* \rightarrow \infty$) behaves similar to the wave equation in flat space. In fact, near the horizon, the equation (4.51) reduces to

$$\left[d^2(d+1)^2(\rho-1)^2 g'_{\mathbf{w}}(\rho) \right]' + \frac{\mathbf{w}^2}{(\rho-1)^2} g_{\mathbf{w}}(\rho) = 0, \quad (\text{C.5})$$

whose independent solutions are precisely given by¹

$$\begin{aligned} g_{\mathbf{w}}^{(\text{out/in})}(\rho) &= e^{\mp \frac{i\mathbf{w}}{d(d+1)(\rho-1)}} \\ &= 1 \mp \frac{i\mathbf{w}}{d(d+1)(\rho-1)} + \mathcal{O}(\mathbf{w}^2). \end{aligned} \quad (\text{C.6})$$

Asymptotically, one has $f(\rho) \rightarrow 1$, so the equation (4.51) reduces to

$$\frac{d}{d\rho} \left[\rho^4 g'_{\mathbf{w}}(\rho) \right] + \mathbf{w}^2 g_{\mathbf{w}}(\rho) = 0, \quad (\text{C.7})$$

¹Note that the dots in (C.2) contain a subleading logarithmic divergence of the form $\sim D \log(\rho-1)$, for some constant D . This factor enters in the expressions for $g_{\mathbf{w}}(\rho)$ as

$$\begin{aligned} g_{\mathbf{w}}^{(\text{out/in})}(\rho) &= (\rho-1)^{\mp iD\mathbf{w}} e^{\mp \frac{i\mathbf{w}}{d(d+1)(\rho-1)}} \\ &= 1 \mp \frac{i\mathbf{w}}{d(d+1)(\rho-1)} \mp i\mathbf{w}D \log(\rho-1) + \mathcal{O}(\mathbf{w}^2), \end{aligned}$$

but it does not affect the term of order $\mathcal{O}(1)$ in frequency.

for arbitrary d . The general solution to (C.7) is given by

$$\begin{aligned} g_{\mathbf{w}}(\rho) &= A_1 \left(1 - \frac{i\mathbf{w}}{\rho}\right) e^{i\mathbf{w}/\rho} + A_2 \left(1 + \frac{i\mathbf{w}}{\rho}\right) e^{-i\mathbf{w}/\rho} \\ &= C_1 \left(1 + \frac{\mathbf{w}^2}{2\rho^2}\right) + C_2 \frac{i\mathbf{w}^3}{3\rho^3} + \mathcal{O}(1/\rho^4), \end{aligned} \quad (\text{C.8})$$

where $C_1 = A_1 + A_2$ and $C_2 = A_1 - A_2$.

In the regime (II) one can expand $g_{\mathbf{w}}(\rho)$ as a power series in the frequency, *i.e.*

$$g_{\mathbf{w}}(\rho) = g_{\mathbf{w}}^{(0)}(\rho) + \mathbf{w}^2 g_{\mathbf{w}}^{(2)}(\rho) + \cdots. \quad (\text{C.9})$$

The first term in the expansion satisfies the equation

$$\frac{d}{d\rho} \left[\rho^4 f(\rho) \frac{d}{d\rho} g_{\mathbf{w}}^{(0)}(\rho) \right] = 0, \quad (\text{C.10})$$

for which we have been able to find analytical solutions only for $d = 2, 3$. Therefore, we now turn our attention to these two particular cases.

C.0.3 Solution for $d = 2$

The general solution of (C.10) for $d = 2$ reads

$$\begin{aligned} g_{\mathbf{w}}^{(0)}(\rho) &= B_1 + B_2 \left[\frac{\sqrt{2}}{2} \tan^{-1} \left(\frac{\rho + 1}{\sqrt{2}} \right) \right. \\ &\quad \left. + \log \left(\frac{3 + \rho(\rho + 2)}{(\rho - 1)^2} \right) - \frac{3}{\rho - 1} \right]. \end{aligned} \quad (\text{C.11})$$

We can allow a frequency dependence for the constants of integration, but in order to have a reliable expansion as in (C.9), we have to require that both B_1 and B_2 are at most linear in \mathbf{w} . We now proceed to find these constants

by expanding (C.11) near the horizon and matching the solution with (C.6).

From (C.9) and (C.11) it follows that

$$g_{\mathfrak{w}}(\rho) = B_1 + B_2 \left[\frac{\sqrt{2}}{2} \tan^{-1}(\sqrt{2}) + \log(6) - 2 \log(\rho - 1) - \frac{3}{\rho - 1} + \mathcal{O}(\rho - 1) \right] + \mathcal{O}(\mathfrak{w}^2). \quad (\text{C.12})$$

Comparing the $\mathcal{O}(1/(\rho - 1))$ and $\mathcal{O}(1)$ terms with the expression in (C.6) we find that

$$B_1^{(\text{out/in})} = 1 \mp \frac{1}{18} i\mathfrak{w} \left(\frac{\sqrt{2}}{2} \tan^{-1} \sqrt{2} + \log 6 \right), \quad (\text{C.13})$$

$$B_2^{(\text{out/in})} = \pm \frac{i\mathfrak{w}}{18}. \quad (\text{C.14})$$

Finally, expanding the general solution in (C.11) for $\rho \rightarrow \infty$ yields

$$g_{\mathfrak{w}}(\rho) = B_1 + B_2 \left[\frac{\pi}{2\sqrt{2}} - \frac{6}{\rho^3} + \mathcal{O}\left(\frac{1}{\rho^4}\right) \right] + \mathcal{O}(\mathfrak{w}^2). \quad (\text{C.15})$$

Comparing equation (C.15) with (C.8) and using (C.13), one obtains the expressions for C_1 and C_2 given in (4.54).

C.0.4 Solution for $d = 3$

The general solution of (C.10) for $d = 3$ takes the form

$$g_{\mathfrak{w}}^{(0)}(\rho) = B_1 + B_2 \left[2\sqrt{2} \tan^{-1} \left(\frac{\rho}{\sqrt{2}} \right) + \tanh^{-1}(\rho) + \frac{3\rho}{\rho^2 - 1} \right]. \quad (\text{C.16})$$

Again, to have a consistent expansion in frequencies, B_1 and B_2 are allowed to be at most of order $\mathcal{O}(\mathfrak{w})$. From (C.9) and (C.16), it follows that

$$g_{\mathfrak{w}}(\rho) = B_1 + B_2 \left[\frac{3}{4} - \frac{\pi i}{2} + \frac{1}{2} \log 2 + 2\sqrt{2} \cot^{-1} \sqrt{2} - \frac{1}{2} \log(\rho - 1) + \frac{3}{2(\rho - 1)} + \mathcal{O}(\rho - 1) \right] + \mathcal{O}(\mathfrak{w}^2). \quad (\text{C.17})$$

Comparing the $\mathcal{O}(1/(\rho - 1))$ and $\mathcal{O}(1)$ terms with (C.6), we obtain

$$B_1^{(\text{out/in})} = 1 \pm \frac{i\mathfrak{w}}{36} \left(\frac{3}{2} - \pi i + 4\sqrt{2} \cot^{-1} \sqrt{2} + \log 2 \right), \quad (\text{C.18})$$

$$B_2^{(\text{out/in})} = \mp \frac{i\mathfrak{w}}{18}. \quad (\text{C.19})$$

Expanding (C.16) for $\rho \rightarrow \infty$ results in

$$g_{\mathfrak{w}}(\rho) = B_1 + B_2 \left[\sqrt{2}\pi - \frac{\pi i}{2} + \frac{6}{\rho^3} + \mathcal{O}\left(\frac{1}{\rho^4}\right) \right] + \mathcal{O}(\mathfrak{w}^2). \quad (\text{C.20})$$

Comparing (C.20) with (C.8), we finally get

$$C_1^{(\text{out/in})} = 1 \pm \frac{i\mathfrak{w}}{36} \left(\frac{3}{2} - 2\sqrt{2}\pi + 4\sqrt{2} \cot^{-1} \sqrt{2} + \log 2 \right) \quad (\text{C.21})$$

$$C_2^{(\text{out/in})} = \mp \frac{1}{\mathfrak{w}^2}. \quad (\text{C.22})$$

Going through the same steps as we did in section 4.5, one easily obtains the following scaling behavior for the imaginary part of the admittance at low frequencies

$$\text{Im } \chi(\omega) \sim \frac{1}{\omega}, \quad (\text{C.23})$$

which using the fluctuation-dissipation theorem results in

$$\langle X(\omega)X(0) \rangle \sim \frac{1}{\omega}. \quad (\text{C.24})$$

Bibliography

- [1] J. Aczel, B. Forte and C. T. Ng, “Why the Shannon and Hartley entropies are natural,” *Adv. Appl. Prob.* **6**, 131 (1974)
- [2] O. Aharony, M. Berkooz, D. Kutasov and N. Seiberg, “Linear dilatons, NS five-branes and holography,” *JHEP* **9810**, 004 (1998), [hep-th/9808149].
- [3] T. Albash and C. V. Johnson, “Evolution of Holographic Entanglement Entropy after Thermal and Electromagnetic Quenches,” *New J. Phys.* **13**, 045017 (2011) [arXiv:1008.3027 [hep-th]].
- [4] M. Alishahiha, E. OColgain and H. Yavartanoo, “Charged Black Branes with Hyperscaling Violating Factor,” arXiv:1209.3946 [hep-th].
- [5] M. Alishahiha and H. Yavartanoo, “On Holography with Hyperscaling Violation,” arXiv:1208.6197 [hep-th].
- [6] A. Allais and E. Tonni, “Holographic evolution of the mutual information,” *JHEP* **1201**, 102 (2012) [arXiv:1110.1607 [hep-th]].
- [7] A. Almheiri, D. Marolf, J. Polchinski and J. Sully, “Black Holes: Complementarity or Firewalls?,” *JHEP* **1302**, 062 (2013) [arXiv:1207.3123 [hep-th]].

- [8] M. Ammon, M. Kaminski and A. Karch, “Hyperscaling-Violation on Probe D-Branes,” arXiv:1207.1726 [hep-th].
- [9] H. Araki and E. H. Lieb, “Entropy inequalities,” Commun. Math. Phys. **18**, 160 (1970).
- [10] F. Ardalan, H. Arfaei and M. M. Sheikh-Jabbari, “Noncommutative geometry from strings and branes,” JHEP **9902**, 016 (1999), [hep-th/9810072].
- [11] C. Asplund, D. Berenstein and D. Trancanelli, “Evidence for fast thermalization in the BMN matrix model,” Phys. Rev. Lett. **107**, 171602 (2011) [arXiv:1104.5469 [hep-th]].
- [12] C. Athanasiou, H. Liu and K. Rajagopal, “Velocity Dependence of Baryon Screening in a Hot Strongly Coupled Plasma,” JHEP **0805**, 083 (2008) [arXiv:0801.1117 [hep-th]].
- [13] A. N. Atmaja, J. de Boer and M. Shigemori, “Holographic Brownian Motion and Time Scales in Strongly Coupled Plasmas,” arXiv:1002.2429 [hep-th].
- [14] V. Balasubramanian, A. Bernamonti, J. de Boer, N. Copland, B. Craps, E. Keski-Vakkuri, B. Muller and A. Schafer *et al.*, “Thermalization of Strongly Coupled Field Theories,” Phys. Rev. Lett. **106**, 191601 (2011) [arXiv:1012.4753 [hep-th]].

- [15] V. Balasubramanian, A. Bernamonti, J. de Boer, N. Copland, B. Craps, E. Keski-Vakkuri, B. Muller and A. Schafer *et al.*, “Holographic Thermalization,” Phys. Rev. D **84**, 026010 (2011)
- [16] K. Balasubramanian and J. McGreevy, “Gravity duals for non-relativistic CFTs,” Phys. Rev. Lett. **101**, 061601 (2008), arXiv:0804.4053 [hep-th].
- [17] T. Banks, W. Fischler, S. H. Shenker and L. Susskind, “M theory as a matrix model: A Conjecture,” Phys. Rev. D **55**, 5112 (1997) [hep-th/9610043].
- [18] J. L. F. Barbon and J. M. Magan, “Chaotic fast scrambling at black holes,” Phys. Rev. D **84**, 106012 (2011) [arXiv:1105.2581 [hep-th]].
- [19] C. Barrabes and W. Israel , “Thin shells in general relativity and cosmology: The Lightlike limit,” Phys. Rev. D **43**, 1129 (1991).
- [20] O. Bergman, J. Erdmenger and G. Lifschytz, “A Review of Magnetic Phenomena in Probe-Brane Holographic Matter,” arXiv:1207.5953 [hep-th].
- [21] E. Berti, V. Cardoso and A. O. Starinets, “Quasinormal modes of black holes and black branes,” Class. Quant. Grav. **26**, 163001 (2009), arXiv:0905.2975 [gr-qc].
- [22] J. Bhattacharya, S. Cremonini and A. Sinkovics, “On the IR completion of geometries with hyperscaling violation,” arXiv:1208.1752 [hep-th].

- [23] D. Bigatti and L. Susskind, “Magnetic fields, branes and noncommutative geometry,” *Phys. Rev. D* **62**, 066004 (2000) [hep-th/9908056].
- [24] D. Birmingham, I. Sachs and S. N. Solodukhin, “Conformal field theory interpretation of black hole quasi-normal modes,” *Phys. Rev. Lett.* **88**, 151301 (2002), [hep-th/0112055].
- [25] N. D. Birrell and P. C. W. Davies, “Quantum Fields In Curved Space,” Cambridge, UK: Univ. Pr. (1982).
- [26] J. de Boer, V. E. Hubeny, M. Rangamani and M. Shigemori, “Brownian motion in AdS/CFT,” *JHEP* **0907**, 094 (2009) [arXiv:0812.5112 [hep-th]].
- [27] S. Bolognesi, F. Kiefer and E. Rabinovici, “Comments on Critical Electric and Magnetic Fields from Holography,” arXiv:1210.4170 [hep-th].
- [28] D. K. Brattan, R. A. Davison, S. A. Gentle and A. O’Bannon, “Collective Excitations of Holographic Quantum Liquids in a Magnetic Field,” arXiv:1209.0009 [hep-th].
- [29] P. Bueno, W. Chemissany, P. Meessen, T. Ortin and C. S. Shahbazi, “Lifshitz-like solutions with hyperscaling violation in ungauged supergravity,” arXiv:1209.4047 [hep-th].
- [30] E. Caceres, M. Chernicoff, A. Guijosa and J. F. Pedraza, “Quantum Fluctuations and the Unruh Effect in Strongly-Coupled Conformal Field Theories,” *JHEP* **1006**, 078 (2010) [arXiv:1003.5332 [hep-th]].

- [31] E. Caceres and A. Kundu, “Holographic Thermalization with Chemical Potential,” JHEP **1209**, 055 (2012) [arXiv:1205.2354 [hep-th]].
- [32] E. Caceres, A. Kundu, J. F. Pedraza and W. Tangarife, “Strong Subadditivity, Null Energy Condition and Charged Black Holes,” JHEP **1401**, 084 (2014) [arXiv:1304.3398 [hep-th]].
- [33] M. Cadoni and S. Mignemi, “Phase transition and hyperscaling violation for scalar Black Branes,” JHEP **1206**, 056 (2012), arXiv:1205.0412 [hep-th].
- [34] M. Cadoni and M. Serra, “Hyperscaling violation for scalar black branes in arbitrary dimensions,” arXiv:1209.4484 [hep-th].
- [35] R. Callan, J. -Y. He and M. Headrick, “Strong subadditivity and the covariant holographic entanglement entropy formula,” JHEP **1206**, 081 (2012) [arXiv:1204.2309 [hep-th]].
- [36] S. Caron-Huot, P. M. Chesler and D. Teaney, “Fluctuation, dissipation, and thermalization in non-equilibrium AdS_5 black hole geometries,” Phys. Rev. D **84**, 026012 (2011) [arXiv:1102.1073 [hep-th]].
- [37] J. Casalderrey-Solana, K. -Y. Kim and D. Teaney, “Stochastic String Motion Above and Below the World Sheet Horizon,” JHEP **0912**, 066 (2009) [arXiv:0908.1470 [hep-th]].

- [38] J. Casalderrey-Solana, H. Liu, D. Mateos, K. Rajagopal and U. A. Wiedemann, “Gauge/String Duality, Hot QCD and Heavy Ion Collisions,” arXiv:1101.0618 [hep-th].
- [39] J. Casalderrey-Solana and D. Teaney, “Heavy quark diffusion in strongly coupled N=4 Yang-Mills,” Phys. Rev. D **74**, 085012 (2006) [hep-ph/0605199].
- [40] J. Casalderrey-Solana and D. Teaney, “Transverse Momentum Broadening of a Fast Quark in a N=4 Yang Mills Plasma,” JHEP **0704**, 039 (2007) [hep-th/0701123].
- [41] H. Casini, “Geometric entropy, area, and strong subadditivity,” Class. Quant. Grav. **21**, 2351 (2004) [hep-th/0312238].
- [42] H. Casini and M. Huerta, “A Finite entanglement entropy and the c-theorem,” Phys. Lett. B **600**, 142 (2004) [hep-th/0405111].
- [43] H. Casini and M. Huerta, “On the RG running of the entanglement entropy of a circle,” Phys. Rev. D **85**, 125016 (2012) [arXiv:1202.5650 [hep-th]].
- [44] A. Chamblin, R. Emparan, C. V. Johnson and R. C. Myers, “Charged AdS black holes and catastrophic holography,” Phys. Rev. D **60**, 064018 (1999), [hep-th/9902170].
- [45] C. Charmousis, B. Gouteraux, B. S. Kim, E. Kiritsis and R. Meyer, “Effective Holographic Theories for low-temperature condensed matter systems,” JHEP **1011**, 151 (2010), arXiv:1005.4690 [hep-th].

- [46] M. Chernicoff and A. Guijosa, “Energy Loss of Gluons, Baryons and k-Quarks in an N=4 SYM Plasma,” JHEP **0702**, 084 (2007) [hep-th/0611155].
- [47] M. Chernicoff and A. Guijosa, “Acceleration, Energy Loss and Screening in Strongly-Coupled Gauge Theories,” JHEP **0806**, 005 (2008) [arXiv:0803.3070 [hep-th]].
- [48] M. Chernicoff, J. A. Garcia and A. Guijosa, “The Energy of a Moving Quark-Antiquark Pair in an N=4 SYM Plasma,” JHEP **0609**, 068 (2006) [hep-th/0607089].
- [49] M. Chernicoff, J. A. Garcia, A. Guijosa and J. F. Pedraza, “Holographic Lessons for Quark Dynamics,” J. Phys. G G **39**, 054002 (2012) [arXiv:1111.0872 [hep-th]].
- [50] C. -S. Chu and C. M. Ho, “Nonequilibrium dynamics in noncommutative spacetime,” JHEP **1002**, 098 (2010) arXiv:0912.1748 [hep-th].
- [51] A. Connes, M. R. Douglas and A. S. Schwarz, “Noncommutative geometry and matrix theory: Compactification on tori,” JHEP **9802**, 003 (1998) [hep-th/9711162].
- [52] K. Copsey and R. Mann, “Singularities in Hyperscaling Violating Spacetimes,” arXiv:1210.1231 [hep-th].
- [53] S. R. Das and B. Ghosh, “A Note on supergravity duals of noncommutative Yang-Mills theory,” JHEP **0006**, 043 (2000), [hep-th/0005007].

- [54] S. R. Das and S.-J. Rey, “Open Wilson lines in noncommutative gauge theory and tomography of holographic dual supergravity,” Nucl. Phys. **B590** 453 (2000), [hep-th/0008042].
- [55] S. R. Das and S. P. Trivedi, “Supergravity couplings to noncommutative branes, open Wilson lines and generalized star products,” JHEP 0102 046 (2001), [hep-th/0011131].
- [56] P. Dey and S. Roy, “Lifshitz-like space-time from intersecting branes in string/M theory,” JHEP **1206**, 129 (2012), arXiv:1203.5381 [hep-th].
- [57] P. Dey and S. Roy, “Lifshitz metric with hyperscaling violation from NS5-Dp states in string theory,” arXiv:1209.1049 [hep-th].
- [58] X. Dong, S. Harrison, S. Kachru, G. Torroba and H. Wang, “Aspects of holography for theories with hyperscaling violation,” JHEP **1206**, 041 (2012), arXiv:1201.1905 [hep-th].
- [59] M. R. Douglas and C. M. Hull, “D-branes and the noncommutative torus,” JHEP **9802**, 008 (1998), [hep-th/9711165].
- [60] M. R. Douglas and N. A. Nekrasov, “Noncommutative field theory,” Rev. Mod. Phys. **73**, 977 (2001) [hep-th/0106048].
- [61] H. Ebrahim and M. Headrick, “Instantaneous Thermalization in Holographic Plasmas,” arXiv:1010.5443 [hep-th].

- [62] M. Edalati, W. Fischler, J. F. Pedraza and W. Tangarife Garcia, “Fast Scramblers and Non-commutative Gauge Theories,” JHEP **1207**, 043 (2012) [arXiv:1204.5748 [hep-th]].
- [63] M. Edalati, J. F. Pedraza and W. Tangarife Garcia, “Quantum Fluctuations in Holographic Theories with Hyperscaling Violation,” Phys. Rev. D **87**, no. 4, 046001 (2013) [arXiv:1210.6993 [hep-th]].
- [64] P. Figueras, V. E. Hubeny, M. Rangamani and S. F. Ross, “Dynamical black holes and expanding plasmas,” JHEP **0904**, 137 (2009) [arXiv:0902.4696 [hep-th]].
- [65] W. Fischler, E. Gorbatov, A. Kashani-Poor, R. McNees, S. Paban and P. Pouliot, “The Interplay between θ and T ,” JHEP **0006**, 032 (2000) [hep-th/0003216].
- [66] W. Fischler, E. Gorbatov, A. Kashani-Poor, S. Paban, P. Pouliot and J. Gomis, “Evidence for winding states in noncommutative quantum field theory,” JHEP **0005**, 024 (2000) [hep-th/0002067].
- [67] W. Fischler, A. Kundu and S. Kundu, “Holographic Entanglement in a Noncommutative Gauge Theory,” JHEP **1401**, 137 (2014) [arXiv:1307.2932 [hep-th]].
- [68] W. Fischler, J. F. Pedraza and W. Tangarife Garcia, “Holographic Brownian Motion in Magnetic Environments,” arXiv:1209.1044 [hep-th].

- [69] V. P. Frolov and D. Fursaev, “Mining energy from a black hole by strings,” *Phys. Rev. D* **63**, 124010 (2001) [hep-th/0012260].
- [70] D. Galante and M. Schvellinger, “Thermalization with a chemical potential from AdS spaces,” *JHEP* **1207**, 096 (2012) [arXiv:1205.1548 [hep-th]].
- [71] G. C. Giecold, E. Iancu and A. H. Mueller, “Stochastic trailing string and Langevin dynamics from AdS/CFT,” *JHEP* **0907**, 033 (2009) [arXiv:0903.1840 [hep-th]].
- [72] D. Gioev and I. Klich, “Entanglement Entropy of Fermions in Any Dimension and the Widom Conjecture,” *Phys. Rev. Lett.* **96**, 100503 (2006).
- [73] B. Gouteraux and E. Kiritsis, “Generalized Holographic Quantum Criticality at Finite Density,” *JHEP* **1112**, 036 (2011), arXiv:1107.2116 [hep-th].
- [74] D. J. Gross, A. Hashimoto and N. Izhaki, “Observables of noncommutative gauge theories,” *Adv. Theor. Math. Phys.* **4**, 893 (2000), [hep-th/0008075].
- [75] S. S. Gubser, “Drag force in AdS/CFT,” *Phys. Rev. D* **74**, 126005 (2006) [arXiv:hep-th/0605182].
- [76] S. S. Gubser, “Momentum fluctuations of heavy quarks in the gauge-string duality,” *Nucl. Phys. B* **790**, 175 (2008) [hep-th/0612143].

- [77] S. S. Gubser, D. R. Gulotta, S. S. Pufu and F. D. Rocha, “Gluon energy loss in the gauge-string duality,” JHEP **0810**, 052 (2008) [arXiv:0803.1470 [hep-th]].
- [78] S. S. Gubser and A. Karch, “From gauge-string duality to strong interactions: A Pedestrian’s Guide,” Ann. Rev. Nucl. Part. Sci. **59**, 145 (2009) [arXiv:0901.0935 [hep-th]].
- [79] S. S. Gubser, I. R. Klebanov and A. M. Polyakov, “Gauge theory correlators from noncritical string theory,” Phys. Lett. B **428**, 105 (1998), [hep-th/9802109].
- [80] S. S. Gubser and F. D. Rocha, “Peculiar properties of a charged dilatonic black hole in AdS_5 ,” Phys. Rev. D **81**, 046001 (2010), arXiv:0911.2898 [hep-th].
- [81] A. Guijosa and J. F. Pedraza, “Early-Time Energy Loss in a Strongly-Coupled SYM Plasma,” JHEP **1105**, 108 (2011) [arXiv:1102.4893 [hep-th]].
- [82] T. Harmark, J. Natario and R. Schiappa, “Greybody factors for d -dimensional black holes,” Adv. Theor. Math. Phys. **14** (2010) 727 [arXiv:0708.0017 [hep-th]].
- [83] S. A. Hartnoll, “Lectures on holographic methods for condensed matter physics,” Class. Quant. Grav. **26**, 224002 (2009) [arXiv:0903.3246 [hep-th]].

- [84] S. A. Hartnoll and E. Shaghoulian, “Spectral weight in holographic scaling geometries,” JHEP **1207**, 078 (2012), arXiv:1203.4236 [hep-th].
- [85] A. Hashimoto and N. Itzhaki, “Noncommutative Yang-Mills and the AdS / CFT correspondence,” Phys. Lett. B **465**, 142 (1999), [hep-th/9907166].
- [86] P. Hayden and J. Preskill, “Black holes as mirrors: Quantum information in random subsystems,” JHEP **0709**, 120 (2007), arXiv:0708.4025 [hep-th].
- [87] M. Headrick, “Entanglement Renyi entropies in holographic theories,” Phys. Rev. D **82**, 126010 (2010) [arXiv:1006.0047 [hep-th]].
- [88] M. Headrick and T. Takayanagi, “A Holographic proof of the strong subadditivity of entanglement entropy,” Phys. Rev. D **76**, 106013 (2007) [arXiv:0704.3719 [hep-th]].
- [89] S. Hemming and E. Keski-Vakkuri, “Hawking radiation from AdS black holes,” Phys. Rev. D **64**, 044006 (2001) [arXiv:gr-qc/0005115].
- [90] C. P. Herzog, A. Karch, P. Kovtun, C. Kozcaz and L. G. Yaffe, “Energy loss of a heavy quark moving through $N = 4$ supersymmetric Yang-Mills plasma,” JHEP **0607**, 013 (2006) [arXiv:hep-th/0605158].
- [91] C. P. Herzog and D. T. Son, “Schwinger-Keldysh propagators from AdS/CFT correspondence,” JHEP **0303**, 046 (2003) [hep-th/0212072].

- [92] G. T. Horowitz and V. E. Hubeny, “Quasinormal modes of AdS black holes and the approach to thermal equilibrium,” *Phys. Rev. D* **62**, 024027 (2000) [hep-th/9909056].
- [93] G. T. Horowitz and V. E. Hubeny, “Quasinormal modes of AdS black holes and the approach to thermal equilibrium,” *Phys. Rev. D* **62**, 024027 (2000), [hep-th/9909056].
- [94] V. E. Hubeny and M. Rangamani, “A Holographic view on physics out of equilibrium,” *Adv. High Energy Phys.* **2010**, 297916 (2010) [arXiv:1006.3675 [hep-th]].
- [95] V. E. Hubeny, M. Rangamani and T. Takayanagi, “A Covariant holographic entanglement entropy proposal,” *JHEP* **0707**, 062 (2007) [arXiv:0705.0016 [hep-th]].
- [96] L. Huijse, S. Sachdev and B. Swingle, “Hidden Fermi surfaces in compressible states of gauge-gravity duality,” arXiv:1112.0573 [cond-mat.str-el].
- [97] N. Iizuka, N. Kundu, P. Narayan and S. P. Trivedi, “Holographic Fermi and Non-Fermi Liquids with Transitions in Dilaton Gravity,” *JHEP* **1201**, 094 (2012), arXiv:1105.1162 [hep-th].
- [98] N. Ishibashi, S. Iso, H. Kawai and Y. Kitazawa, “Wilson loops in noncommutative Yang-Mills,” *Nucl. Phys. B* **573**, 573 (2000), [hep-th/9910004].

- [99] W. Israel, “Singular hypersurfaces and thin shells in general relativity,”
Nuovo Cim. B **44S10**, 1 (1966) [Erratum-ibid. B **48**, 463 (1967)] [Nuovo
Cim. B **44**, 1 (1966)].
- [100] S. Janiszewski and A. Karch, “Moving Defects in AdS/CFT,” JHEP
1111, 044 (2011) [arXiv:1106.4010 [hep-th]].
- [101] K. Jensen, “Chiral anomalies and AdS/CMT in two dimensions,” JHEP
1101, 109 (2011) [arXiv:1012.4831 [hep-th]].
- [102] S. Kachru, X. Liu and M. Mulligan, “Gravity Duals of Lifshitz-like Fixed
Points,” Phys. Rev. D **78**, 106005 (2008), arXiv:0808.1725 [hep-th].
- [103] J. I. Kapusta and C. Gale, “Finite-temperature field theory: Principles
and applications,” Cambridge University Press, 2006.
- [104] B. S. Kim, “Schrödinger Holography with and without Hyperscaling
Violation,” JHEP **1206**, 116 (2012), arXiv:1202.6062 [hep-th].
- [105] B. S. Kim, “Hyperscaling violation : a unified frame for effective holo-
graphic theories,” arXiv:1210.0540 [hep-th].
- [106] E. Kiritsis, “Lorentz violation, Gravity, Dissipation and Holography,”
arXiv:1207.2325 [hep-th].
- [107] C. Hoyos and P. Koroteev, “On the Null Energy Condition and Causality
in Lifshitz Holography,” Phys. Rev. D **82**, 084002 (2010), [Erratum-ibid.
D **82**, 109905 (2010)], arXiv:1007.1428 [hep-th].

- [108] P. K. Kovtun and A. O. Starinets, “Quasinormal modes and holography,” *Phys. Rev. D* **72**, 086009 (2005), [hep-th/0506184].
- [109] P. Kovtun, D. T. Son and A. O. Starinets, “Viscosity in strongly interacting quantum field theories from black hole physics,” *Phys. Rev. Lett.* **94**, 111601 (2005) [hep-th/0405231].
- [110] C. Krishnan, “Baryon Dissociation in a Strongly Coupled Plasma,” *JHEP* **0812**, 019 (2008) [arXiv:0809.5143 [hep-th]].
- [111] R. Kubo, “The fluctuation-dissipation theorem,” *Rep. Prog. Phys.* **29**, 255-284 (1966).
- [112] B. Kursunoglu, “Brownian Motion in a Magnetic Field” *Ann. Phys.* **17**, 259 (1962).
- [113] N. Lashkari, D. Stanford, M. Hastings, T. Osborne and P. Hayden, “Towards the fast scrambling conjecture,” arXiv:1111.6580 [hep-th].
- [114] A. E. Lawrence and E. J. Martinec, “Black hole evaporation along macroscopic strings,” *Phys. Rev. D* **50**, 2680 (1994) [hep-th/9312127].
- [115] E. W. Leaver, “Quasinormal modes of Reissner-Nordstrom black holes,” *Phys. Rev. D* **41**, 2986 (1990).
- [116] M. Le Bellac. “Thermal Field Theory”, Cambridge University Press (1996).

- [117] E. H. Lieb and M. B. Ruskai, “Proof of the strong subadditivity of quantum-mechanical entropy,” J. Math. Phys. **14**, 1938 (1973).
- [118] H. Liu, “*-Trek II: $*_n$ Operations, open Wilson lines and the Seiberg-Witten map,” Nucl. Phys. **B614** 305 (2001) [hep-th/0011125].
- [119] H. Liu and J. Michelson, “Supergravity couplings of noncommutative D-branes,” Nucl. Phys. **B615** 169 (2001) [hep-th/0101016].
- [120] H. Liu, K. Rajagopal and U. A. Wiedemann, “An AdS/CFT Calculation of Screening in a Hot Wind,” Phys. Rev. Lett. **98**, 182301 (2007) [hep-ph/0607062].
- [121] J. M. Maldacena, “The Large N limit of superconformal field theories and supergravity,” Adv. Theor. Math. Phys. **2**, 231 (1998), Int. J. Theor. Phys. **38**, 1113 (1999), [hep-th/9711200].
- [122] J. M. Maldacena, “Eternal black holes in anti-de Sitter,” JHEP **0304**, 021 (2003) [hep-th/0106112].
- [123] J. M. Maldacena, J. G. Russo, “Large N limit of noncommutative gauge theories,” JHEP **9909**, 025 (1999), [hep-th/9908134].
- [124] T. Matsuo, D. Tomino and W. -Y. Wen, “Drag force in SYM plasma with B field from AdS/CFT,” JHEP **0610**, 055 (2006) [hep-th/0607178].
- [125] A. Matusis, L. Susskind and N. Toumbas, “The IR / UV connection in the noncommutative gauge theories,” JHEP **0012**, 002 (2000) [hep-th/0002075].

- [126] J. McGreevy, “Holographic duality with a view toward many-body physics,” *Adv. High Energy Phys.* **2010**, 723105 (2010) [arXiv:0909.0518 [hep-th]].
- [127] S. Minwalla, M. Van Raamsdonk and N. Seiberg, “Noncommutative perturbative dynamics,” *JHEP* **0002**, 020 (2000) [hep-th/9912072].
- [128] S. Minwalla and N. Seiberg, “Comments on the IIA (NS)five-brane,” *JHEP* **9906**, 007 (1999), [hep-th/9904142].
- [129] H. Mori, “Transport, collective motion, and Brownian motion,” *Prog. Theor. Phys.* **33**, 423 (1965).
- [130] R. C. Myers and A. Sinha, “Seeing a c-theorem with holography,” *Phys. Rev. D* **82**, 046006 (2010) [arXiv:1006.1263 [hep-th]].
- [131] R. C. Myers and A. Sinha, “Holographic c-theorems in arbitrary dimensions,” *JHEP* **1101**, 125 (2011) [arXiv:1011.5819 [hep-th]].
- [132] K. Narayan, “On Lifshitz scaling and hyperscaling violation in string theory,” *Phys. Rev. D* **85**, 106006 (2012), arXiv:1202.5935 [hep-th].
- [133] M. A. Nielsen and D. Petz, “A simple proof of the strong subadditivity inequality,” [arXiv:0408130 [quant-ph]].
- [134] W. Ochs, “A new axiomatic characterization of the von Neumann entropy,” *Rev. Mod. Phys.* **50**, 221 (1978)

- [135] N. Ogawa, T. Takayanagi and T. Ugajin, “Holographic Fermi Surfaces and Entanglement Entropy,” JHEP **1201**, 125 (2012), arXiv:1111.1023 [hep-th].
- [136] A. Ori, “Charged null fluid and the weak energy condition,” Class. Quantum Grav. **8** 1991, 1559-1575
- [137] K. Peeters, J. Sonnenschein and M. Zamaklar, “Holographic melting and related properties of mesons in a quark gluon plasma,” Phys. Rev. D **74**, 106008 (2006) [hep-th/0606195].
- [138] E. Perlmutter, “Hyperscaling violation from supergravity,” JHEP **1206**, 165 (2012), arXiv:1205.0242 [hep-th].
- [139] G. Policastro, D. T. Son and A. O. Starinets, “The Shear viscosity of strongly coupled N=4 supersymmetric Yang-Mills plasma,” Phys. Rev. Lett. **87**, 081601 (2001) [hep-th/0104066].
- [140] M. Rangamani, “Gravity and Hydrodynamics: Lectures on the fluid-gravity correspondence,” Class. Quant. Grav. **26**, 224003 (2009) [arXiv:0905.4352 [hep-th]].
- [141] L. J. Romans, “Supersymmetric, cold and lukewarm black holes in cosmological Einstein-Maxwell theory,” Nucl. Phys. B **383**, 395 (1992), [hep-th/9203018].

- [142] S. Roy, “Holography and drag force in thermal plasma of non-commutative Yang-Mills theories in diverse dimensions,” *Phys. Lett. B* **682**, 93 (2009) [arXiv:0907.0333 [hep-th]].
- [143] S. Ryu and T. Takayanagi, “Holographic derivation of entanglement entropy from AdS/CFT,” *Phys. Rev. Lett.* **96**, 181602 (2006) [hep-th/0603001].
- [144] S. Ryu and T. Takayanagi, “Aspects of Holographic Entanglement Entropy,” *JHEP* **0608**, 045 (2006) [hep-th/0605073].
- [145] J. Sadeghi, B. Pourhassan and A. Asadi, “Thermodynamics of string black hole with hyperscaling violation,” arXiv:1209.1235 [hep-th].
- [146] J. Sadeghi, B. Pourhasan and F. Pourasadollah, “Schrödinger black holes with hyperscaling violation,” arXiv:1209.1874 [hep-th].
- [147] J. H. Schwarz, “Covariant field equations of chiral $N = 2$ $D = 10$ supergravity,” *Nucl. Phys.* **B226**, 269 (1983).
- [148] N. Seiberg and E. Witten, “String theory and noncommutative geometry,” *JHEP* **9909**, 032 (1999), [hep-th/9908142].
- [149] Y. Sekino and L. Susskind, “Fast scramblers,” *JHEP* **0810**, 065 (2008), arXiv:0808.2096 [hep-th].
- [150] E. Shaghoulian, “Holographic Entanglement Entropy and Fermi Surfaces,” *JHEP* **1205**, 065 (2012), arXiv:1112.2702 [hep-th].

- [151] H. Singh, “Special limits and non-relativistic solutions,” JHEP **1012**, 061 (2010), arXiv:1009.0651 [hep-th].
- [152] H. Singh, “Lifshitz/Schrödinger Dp-branes and dynamical exponents,” JHEP **1207**, 082 (2012), arXiv:1202.6533 [hep-th].
- [153] A. Sinha, “On higher derivative gravity, c -theorems and cosmology,” Class. Quant. Grav. **28**, 085002 (2011) [arXiv:1008.4315 [hep-th]].
- [154] D. T. Son, “Toward an AdS/cold atoms correspondence: A Geometric realization of the Schrodinger symmetry,” Phys. Rev. D **78**, 046003 (2008), arXiv:0804.3972 [hep-th].
- [155] D. T. Son and A. O. Starinets, “Minkowski-space correlators in AdS/CFT correspondence: Recipe and applications,” JHEP **0209**, 042 (2002), [hep-th/0205051].
- [156] D. T. Son and A. O. Starinets, “Viscosity, Black Holes, and Quantum Field Theory,” Ann. Rev. Nucl. Part. Sci. **57**, 95 (2007) [arXiv:0704.0240 [hep-th]].
- [157] D. T. Son and D. Teaney, “Thermal Noise and Stochastic Strings in AdS/CFT,” JHEP **0907**, 021 (2009) [arXiv:0901.2338 [hep-th]].
- [158] L. Susskind, “The World as a hologram,” J. Math. Phys. **36**, 6377 (1995) [hep-th/9409089].
- [159] L. Susskind, “Addendum to fast scramblers,” arXiv:1101.6048 [hep-th].

- [160] L. Susskind, L. Thorlacius and J. Uglum, “The Stretched horizon and black hole complementarity,” *Phys. Rev. D* **48**, 3743 (1993) [hep-th/9306069].
- [161] B. Swingle, “Entanglement Entropy and the Fermi Surface,” *Phys. Rev. Lett.* **105**, 050502 (2010), arXiv:0908.1724 [cond-mat.str-el].
- [162] B. Swingle, “Conformal Field Theory on the Fermi Surface,” *Phys. Rev. B* **86**, 035116 (2012), arXiv:1002.4635 [cond-mat.str-el].
- [163] T. Takayanagi, “Entanglement Entropy from a Holographic Viewpoint,” *Class. Quant. Grav.* **29**, 153001 (2012) [arXiv:1204.2450 [gr-qc]].
- [164] J. B. Taylor, “Diffusion of Plasma Across a Magnetic Field,” *Phys. Rev. Lett.* **6**, 262 (1961).
- [165] G. 't Hooft, “Dimensional reduction in quantum gravity,” gr-qc/9310026.
- [166] K. S. Thorne, R. H. Price and D. A. Macdonald, “Black Holes: The Membrane Paradigm,” Yale University Press, 1986.
See also L. Susskind and J. Lindesay, “An introduction to black holes, information and the string theory revolution: The holographic universe,” World Scientific, 2005.
- [167] D. Tong and K. Wong, “Fluctuation and Dissipation at a Quantum Critical Point,” arXiv:1210.1580 [hep-th].
- [168] A. C. Wall, “Maximin Surfaces, and the Strong Subadditivity of the Covariant Holographic Entanglement Entropy,” arXiv:1211.3494 [hep-th].

- [169] E. Witten, “Anti-de Sitter space and holography,” *Adv. Theor. Math. Phys.* **2**, 253 (1998), [hep-th/9802150].
- [170] E. Witten, “Anti-de Sitter space, thermal phase transition, and confinement in gauge theories,” *Adv. Theor. Math. Phys.* **2**, 505 (1998), [hep-th/9803131].
- [171] M. M. Wolf, “Violation of the entropic area law for Fermions,” *Phys. Rev. Lett.* **96**, 010404 (2006), [quant-ph/0503219].
- [172] Y. Zhang, T. Grover, A. Vishwanath, Entanglement entropy of critical spin liquids, *Phys. Rev. Lett.* 107 (2011), 067202, arXiv:1102.0350[cond-mat].

Vita

Walter Tangarife was born in Medellín, Antioquia, Colombia. He received a canonical Bachelor of Philosophy diploma from Universidad Pontificia Bolivariana, Medellín, in 2002. Afterwards, he went to La Universidad de Antioquia, where he got a Bachelor of Science degree in Physics in 2008 with a senior thesis titled “Supersymmetric $SU(5) \times U(1)$ model and quark Yukawa couplings”. He joined the graduate program in Physics at The University of Texas at Austin in August 2008.

Email address: walter.tangarife@gmail.com

This dissertation was typeset with \LaTeX^\dagger by the author.

[†] \LaTeX is a document preparation system developed by Leslie Lamport as a special version of Donald Knuth’s \TeX Program.